The role of glia and CED-1/MEGF10 in *C. elegans* models of Parkinson's disease

German Rojas

A dissertation

submitted in partial fulfillment of the

requirements for the degree of

Doctor of Philosophy

University of Washington

2025

Reading Committee:

Aakanksha Singhvi, Chair

Jihong Bai

Jonathan R. Weinstein

Program Authorized to Offer Degree:

Neuroscience

University of Washington

Abstract

The role of glia and CED-1/MEGF10 in *C. elegans* models of Parkinson's disease

German Rojas

Chair of Supervisory Committee:

Aakanksha Singhvi

Department of Neurobiology and Biophysics

Parkinson's disease (PD) is marked by progressive dopamine neuron degeneration, but the phagocytic receptors and cells that clear dopamine neuron corpses are unknown. Further, while other cell types like glia, skin, and muscle are also affected in PD, their role in disease progression is unclear. In my thesis project, I found that astrocyte-like CEPsh glia are neurotoxic in *C. elegans* PD models by regulating the neuronal dopamine biosynthesis enzyme CAT-2/tyrosine hydroxylase. I also identified epithelia and muscle as the phagocytes for dopamine neuron corpses. They engulf by recognizing phosphatidylserine on necrotic-like neuron corpses via the conserved receptor CED-1/Draper/MEGF10. Loss of *ced-1* protects from loss of dopamine neurons but does not protect against the impairment of associated dopaminergic behaviors. Altogether, my thesis work provides evidence for the involvement of glia, muscle, and epithelial cells as potential mediators of dopamine neuron degeneration. Thus, my thesis work suggests that PD may be a disease of multi-organ dysfunction and could inform future therapeutic interventions.

Dedications and Acknowledgements

I would like to dedicate this thesis to my mentors, friends, and family.

First, I would like to thank Aakanksha whose continual support was crucial for the completion of this degree. Thank you for teaching me how to see a project through until the end. Thank you for your patience and for encouraging a lab environment where we celebrate, uplift, and support each other.

I would also like to thank my undergraduate mentors – Karen Parfitt, Karl Johnson, and Elizabeth Glater. Your support, care, and guidance helped me become the scientist that I am today. Without you, I never would have known that grad school was something that I could pursue. Thank you for opening my mind to the many possibilities of this (scientific) world.

I would like to thank my committee members – Jihong Bai, Sharona Gordon, Dana Miller, and Jonathan Weinstein. I enjoyed our conversations, both the scientific curiosities and the not so scientific ones, and I greatly appreciated the support and grace you showed me throughout my graduate career.

I want to thank all past and present GPN staff members, as well as the admin and IT staff in the Basic Sciences Division. I would not be able to do any science without your support. Thank you.

I would like to thank everyone in the Singhvi Lab, past and present, for making the lab feel so welcoming and fun. I will miss you and our yap sessions. I will miss rushing and trying to finish a thousand experiments while everyone crowds around my bench to yap. Thank you for always being kind and thoughtful with your comments and feedback. I will always appreciate

how you supported me during tough times. Finally, I would like to thank Solomon, Sneha, and Irini for their help on the manuscript.

Finally, I would like to thank my friends and family who kept me afloat throughout this entire journey. Thank you to my cohort for showing me what it takes to fight unjust systems, and for the many Heists. As they say, from gnomes we came, to gnomes we return. Thank you to my friends from back home and from college for staying connected and their support. Alex, thank you for never giving up on calling me on the phone. Soleil and Esme, thank you for your support from afar and for watching the CATS movie with me. A big thank you my friends here in Seattle, in particular the Noblets – Sneha, Pralaksha, Trisha, Iissaac, and Mike. Thank you for feeding me, nurturing our love of games, and nurturing our friendship. I never would have broken my foot without you all, and I don't regret it one bit. Thank you for expanding my world and always being willing to try new things together. You have made Seattle feel like home. Sneha, thank you for being a caring and supportive partner. I love you. Also, a huge shoutout to your car. It would have taken me an extra year to finish without it. Finally, I would like to thank my family – my dad, my mom, Maria, Jenny, Javi, and Mateo. Los queiro muchisimo. Gracias por su amor y apoyo incondicional. Siempre han apoyado mis sueños. Nunca dudé de su fe en mí. Soy muy afortunado de tener una familia tan amorosa.

Finally finally, I would like to thank the many many cats in my life – Hotdog, Bella, Sophie, Ella, Soba, Kiwi, Fib, Voxel, Beetle, Poe, Zazu, Mr. Man. Thank you for teaching me how to love and what personal boundaries are.

Table of Contents

Chapter 1

INTRODUCTION

> "If you do not have a proven treatment for certain illnesses, bide your time, do what you can, but do not harm your patients."
>
> Jean-Martin Charcot, 1888

Descriptions of Parkinson's-like symptoms can be found in several ancient texts such as the Old Testament (2000-440 BC), the Caraka Samhita on Ayurvedic medicine (~1000 BC), the Yellow Emperor Internal Classic on traditional Chinese medicine (425-221 BC), a papyrus from Egypt (1350 – 1200 BC), and the Akkadian Diagnostic Handbook from Mesopotamia (1069 – 1046 BC) to name a few (Li and Le, 2017; Raudino, 2012). People continued to record these descriptions into modern times, but the biological basis of the disease remained unclear. Finally, in 1817, James Parkinson published the first description of Parkinson's disease as a neurological disorder in a monograph titled "An Essay on the Shaking Palsy" (Li and Le, 2017; Parkinson, 2002). Over 50 years later, Jean-Martin Charcot and his students furthered our understanding of the disease. He recognized that there was a spectrum of symptoms, and that paralysis and tremor were not always present (Charcot 1872). Thus, he rejected the designation of the disease as a shaking palsy and was the first to suggest the name "Parkinson's disease" after James

Parkinson's seminal work (Goetz, 2011). Finally, in 1899, Édouard Brissaud suggested that Parkinson's originated from damage to the substantia nigra (Brissaud 1899).

Around the same time, our understanding of neurons and glia as the core units of the brain was just beginning to develop. The early characterization of neurons and glia came solely from morphological studies (Fan and Agid, 2018). Based on these studies, in 1856, Rudolf Virchow coined the term "Nervenkitt" or "neuroglia" and referred to glia as being the connective tissue that held neuronal elements together (Fan and Agid, 2018). The idea of glia being the "glue" that held the brain together persisted, and the lack of tools to examine the physiology of glial cells further stagnated their study. In contrast, the physiological study of neurons began to advance rapidly, and in 1868, Julius Bernstein recorded the first resting and action potentials from a neuron (Fan and Agid, 2018). However, based simply on the morphology of glial cells, Ramon y Cajal and others hypothesized roles for glia in synaptic transmission, sleep, learning and memory, attention, and cognition ((Fan and Agid, 2018).

Since then, our understanding of Parkinson's disease, neurons, and glia have grown exponentially. We now appreciate the many genetic factors, neuropathological features, and neurochemical process that are involved in Parkinson's disease. This growth in knowledge has advanced our therapeutic interventions, but despite these advancements, we still lack a "cure" for Parkinson's. In addition, much like our physiological understanding of glia trailed behind neurons, our understanding of glia in Parkinson's disease has trailed behind neurons as well. However, post-mortem morphological studies have shown that both neurons and glia are impacted in Parkinson's disease. Thus, this raises an important yet unanswered question: what is the role of glia in Parkinson's disease? Just as our understanding of the neuronal basis of

Parkinson's disease advanced our therapies, understanding how glial cells and other impacted cell types are affected in Parkinson's disease will be crucial for developing new interventions.

In my thesis, I use *C. elegans* models of Parkinson's disease to address the question of glial and non-neuronal roles in the degeneration of dopamine neurons and the clearance of neuronal corpses. In Chapter 1, I provide a brief introduction on the etiology and pathophysiology of Parkinson's disease. I next review the existing literature for the roles of glial, muscle, and epithelial cells in the nervous system. Finally, I provide background on genetic and toxin models of Parkinson's disease and the role of cell death and phagocytosis in *C. elegans.* In Chapters 2 and 3, I describe my thesis findings on how glia, muscle, and epithelial cells independently regulate dopamine neurodegeneration in *C. elegans* models of Parkinson's disease. Finally, in Chapter 4, I will discuss the importance and future directions of my findings.

1 PARKINSON'S DISEASE

Parkinson's disease (PD) is the second most common and fasting growing neurodegenerative disorder worldwide (Dorsey et al., 2018). The characteristic motor symptoms of PD – rigidity, tremor, loss of balance – are primarily caused by a loss of dopaminergic neurons in the substantia nigra pars compacta (Day and Mullin, 2021). Another characteristic of PD is the accumulation of Lewy bodies – abnormal aggregations of proteins composed mostly of α-synuclein – in both neurons and glial cells (Calabresi et al., 2023). However, degeneration is also seen in other brain regions and is not limited to dopaminergic neurons (Braak et al., 2003; Day and Mullin, 2021). This widespread degeneration is thought to drive the cognitive symptoms prevalent in PD such as anxiety, depression, lack of sleep, and loss of smell (Day and Mullin,

2021; Fullard et al., 2017). There is currently no cure for PD, and there are no available therapies to replace dopaminergic neurons that have degenerated. The current "gold standard" treatment for PD is supplementation with L-DOPA, a precursor for dopamine, to compensate for the reduced dopamine signaling; however, this treatment mostly targets the motor symptoms and can result in unpleasant side effects (Day and Mullin, 2021).

1.1 Pathogenesis of Parkinson's disease

The etiology of PD is thought to be complex and due to a combination of genetic and environmental risk factors with age being the largest risk factor (Day and Mullin, 2021). Less than 10% of PD patients have a familial history of the disease, while the rest of the cases are sporadic (Day and Mullin, 2021). Out of those familial cases, around 35% are due to a single gene mutation (Day and Mullin, 2021). In addition to the monogenic cases, there are also cases of toxin-induced PD such as the accidental ingestion of MPTP (Blum et al., 2001). Interestingly, there is substantial overlap in the clinical features present between familial and sporadic PD suggesting common mechanisms that drive the disease (Kouli et al., 2018). Indeed, two similarities between the sporadic and familial cases are the aggregation and spread of α-synuclein and the eventual degeneration of dopamine neurons in the substantia nigra. Thus, α-synuclein aggregation is thought to be central to the progression of the disease and causal to the degeneration of dopamine neurons. However, other mechanisms are thought to be involved. For example, apart from mutations in α-synuclein, the other monogenic forms of PD include mutations in Pink1, Parkin, DJ-1, and LRRK-2 to name a few (Calabresi et al., 2023; Day and Mullin, 2021; Rui et al., 2018). These genes impact several cellular processes such as mitochondrial health, oxidative stress responses, proteostasis, endolysosomal processing,

autophagy, and synaptic signaling (Kouli et al., 2018). Based on these studies, mitochondrial dysfunction and protein degradation dysfunction appear to be key for the pathogenesis of Parkinson's disease (Kouli et al., 2018). In addition, dopaminergic neurons in the substantia nigra appear to be particularly susceptible to mitochondrial and oxidative stressors (Haddad and Nakamura, 2015). How and why these dysfunctions drive the degeneration of dopamine neurons in the substantia nigra remains unclear. In addition, whether the degeneration is due to intrinsic features of these dopaminergic cells or due to extrinsic factors such as dysfunctions in neighboring cells is debated (Poewe et al., 2017). In fact, several PD-associated genes are also expressed in non-neuronal cells such as glia, epithelial cells, and muscle cells suggesting non-neural tissues may also be impacted in PD (Clairembault et al., 2015; Derkinderen, 2017; Gibbons et al., 2024; Tamo et al., 2007). Indeed, patients with PD also report increased sweating, constipation, muscle stiffness, muscle pain, and urinary issues (Dickson et al., 2009; Kouli et al., 2018). However, whether glial, epithelial, and muscle cells impact PD progression remains unclear. Thus, to better treat PD, we need to understand the cellular and molecular basis for the loss of dopamine neurons and how PD impacts or may be driven by non-neural tissues.

2 GLIAL CELLS IN NERVOUS SYSTEM HEALTH AND DISEASE

The nervous system comprises two major cell types, neurons and glia, whose close interactions are critical for neural development and functions (Allen and Eroglu, 2017; Khakh and Sofroniew, 2015; Purice et al., 2024; Singhvi et al., 2024). Glial cells are known to regulate various aspects of nervous system health such as ion homeostasis, synaptic transmission, trophic support, nutrient support, immune support, and structural support (Allen and Eroglu, 2017;

Khakh and Sofroniew, 2015; Purice et al., 2024; Singhvi et al., 2024). However, the molecular mechanisms underlying these roles have only recently been uncovered, and even less is known about glial roles in disease contexts.

2.1 Glial phagocytosis regulates nervous system health and development

One way that glial cells modulate the nervous system is through a process known as glial engulfment where glial cells phagocytose neurons and their processes (Raiders et al., 2021b). In the central nervous system (CNS), glia such as ectoderm-lineage derived astrocyte glia and mesoderm-lineage derived microglia can act as phagocytes (Allen and Eroglu, 2017; Reemst et al., 2016). During development, both astrocytes and microglia engulf pre- and post-synaptic elements of living neurons as well as excess apoptotic neurons generated during neurogenesis to modify neuronal circuits (Chung et al., 2024; Reemst et al., 2016). Astrocytes use engulfment receptors such as Draper/JED-1/MEGF10 and MERTK, while microglia use AXL, MERTK, TREM2, and the complement receptor CR3 to engulf neurons (Chung et al., 2013; Iram et al., 2016; Rueda-Carrasco et al., 2023; Tremblay et al., 2019a).

In addition to refining neuronal circuits, glia engulf neurons after injury to remove cellular debris. In *Drosophila*, astrocyte-like glia engulf axonal debris after nerve crush injuries using Draper, a MEGF10 ortholog (Purice et al., 2017). Cultured microglia can engulf axonal debris from laser-transected rat cortical axons (Neumann et al., 2009). In mice, astrocytes and microglia coordinate their efforts to engulf laser-ablated neurons using the MERTK receptor (Damisah et al., 2020). In this case, microglia migrate towards the apoptotic neurons and engulf the cell bodies and proximal dendrites. In contrast, astrocytes send out processes to engulf the distal debris (Damisah et al., 2020). In the absence of microglia, astrocytes could engulf the

apoptotic somas (Damisah et al., 2020). In summary, multiple glial cells use conserved phagocytic receptors to engulf both living and damaged or apoptotic neurons to regulate nervous system health and development.

2.2 Parkinson's disease and glial phagocytosis

The causal relationship between glial phagocytosis and PD remains unclear. Although microglia are known as the resident immune cells of the CNS, both astrocytes and microglia are inflammatory cells that regulate both innate and reactive immune responses in the CNS (Tremblay et al., 2019a). Both astrocytes and microglia can take on "reactive" states in response to neuronal stress or damage (Tremblay et al., 2019a). These "reactive" responses can alter the shape and function of both astrocytes and microglia to increase their phagocytic capacity (Tremblay et al., 2019a). Post-mortem brain analyses of PD patients identified "activated" microglia with phagocyte morphologies near the remaining dopamine neurons in the substantia nigra (Joers et al., 2017; Jyothi et al., 2015). Microglia also show reactive phenotypes in animal models of PD that use toxins such as 6-OHDA or MPTP (Barcia et al., 2013; Tremblay et al., 2019a). In mice, dopaminergic debris was found in microglia following MPTP treatment (Depboylu et al., 2012). In rats, dopaminergic debris was found in astrocytes following 6-OHDA treatment (Morales et al., 2017). The receptors used to engulf this debris remain unknown.

Recent studies have also shown that microglia and astrocytes can engulf α-synuclein, suggesting a protective role for glia in the clearance of α-synuclein (Gómez-Benito et al., 2020; Tremblay et al., 2019). However, extracellular aggregated α-synuclein can also inhibit phagocytosis in microglia (Tremblay et al., 2019). In addition, intracellular deposits of α-synuclein in astrocytes can disrupt lysosome function, mitochondrial homeostasis, and may be

transferred to other glia or neurons (Tremblay et al., 2019). Thus, engulfment of α-synuclein may prove detrimental to glial and neuronal health.

In addition, gain-of-function and loss-of-function mutations in other PD-associated genes can either enhance or inhibit microglial phagocytosis (Cabello et al., 2014; Tremblay et al., 2019; Xiong et al., 2017). Whether these effects on glial phagocytosis impact dopamine neuron health remain unclear. It has been proposed that glial phagocytosis can kill neurons in a process known as phagoptosis. Indeed, several *in vitro* studies found that exposing microglia to inflammatory molecules like lipopolysaccharide or amyloid-beta can drive phagocytosis of stressed but living neurons (Bodea et al., 2014; Brown and Neher, 2014). This phagoptosis was prevented by blocking phosphatidylserine exposure in neurons or by removing microglia altogether (Brown and Neher, 2014). Some evidence suggests glial phagocytosis as a mechanism that drives neurodegeneration in PD. In a PD mouse model that overexpressed α-synuclein in motor neurons in the spinal cord, knockdown of both MERTK and AXL increased the lifespan of the animal suggesting that these engulfment receptors were promoting the death of neurons (Fourgeaud et al., 2016). In several toxin models of PD, disrupting microglial phagocytosis prevented the loss and death of neurons (Tremblay et al., 2019a).

2.3 Glial regulation of synaptic transmission

Another major glial role is the regulation of synaptic transmission. Synaptic transmission is the process by which neurons release signaling molecules known as neurotransmitters to evoke a response in other neurons (Allen and Eroglu, 2017). Synaptic transmission occurs at structures known as chemical synapses where a pre-synaptic neuron releases neurotransmitters onto a receiving post-synaptic neuron (Allen and Eroglu, 2017). Astrocytes can send projections into

these synapses to form structures known as tripartite synapses (Chung et al., 2024). At tripartite synapses, astrocytes use transporters to help remove released neurotransmitters and regulate neurotransmitter diffusion to modify synaptic transmission (Chung et al., 2024). Astrocytes can express transporters for several neurotransmitters including dopamine and glutamate (Pajarillo et al., 2019; Zhao et al., 2023). Astrocytes can also release signaling molecules of their own into synapses to alter synaptic activity (Chung et al., 2024; de Ceglia et al., 2023). Microglia can also alter synaptic transmission by releasing cytokines and neurotrophic factors that alter synaptic receptors in neurons and glutamate release from astrocytes (Tremblay et al., 2019a).

2.4 Synaptic dysfunction in Parkinson's disease

Synaptic dysfunction and axonal degeneration are hypothesized to precede the degeneration of dopamine neurons in Parkinson's disease. Functional imagining and postmortem studies demonstrate a loss of dopamine transporter (DAT-1) and tyrosine hydroxylase (TH) in dopamine axon terminals that precedes and is greater than DAT-1 and TH loss in dopaminergic neuron cell bodies (Kordower et al., 2013). However, one postmortem study found an increase in the expression of the 2nd isoform of TH in surviving dopamine neurons (Shehadeh et al., 2019). Whether these changes to DAT-1 and TH cause dopaminergic degeneration or are effects of disease progression remain unclear. TH synthesizes L-DOPA which is the precursor to dopamine (Tabrez et al., 2012). While some studies have shown that L-DOPA treatment can be neuroprotective, others have shown that increased TH expression can drive dopamine neuron degeneration (Tabrez et al., 2012). In addition, dopamine itself can oxidize into reactive oxidative species, and dysregulation of dopamine storage and metabolism can drive oxidative

stress in dopamine neurons (Zhou et al., 2023). Thus, whether increased TH activity drives neurodegeneration in PD remains contentious.

Glutamatergic synapses in the striatum are also altered in PD (Gcwensa et al., 2021; Wang et al., 2020). Postmortem studies show a robust reduction in dendritic spine density onto GABAergic spiny projection neurons in the striatum (Villalba and Smith, 2018). Since these synapses are primarily glutamatergic these results suggest a reduction in glutamatergic synapses. In addition, loss of dopamine signaling can reduce glutamatergic synapses in the striatum (Gcwensa et al., 2021). However, functional imagining studies also found slight alterations in glutamate content that suggest increase glutamate signaling (Gröger et al., 2014; O'Gorman Tuura et al., 2018; Weingarten et al., 2015). Indeed, subsequent animal studies have also shown a reduction in glutamate transporter (GLT-1) expression and an increase in extracellular glutamate in both acute and genetic PD models (Iovino et al., 2020; Pajarillo et al., 2019; Wang et al., 2020). In addition, murine and invertebrate studies have shown that dysregulated and increased glutamate signaling onto dopamine neurons can drive dopamine neurodegeneration (Iovino et al., 2020). Finally, astrocytic downregulation of GLT-1 in the substantia nigra in mice induced progressive motor deficits and dopamine neuron loss (Beccano-Kelly et al., 2014). Thus, glutamate-induced excitotoxicity of dopamine neurons is hypothesized as a potential mechanism that drives dopaminergic degeneration in PD.

3 EPITHELIAL AND MUSCLE CELLS IN NERVOUS SYSTEM HEALTH AND DISEASE

Both neurons and glia in the nervous system interact with several epithelial and muscle tissues to regulate nervous system function and health (Alberts et al., 2002; Yu et al., 2020). In the CNS, these interactions occur primarily between glial cells and muscle cells. In the PNS, both peripheral nerves and glia are embedded in epithelial and muscle tissue. However, the cellular and molecular interactions between these many cell types are only recently being studied, and very little is known about their interactions in disease.

3.1 Epithelial roles in the nervous system

Currently, there are only two known epithelial cells in the CNS: ependymal cells that line the ventricles and central canal of the spinal cord, and Choroid Plexus Epithelial cells. Ependymal cells are specialized neuroepithelial cells that help produce and circulate cerebral spinal fluid (Bitanihirwe et al., 2022). Choroid plexus epithelial cells are also specialized epithelial cells that resemble glia and help maintain a barrier between CSF and the blood (Bitanihirwe et al., 2022). Although previously understudied, both of these cell types are now being appreciated for their potential roles in maintaining nervous system health (Bitanihirwe et al., 2022).

In the PNS, sensory epithelia such as olfactory epithelia, auditory epithelia, and retinal epithelia interact with neurons and glia to ensure proper neuronal function (Alberts et al., 2002; Bigdai and Samoilov, 2022). For example, in the retina, retinal pigment epithelial cells phagocytose photoreceptor outer segments, provide oxidative protection, and help maintain the

retinal blood brain barrier (Yang et al., 2021). The intestinal epithelium in the gastrointestinal (GI) tract also interacts closely with the enteric nervous system (Gulbransen and Sharkey, 2012; Walsh and Zemper, 2019). The bidirectional communication between enteric neurons, enteric glial cells, and enteric epithelial cells is important for maintaining epithelial barrier function and for connecting the enteric nervous system with the central nervous system (Dowling et al., 2022). Finally, skin-neuron-glia interactions in the PNS are also important for wound healing and pain sensation (Abdo et al., 2019; Parfejevs et al., 2018).

3.2 Muscle roles in the nervous system

In the CNS, both astrocytes and microglia interact with mast cells such as smooth muscle cells and pericytes in the vasculature that supplies blood to the brain to form the neurovascular unit/complex (Yu et al., 2020). Astrocytes extend specialized projections called end-feet that wrap around the vasculature in the brain to regulate the blood brain barrier, cerebral blood flow, nutrient uptake, and waste clearance (Abbott, 2002; Langen et al., 2019). Microglia also localize to capillaries in the brain and help to regulate vasculature tone (Bisht et al., 2021).

In the PNS, neuromuscular junctions (NMJs) are tripartite chemical synapses between motor neurons, muscle fibers, and peripheral glial cells known as perisynaptic Schwann cells or terminal Schwann cells (Alvarez-Suarez et al., 2020). Like astrocytes, perisynaptic Schwann cells regulate synaptic transmission, synapse formation and elimination, and debris clearance at NMJs (Alvarez-Suarez et al., 2020). Thus, both the central and peripheral nervous system interact with several muscle and epithelial cells to regulate nervous system health and function.

3.3 Epithelia and muscle in Parkinson's disease

Both epithelial and muscle cells in the CNS and PNS express PD-linked genes, are impacted early in disease, and have dopamine-driven functions. For example, in the retina, α-synuclein aggregations were found in the retinal pigment epithelium in post-mortem samples of PD patients (Veys et al., 2019). In addition, the progression of α-synuclein aggregation in the retina may be related to the level of aggregation in the brain (Veys et al., 2019). In fact, a recent study also suggests that the retina may be an initial site of α-synuclein aggregation that then spreads to the brain (Pérez-Acuña et al., 2023). The aggregation of α-synuclein in the retina is also thought to drive the vision impairments seen in many PD patients since L-DOPA treatment can temporarily alleviate their symptoms (Veys et al., 2019). Indeed, a recent study demonstrated that α-synuclein overexpression in adult mice caused dopaminergic amacrine cell death and vision impairments (Marrocco et al., 2020).

Olfactory dysfunction can also predate clinical diagnosis in PD patients, and the olfactory bulb is an early site of Lewy body pathology (Braak et al., 2003; Fullard et al., 2017; Martin-Lopez et al., 2023). Further, dopamine acts on olfactory sensory epithelia to regulate olfactory neuron maturation (Bigdai and Samoilov, 2022). Similarly, enteric nervous system neurons express dopamine, and GI motility and intestinal epithelial barrier functions are altered early in PD (Chalazonitis et al., 2022; Clairembault et al., 2015). Post-mortem samples also show aggregates of α-synuclein in several tissues in the GI tract, and these aggregates can both disrupt intestinal epithelial functions and spread from these tissues into the brain through the vagus nerve (Montanari et al., 2023).

Vascular endothelia also express some PD-genes, and meningeal dysfunction is thought to aggravate α-synuclein pathology (Ding et al., 2021; Tamo et al., 2007, 2002; Zou et al., 2019).

In addition, recent studies have identified α-synuclein deposits in the skin and suggest that skin biopsies may be a potential early diagnostic for identifying Parkinson's disease before the motor symptoms occur (Gibbons et al., 2024; Niemann et al., 2021). Finally, skeletal muscle impairment is reported in PD, and exercise-induced myokines can impede neurodegeneration (Kam et al., 2022; Murphy and Lynch, 2023).

4 MODELS TO STUDY PARKINSON'S DISEASE

There are several genetic and toxin-based animal models that have been established to study dopamine neurodegeneration in PD (Gómez-Benito et al., 2020; Schober, 2004; Xiong et al., 2017). Here I focus on two that are relevant to my thesis project: the 6-hydroxydopamine toxin model and the α-synuclein genetic model.

4.1 6-hydroxydopamine model of Parkinson's Disease

A well-established toxin model for PD is 6-hydroxydopamine (6-OHDA), a neurotoxic compound derived from dopamine which acts by inducing intracellular oxidative stress (Schober, 2004). 6-OHDA has been shown to interact with norepinephrine and dopamine and also accumulates selectively in both noradrenergic and noradrenergic neurons (Schober, 2004). 6-OHDA is structurally similar to both dopamine and norepinephrine, and it exhibits high affinity to the reuptake transporters of these neurotransmitters (Blum et al., 2001). Once it enters dopaminergic neurons through these transporters, 6-OHDA oxidizes to form reactive oxygen species (ROS) and inhibits complex I and IV of the mitochondrial electron transport chain (Schober, 2004). The production of ROS and the depletion of energy production is thought to

drive 6-OHDA-induced neurodegeneration (Glinka et al., 1997). Although 6-OHDA models of PD do well to recapitulate the degeneration of nigral dopamine neurons, they fail to demonstrate α-synuclein aggregation, another key characteristic of PD. Nonetheless, the cellular specificity of 6-OHDA makes it an important tool to examine dopamine neurodegeneration.

4.2 α-synuclein models of Parkinson's Disease

Given that in both sporadic and familial cases of PD exhibit α-synuclein aggregation, many studies have investigated its role in pathogenesis. To do so, several genetic models of α-synuclein overexpression and α-synuclein mutants have been studied (Calabresi et al., 2023; Gómez-Benito et al., 2020). A-synuclein is a small 14kDa protein expressed in neurons and glia (Gómez-Benito et al., 2020). Although its functions in normal physiological conditions are still not well understood, it is currently thought to regulate synaptic transmission, particularly dopamine neurotransmission, and aid in DNA repair (Calabresi et al., 2023). Under normal conditions, α-synuclein exists in an equilibrium between its monomeric form and as a tetramer (Lashuel et al., 2013). The disruption of this equilibrium and an increase in its monomeric form is thought to facilitate its aggregation into oligomers, protofibrils, and insoluble fibers that are found in Lewy bodies (Gómez-Benito et al., 2020). The oligomers and protofibrils are thought to be the main drivers of neurodegeneration (Delenclos et al., 2019; Gómez-Benito et al., 2020; Lashuel et al., 2013). Overexpression of α-synuclein and its variants in animal models recapitulates dopamine neuron degeneration and proteinaceous inclusions seen in PD (Gómez-Benito et al., 2020). Thus, α-synuclein overexpression models are an invaluable tool to study dopamine neurodegeneration in PD.

4.3 *C. elegans* as a model organism to study dopamine neuron degeneration

The *C. elegans* nervous system is comprised of 302 neurons and 56 glia (White et al., 1986). In addition, the animal is optically transparent, has an invariant life cycle, a fully mapped connectome, and a robust molecular and genetic toolkit allowing for *in vivo* cellular and molecular studies. The *C. elegans* hermaphrodite has eight dopamine neurons distributed amongst three mechanosensory sense-organs – 4 cephalic neurons (CEP), 2 anterior deirid neurons (ADE), and 2 posterior deirid neurons (PDE) (Nass et al., 2002; Sulston et al., 1975). These eight neurons mediate several locomotory behaviors including food-seeking and swimming behaviors (Sulston et al., 1975). In my studies, I focused on the four CEP neurons which are the bilateral CEP ventral and CEP dorsal pairs. Anatomically, CEP neurons are components of the cephalic sense organ along with the **cep**halic **sh**eath glia (**CEPsh**) and **cep**halic **so**cket glia (CEPso) (White et al., 1986). CEP neurons send dendritic projections anteriorly towards the nose tip of the animal. Here, the ciliated endings of the CEP neurons traverse through a channel formed by CEPsh glia and CEPso glia before embedding into the cuticle. CEP neuron axons terminate in the nerve ring, the neuropil of the animal, where they form synapses with several interneurons and chemosensory neurons. CEP axons are ensheathed by the CEPsh glial posterior sheath-like structure in the nerve ring (Chapter 2 Fig. 1 B). CEPsh glia exhibit astrocyte-like molecular signatures, regulate axon guidance in the embryo, and maintain dopamine and glutamate neurotransmitter balance in post-embryo adults (Gibson et al., 2018; Katz et al., 2018; McDonald et al., 2007; Purice et al., 2023; Yoshimura et al., 2008). In addition to contacting CEPsh and CEPso glia, CEPD somas contact mesoderm-lineage derived GLR glia and body wall muscle cells, while CEPV somas contact epithelia, and body wall muscle cells (Chapter 2 Fig. 1, A-A'', and B).

4.4 *C. elegans* and 6-OHDA model

After exposure to 6-OHDA, the 4 CEP neurons and 2 ADE neurons display blebbed processes, rounded cell bodies, and are eventually completely lost (Nass et al., 2002). As in other organisms, mutations in the dopamine transporter (DAT-1) inhibit 6-OHDA degeneration suggesting that 6-OHDA is taken up by DAT-1 into dopamine neurons (Nass et al., 2002). Chromatin condensation, a feature of apoptotic cell death, is evident; however, mutations in the classical apoptosis pathway do not prevent dopaminergic neurodegeneration (Nass et al., 2002). Surprisingly, features of necrotic cell death such as membranous whorls, swollen organelles or cell bodies are absent as well (Nass et al., 2002).

Using the 6-OHDA model in *C. elegans,* several studies have identified genes that confer protection and sensitivity to dopamine neurodegeneration (Masoudi et al., 2014; Offenburger et al., 2018a, 2018b; Schober, 2004). Like in other 6-OHDA models, the role of TH in dopamine degeneration in *C. elegans* is complex. On one hand, overexpression of the L-DOPA synthesis enzyme CAT-2/TH protects CEP neurons against 6-OHDA toxicity in *C. elegans* (Masoudi et al., 2014). However, in the absence of 6-OHDA exposure, overexpression of CAT-2/TH was shown to induce age-dependent dopaminergic cell death (Cao et al., 2005; Masoudi et al., 2014). Recently, a study found that loss of function mutations in phagocytic genes (*ced-2, ced-6, ced-10)* confers protection against 6-OHDA degeneration, suggesting a role for phagocytosis in the degeneration of dopamine neurons (Offenburger et al., 2018a). In addition, a single EM micrograph study indicated that degenerating CEP neurons could be eliminated and cleared after 6-OHDA treatment, possibly by GLR glial cells (Nass et al., 2002). However, the phagocytic receptor used to clear CEP neurons remains unknown.

4.5 *C. elegans* and α-synuclein model

Although *C. elegans* do not express orthologs to α-synuclein, overexpression of human α-synuclein has been an invaluable tool to examine α-synuclein aggregation and pathology (Gaeta et al., 2019; Gómez-Benito et al., 2020). Multi-copy expression of human α-synuclein in dopamine neurons in *C. elegans* has shown to induce progressive CEP neurodegeneration that worsens with age (Cao et al., 2005; Vozdek et al., 2022). Using this model, studies have identified several chemicals and genes that confer neuroprotection against α-synuclein toxicity and aggregation (Gaeta et al., 2019). These studies identified several molecules involved in autophagy, lysosomal function, trafficking, and G-protein signaling (Gaeta et al., 2019). Single-copy expression of α-synuclein has been used as well, but these transgenic animals do not show the same degree of degeneration as the multi-copy worms (Cooper et al., 2018). However, singly-copy expression in conjunction with loss-of-function mutations in PD familial genes worsened the degeneration of the CEP neurons (Cooper et al., 2018). In summary, human α-synuclein expression in *C. elegans* is a valuable tool to understand factors that regulate both neurodegeneration and aggregation.

5 CELL DEATH AND PHAGOCYTOSIS IN *C. ELEGANS*

There are several genetically programmed types of cell death (Yarychkivska et al., 2024). In addition, several mechanisms exist to remove cell corpses after programmed cell death (Wang and Yang, 2016). Much of our knowledge surrounding programmed cell death and phagocytosis emerged from studies in *C. elegans* (Hengartner and Robert Horvitz, 1994). Amazingly, these

mechanisms appear to be highly conserved across species (Yarychkivska et al., 2024). Here I review the molecular mechanisms underlying programmed cell death and phagocytosis in *C. elegans.*

5.1 Apoptotic cell death in *C. elegans*

Apoptosis and necrosis are two morphologically distinct types of cell death in *C. elegans*. Apoptosis is a genetically programmed type of cell death and characterized by cytoplasm compaction, cell shrinkage and rounding-up, nuclear fragmentation, chromatin condensation and plasma membrane blebbing (Yarychkivska et al., 2024). Apoptosis is mediated by a conserved caspase-dependent pathway, first described in *C. elegans* (Hengartner and Robert Horvitz, 1994). In the canonical apoptosis pathway, the Apaf-1 homolog CED-4 activates CED-3/caspase into an active protease (Yarychkivska et al., 2024). The pro-apoptotic function of CED-4/Apaf1 is inhibited by CED-9, a homolog of the mammalian BCL-2 (Yarychkivska et al., 2024). EGL-1/BH3-only promotes CED-3/caspase activation by interacting with CED-9/BCL-2 and inhibiting the anti-apoptotic CED-9/CED-4 complex formation (Yarychkivska et al., 2024). In *C. elegans,* apoptosis occurs in both somatic and germline cells during development (Yarychkivska et al., 2024).

5.2 Necrotic cell death in *C. elegans*

Necrosis was initially thought to be an alternative to apoptosis and was not regarded as genetically programmed. However, research suggests that necrosis is also tightly regulated by a conserved set of mechanisms (Nikoletopoulou and Tavernarakis, 2014). These mechanisms are mostly distinct from apoptosis, since necrotic-like deaths are not affected by mutations in

apoptotic genes (Reddien and Horvitz, 2004). In addition, necrotic cell death is morphologically distinct from apoptosis and is characterized by osmotic swelling of organelles, increased cell volume, and rupture of the plasma membrane (Nikoletopoulou and Tavernarakis, 2014). There are a few necrotic-like cell deaths during *C. elegans* development, but most necrotic cell deaths studied were evoked by environmental insults such as heat stress, hypoxia or hypo-osmotic shock, or by genetically encoded insults such as gain-of-function ion channels (Nikoletopoulou and Tavernarakis, 2014). Interestingly, the morphological and mechanistic features between necrotic cell death induced from gain-of-function ion channels in *C. elegans* and glutamatergic excitotoxic cell death in mammalian neurons appear to be conserved (Nikoletopoulou and Tavernarakis, 2014). In both cases, Ca2+ dysregulation is a key feature (Nikoletopoulou and Tavernarakis, 2014). In *C. elegans,* cytosolic Ca2+ levels may increase by influx through voltage-gated channels or by release from intracellular stores in the endoplasmic reticulum (Nikoletopoulou and Tavernarakis, 2014). Excessive cytoplasmic Ca2+ causes activation of Ca2+-dependent calpain proteases and lysosomal rupture, which in turn lead to the release of lysosomal cathepsin proteases, and the acidification of the cytoplasm (Danese et al., 2021; Zhivotovsky and Orrenius, 2011). Finally, both necrotic and apoptotic cells are engulfed and cleared by phagocytic cells (Nikoletopoulou and Tavernarakis, 2014; Yarychkivska et al., 2024).

5.3 Phagocytic clearance in *C. elegans*

The molecular mechanisms detailing cell corpse removal were first identified in *C. elegans* (Reddien and Horvitz, 2004). These mechanisms appear to be conserved across species (Ghose and Wehman, 2021). In *C. elegans*, phagocytic clearance of dead cells is important for tissue remodeling and the regulation of immune responses (Reddien and Horvitz, 2004). In

contrast to mammals, there are no specialized phagocytes in *C. elegans* (Ghose and Wehman, 2021). Instead, epithelial, muscle, intestinal, and pharyngeal cells take on phagocytic roles and engulf their dying neighboring cells (Reddien and Horvitz, 2004). Mechanistically, the process of engulfment begins with the presentation of the conserved "eat-me" signal, the phospholipid phosphatidylserine (PS), on the extracellular surface of apoptotic and necrotic cells (Nagata et al., 2016). Two partially redundant pathways in engulfing cells mediate the recognition of exposed PS (Conradt et al., 2016). In one pathway, the PS receptor PSR-1/JMJD6 or the integrin receptor INA-1 can bind to PS and signal through CED-2/CRKII, CED-5/DOCK180 and CED-12/ELMO, which in turn activate the small GTPase CED-10/Rac1 (Hsu and Wu, 2010; Yang et al., 2015). CED-10 activation leads to the reorganization of the actin cytoskeleton to form the phagocytic cup (Conradt et al., 2016). The Frizzled homolog MOM-5 can also act as an engulfment receptor and acts through the CED-2/5/12 pathway, but its ligand remains unknown (Cabello et al., 2010). In the second pathway, the phagocytic receptor CED-1/Draper/MEGF10 recognizes PS with the help of the two secreted proteins TTR-52 and NRF-5, as well as the ABC transporter CED-7/ABCA1 (Mapes et al., 2012; Zhang et al., 2012; Zhou et al., 2001). CED-1/MEGF10 transduces this signal through CED-6/GULP to activate DYN-1 and CED-10 (Yu et al., 2006; Zhou et al., 2001). In addition to the relay via TTR-52, CED-1 may also bind directly to PS (Li et al., 2015). In summary, two partially overlapping pathways regulate the clearance of apoptotic and necrotic cells in *C. elegans.*

In *C. elegans*, there are several mechanisms regulating extracellular phosphatidylserine (PS) exposure in apoptotic cells. Typically, PS is actively and asymmetrically maintained on the inner leaflet of the plasma membrane (Nagata et al., 2016). To act as an "eat-me" signal, PS needs to be translocated from the inner leaflet to the outer leaflet of the plasma membrane of the

dying cell (Eroglu and Derry, 2016). The aminophospholipid translocase TAT-1 actively maintains PS on the inner leaflet of the plasma (Darland-Ransom et al., 2008; Zullig et al., 2007). *tat-1* knockdown was reported to lead to abnormal PS exposure and the subsequent removal of living cells (Darland-Ransom et al., 2008). In addition, the phospholipid scramblase SCRM-1 translocates PS from the inner to the outer leaflet of the plasma membrane after being activated by the apoptosis-inducing factor (AIF) homologue WAH-1 (Wang et al., 2007). CED-8/Xkr8 also mediates PS exposure during apoptosis after being activated by caspase cleavage (Chen et al., 2013; Suzuki et al., 2013). In necrotic cells, Ca2+ influx activates the neuronal PS-scramblase and TMEM16F homologue ANOH-1, which mediates cell surface exposure of PS (Li et al., 2015). In addition, CED-7 also promotes PS exposure and removal of necrotic cells (Li et al., 2015). Lastly, CED-8 has a role in the removal of necrotic cells and was proposed to act redundantly with ANOH-1 (Li et al., 2015). Amazingly, these factors also appear to be conversed across species. To summarize, CED-7, CED-8, ANOH-1, SCRM-1, and TAT-1 are important for proper PS exposure in dying cells.

Chapter 2

Glia and CED-1/MEGF-10 independently drive dopamine neurodegeneration in Parkinson's disease models

German Rojas[1, 2, 3], Solomon Wossene[1], Sneha Ray[1], Irini Topalidou[1], Aakanksha Singhvi[1, 2, 3, *]

[1]Division of Basic Sciences, Fred Hutchinson Cancer Center, Seattle, WA 98109

[2]Graduate Program in Neuroscience, University of Washington, Seattle, WA 98195

[3]Department of Neurobiology and Biophysics, University of Washington School of Medicine, Seattle, WA 98195

*Lead Contact:

Email: asinghvi@fredhutch.org | Tel (206) 667-3606

ABSTRACT

Parkinson's Disease (PD) is marked by progressive dopamine neuron degeneration, but the phagocytic receptors and cells that clear dopamine neuron corpses are unknown. Further, while other cell types like glia, skin, and muscle are also impacted in PD, their roles in disease progression is unclear. We report that astrocyte-like CEPsh glia are neurotoxic in *C. elegans* PD models by regulating the neuronal dopamine biosynthesis enzyme CAT-2/tyrosine hydroxylase. We also identify epithelia and muscle as the phagocytes for dopamine neuron debris. They engulf by recognizing phosphatidylserine on necrotic-like neuron corpses via the conserved receptor CED-1/Draper/MEGF10and the ABC transporter CED-7/ABCA1. Loss of *ced-1* protects from loss of dopamine neurons and the impairment of associated animal behaviors. Thus, multiple non-neuronal cell-types independently dictate dopamine neurodegeneration. Evolutionary conservation of all underlying molecules identified, and their effect across PD models, implies that multi-organ engagement may impact neuron degeneration in Parkinson's disease broadly.

Key Words: Parkinson's disease, glia, neurodegeneration, engulfment, *C. elegans*, CED-1/MEGF10

INTRODUCTION

The nervous system comprises two major cell types, neurons and glia, whose close interactions are critical for neural development and functions (Allen and Eroglu, 2017; Khakh and Sofroniew, 2015; Purice et al., 2024; Singhvi et al., 2024). Glia of both the **c**entral and **p**eripheral **n**ervous **s**ystems (CNS/PNS) as well as free nerve-endings of the PNS also interact with non-neural cell types like muscle (e.g. endothelial vasculature in CNS; peripheral muscle at NMJ), and epithelia (e.g. choroid plexus, ependymal cells in CNS; skin or sensory epithelia in PNS) (Abbott, 2002; Derk et al., 2021; Gulbransen and Sharkey, 2012; Langen et al., 2019; Martin et al., 2024). How neurons interact with glia or non-neural cell types in health or disease is only recently starting to be explored at molecular and cellular resolution.

Parkinson's disease (PD) is the second most common and fastest growing neurodegenerative disorder worldwide (Dorsey et al., 2018; Poewe et al., 2017). Clinically, it is characterized by motor deficits, degeneration of CNS striatal dopamine neurons, and accumulation of Lewy bodies containing α-synuclein in neurons and glia (Damier et al., 1999; Dickson et al., 2009; Fearnley and Lees, 1991). Mechanistic evidence suggests oxidative stress and mitochondrial dysfunction drive dopamine neuron degeneration, associated in part with a growing list of PD-linked gene lesions (Chang and Chen, 2020; Day and Mullin, 2021; Dias et al., 2013).

Non-neuronal cells like glia also express PD-associated genes, and are impacted in PD as summarized below, but their contributions to PD progression is unclear (Zhang et al., 2022). In the CNS, multiple glia types including astrocytes and microglia exhibit altered properties in PD (Lee et al., 2021). Three major CNS glial functions may be at play. One, their regulation of

neurotransmitter release and diffusion may be impacted since the balance of neurotransmitters like dopamine and glutamate is altered in the striatum of rodent PD models (Barcomb and Ford, 2023; de Ceglia et al., 2023; Iovino et al., 2020; Zhao et al., 2023). Two, multiple glia can phagocytose neuronal debris in health, injury, or neurodegenerative states like in Alzheimer's disease (AD) models (Coutinho-Budd et al., 2024; Hong et al., 2016; Liu et al., 2022; Reemst et al., 2016; Rueda-Carrasco et al., 2023; Tremblay et al., 2019b; Zuchero and Barres, 2015). Mechanistically, some do so via opsonic receptors like CR3 and MEGF10/Draper (Raiders et al., 2021b). While recent studies suggest that astrocytes and microglia phagocytose dopamine neurons in PD models, the extent of this function or its molecular drivers in PD remain unknown (Morales et al., 2017; Vilalta and Brown, 2018). Three, studies have shown that glial responses to injury and oxidative stress have both protective and harmful effects on neurons (Lee et al., 2021). Whether any of these glial functions contribute to neurodegeneration or are a secondary response to neuronal defects remains to be determined.

Other non-neural cells of the PNS, such as epithelia and muscle, also express PD genes, are impacted early in disease, and have dopamine-driven functions. For example, olfactory dysfunction can predate clinical diagnosis in PD patients, and the olfactory bulb is an early site of Lewy body pathology (Braak et al., 2003; Fullard et al., 2017; Martin-Lopez et al., 2023). Further, dopamine acts on olfactory sensory epithelia to regulate olfactory neuron maturation (Bigdai and Samoilov, 2022). Similarly, enteric nervous system neurons express dopamine, and GI motility and intestinal epithelial barrier functions are altered early in PD (Chalazonitis et al., 2022; Clairembault et al., 2015). Vascular endothelia also express some PD-genes, and meningeal dysfunction is thought to aggravate α-synuclein pathology (Ding et al., 2021; Tamo et

al., 2007, 2002; Zou et al., 2019). Finally, skeletal muscle impairment is reported in PD, and exercise-induced myokines can impede neurodegeneration (Kam et al., 2022; Murphy and Lynch, 2023) However, if or how any of these cell-types impact disease etiology is unclear.

To systematically examine dopamine neurodegeneration with cell-type specificity and molecular resolution, we leveraged *C. elegans* as an experimental model. The *C. elegans* hermaphrodite (somatic female) has eight dopamine neurons distributed amongst three mechanosensory sense-organs that mediate food-seeking and swimming behaviors (Sulston et al., 1975). Four of these are the bilateral dorsal and ventral **cep**halic (**CEP**) neurons, CEPD and CEPV, respectively. These neurons are the best studied in *C. elegans* PD models. Similar to other animal systems, *C. elegans* PD models include neurotoxicity models using the canonical drugs 6-hydroxydopamine (6-OHDA) or 1-methyl-4-phenyl-1,2,3,6-tetrahydropyridine (MPTP), and genetic models bearing either mutations in PD-linked genes, or over-expressing PD genes such as human α-synuclein (Blum et al., 2001; Gaeta et al., 2019; Gómez-Benito et al., 2020; Hernandez-Baltazar et al., 2017; Nass et al., 2002; Schober, 2004). These models all exhibit degeneration of *C. elegans* dopamine neurons, with the CEP neurons being the most susceptible (Masoudi et al., 2014; Nass et al., 2002; Offenburger et al., 2018a, 2018b). EM studies indicate that degenerating CEP neurons are likely eliminated and cleared, at least after 6-OHDA (Nass et al., 2002). However, like in other species, the phagocytic cell and receptor for CEP remain to be identified in this context.

Anatomically, CEP neurons are components of the cephalic sense organ along with the **cep**halic **sh**eath glia (**CEPsh**) and **cep**halic **so**cket glia (CEPso) (White et al., 1986). CEPsh glia exhibit

astrocyte-like molecular signatures, regulate axon guidance in the embryo, and maintain dopamine and glutamate neurotransmitter balance in post-embryo adults (Gibson et al., 2018; Katz et al., 2018; McDonald et al., 2007; Purice et al., 2023; Yoshimura et al., 2008). While another astrocyte-like glia in *C. elegans* (AMsh glia) phagocytoses neuron fragments, this glial function has not yet been examined for CEPsh glia (Raiders et al., 2021a). CEPD neurons contact CEPsh glia, mesoderm-lineage derived GLR glia, and body wall muscle cells at their cell somas (Fig. 1, A-A', and B). CEPV neurons contact CEPsh glia, epithelia, and muscle cells at their cell somas (Fig. 1, A, A'', and B). CEP neuron axons and synapses terminate in the nerve ring, which is the "brain" neuropil of the animal, where they are ensheathed by the CEPsh glial posterior sheath-like structure (Fig. 1 B). The invariant and mapped cell-cell contacts in this experimental system, along with the powerful molecular-genetic toolkit of this animal model offers an unparalleled setting to definitively identify the molecular machinery and role of each individual cell-type in CEP neurodegeneration.

We report here that dopamine neurodegeneration has a multi-organ etiology in *C. elegans*, with different cell-types acting independently. Briefly, CEPsh glia are neurotoxic and drive CEP neurodegeneration by modulating dopamine levels through the rate-limiting biosynthesis enzyme CAT-2/tyrosine hydroxylase. Independently, adjacent muscle and epithelia phagocytose CEP neuron corpses via the phagocytosis receptor CED-1/MEGF10/Draper. They subcellularly recruit CED-1 around phosphatidylserine exposed by dying neuron corpses. Loss of *ced-1* protects animals against neurodegeneration and partially protects associated behavior defects. Conservation of all molecular players identified implies that analogous multi-tissue engagement may similarly cooperate to drive PD progression in other species.

RESULTS

CEPsh glia are neurotoxic in a 6-OHDA degeneration model

To monitor CEP neuron clearance quantitatively, we first evaluated two stable transgenic fluorescent reporter strains that label the dopaminergic CEP neurons with either GFP or mCherry (Bertrand and Hobert, 2009; Nass et al., 2002). We examined CEP clearance over 72 hours in these reporter strains after 50mM 6-OHDA exposure in larval stage L1 or L3 animals (Fig. 1 C). We found that CEP clearance occurs in two stages after 6-OHDA insult: normal CEP neurons (non-rounded) first adopt a button-like apoptotic corpse morphology by DIC and fluorescence imaging (rounded) before being cleared (missing) (Fig. 1, D and D'). In line with prior reports, we noted CEP neuron clearance as early as 12 hours in L1-treated animals (Fig. S1, A and B) (Masoudi et al., 2014; Nass et al., 2002; Offenburger et al., 2018a). Most CEP neurons were cleared by 72 hours in both L1- and L3-treated animals (Fig. 1 E and Fig. S1 A and B). Similar kinetics of both GFP and mCherry fluorophores indicated that CEP clearance was not biased by reporter transgene variance (Fig. S1, A and B). Thus, all subsequent experiments were done using 50mM 6-OHDA exposure to L3 animals in GFP-labeled animals and assayed at 24 or 72 hours, unless noted otherwise.

To examine if CEPsh glia impact CEP neurodegeneration, we first examined if CEPsh glia themselves are impacted by 6-OHDA exposure. We exposed transgenic animals expressing GFP under the CEPsh glia-specific *hlh-17* promoter to 6-OHDA (Yoshimura et al., 2008). 24h post-exposure, CEPsh glia exhibited GFP aggregates in their posterior sheaths, and this was resolved by 72 hours post-exposure when we observe maximal loss of CEP neurons (Fig. 1, F and G). Thus, cellularly, CEPsh glia monitor and react to CEP neuron stress after neurotoxic insult.

Next, we evaluated animals whose CEPsh glia were genetically ablated in post-embryo larva (Chelur and Chalfie, 2007; Katz et al., 2018). We reasoned this would avoid pleiotropic effect on CEP neurodevelopment, given CEPsh glia's roles in the animal's nerve ring ("brain" neuropil) assembly (Rapti et al., 2017; Wadsworth et al., 1996; Yoshimura et al., 2008). Glia ablation alone did not affect CEP neuron survival, implying it is dispensable for neuron trophic support (Fig. 1, H and I) (Yoshimura et al., 2008). However, we noted ectopic GFP reporter expression in two cells located ventrally which confounded conclusive identification of CEPV neurons (Fig. 1 H). So, we focused quantification on CEPD neurons. We found that their neurodegeneration was strongly suppressed in CEPsh glia-ablated animals with CEPD neurons maintaining "non-rounded" morphology after drug insult (Fig. 1 I). Thus, loss of CEPsh glia protects against CEP neuron death post 6-OHDA insult, implying their presence is required for the full neurotoxic effect of 6-OHDA.

To confirm this result in an orthogonal approach, we examined mutations in two genes that regulate CEPsh glia development, *mls-2* and *vab-3.* MLS-2 preferentially affects ventral CEPsh development, while VAB-3 preferentially regulates dorsal CEPsh development (Chisholm and Horvitz, 1995; Jiang et al., 2005; Yoshimura et al., 2008). Like the glia ablation strain, *vab-3(ot276)* mutants showed ectopic $P_{dat\text{-}1}$:GFP expression which precluded conclusive assessment of CEPV neurons in this strain. Nonetheless, as expected, *mls-2(ns329)* mutation preferentially protected CEPV neurons, while the *vab-3(ot276)* mutation protected CEPD neurons post 6-OHDA (Fig. 1 J). Thus, both dorsal and ventral CEPsh glia are required for the full neurotoxic effect of 6-OHDA on cognate CEP dopamine neurons.

Finally, we asked if CEPsh were neurotoxic only for 6-OHDA insult or across PD models. Loss of CEPsh glia also protected CEP neurons from degenerating against human α-synuclein over-expression in Day 6 aged animals (Fig. 1 K). Thus, CEPsh glial neurotoxicity is a general feature of CEP dopamine neuron degeneration.

The phagocytic receptor CED-1/MEGF10 regulates CEP neuron clearance

Core components of the apoptosis and the corpse engulfment pathways, discovered first in *C. elegans*, are implicated also in 6-OHDA mediated degeneration of CEP neurons (Conradt et al., 2016; Mapes et al., 2012; Offenburger et al., 2018a, 2018b; Wang et al., 2010, 2003; Zhou et al., 2001) (Fig. S1, C and D). However, neither the phagocytic receptor nor the phagocytic cell has been determined. Multiple astrocyte-like glial cells also repurpose this phagocytosis machinery to engulf neuron fragments across species, including *C. elegans*, and many of these cells act via the conserved phagocytic receptor CED-1/MEGF10/Draper (Chung et al., 2013; MacDonald et al., 2006; Zhou et al., 2001). Given that loss of CEPsh glia leads to neuron survival, we hypothesized that CEPsh glia phagocytose dying neurons, likely via the conserved receptor CED-1/MEGF10/Draper.

To test this, we examined two loss of function mutations in *ced-1* (Fig. S1 E). Like CEPsh glia ablation, both mutations exhibited dramatically reduced clearance of CEP neurons (Fig. 2 A). Remarkably, besides persistent cell corpses, we also noted a greater fraction of "normal" non-rounded CEP neurons suggesting a protection against degeneration. We also tested a loss of function mutation in *psr-1(tm469)* since some studies proposed PSR-1/JmJD6 as a second PS

receptor in apoptotic corpse phagocytosis (Raiders et al., 2021a; Wang et al., 2003; Yang et al., 2015). While *psr-1* mutants partially protected against degeneration, *psr-1;ced-1* double mutants did not enhance the clearance defects of *ced-1* single mutants (Fig. 2 A). Lastly, loss of *ced-1* also suppressed CEP degeneration in the *C. elegans* α-synuclein model (Fig. 2 B) (Vozdek et al., 2022b). Together, these results identify CED-1/MEGF10 as the major phagocytic receptor to facilitate both death and clearance of CEP neurons across PD models.

Epithelia and muscle, but not glia, phagocytose dying CEP neurons via CED-1

The similar phenotypes of CEPsh glia ablation and *ced-1* mutants in both models were consistent with CED-1 acting in glia. To test this, we first used RT-qPCR to examine *ced-1* mRNA transcript levels in CEPsh ablated animals. Loss of CEPsh glia showed a trend towards decreased *ced-1* expression, but it was not significant (Fig. S2 A). Next, we performed cell-specific rescue studies. We expressed CED-1 under a pan-glial promoter ($P_{mir\text{-}228}$) in animals mutant for *ced-1* and exposed these animals to 6-OHDA (Pierce et al., 2008; Purice et al., 2023). Surprisingly, this failed to rescue the *ced-1(1754)* mutant phenotype (Fig. S2 B). The only glia not covered by this promoter were the mesoderm lineage derived GLR glia, which had been proposed to engulf dying CEP neurons based on a single EM observation (Nass et al., 2002). However, expression of CED-1 under a GLR-specific promoter ($P_{nep\text{-}2s}$) also did not rescue the clearance defect of *ced-1(1754)* animals (Fig. S2 C) (Yamada et al., 2010). Thus, surprisingly, these data showed that neither CEPsh glia nor GLR glia phagocytose dying CEP neurons via CED-1/MEGF10.

To identify the phagocytic cell, we re-examined the animal's anatomy and noted that CEPV cell somas contact CEPsh glia and epithelial cells, while CEPD cell somas are physically adjacent to

CEPsh glial sheath processes, GLR dorsal glia, and dorsal body wall muscles (Fig. 1, A-A'') (White et al., 1986). We found that expressing CED-1 under a muscle-specific promoter (P_{myo-3}) rescued the clearance defects of CEPD but not CEPV neurons in *ced-1* mutant animals (Fig. 2 C). In contrast, expressing CED-1 under an epithelial-specific promoter (P_{dpy-7}) rescued the clearance defects of CEPV neurons but not CEPD neurons in *ced-1* mutants (Fig. 2 D) (Gilleard et al., 1997). Further, over-expression of CED-1 in epithelia but not muscle increased degeneration of both CEPD and CEPV neurons in WT animals (Fig. 2, C and D). Thus, CED-1/MEGF10 is necessary and sufficient in muscle and epithelia to engulf nearby dying CEP neurons, and epithelial CED-1 levels are rate-limiting for CEP neurodegeneration.

This result implied that these cell types endogenously express CED-1. To probe this, we leveraged the split-GFP system (Goudeau et al., 2021). Briefly, we expressed two GFP fragments under either a cell type-specific or the *ced-1* promoter, reasoning that GFP fluorescence will reconstitute only if both fragments express together in one cell. By this assay, we observed GFP reconstitution in both epithelia and muscle when the respective cell type promoter was used (Fig. S2, D and E). Thus, both epithelia and muscle express *ced-1*.

Finally, we performed cell-specific real-time imaging to conclusively visualize if muscle or epithelia engulf dying CEP neurons. We examined wild type transgenic animals with their muscle or epithelia labeled with a cytosolic mKate2 reporter and CEP neurons with a transcriptional GFP reporter. First, as expected from EM, epithelia were physically adjacent to CEPV neurons, and body wall muscle was adjacent to CEPD neurons (Fig. 2, E-F). 24h after 6-OHDA exposure, we found rounded CEPD neurons within the body wall muscle and rounded

CEPV neurons within the epithelia, as expected (Fig. 2, E-F). Thus, muscle and epithelia phagocytose dying CEPD or CEPV neurons, respectively, through CED-1/MEGF10.

CED-1 recruitment, not expression, drives CEP degeneration

If CED-1 is the phagocytic receptor, it should localize to dying CEP soma. To probe this, we generated a double-transgenic animal strain with GFP labeled CED-1 expressed under the *ced-1* promoter and mCherry labeled CEP neurons We subjected these animals to our 6-OHDA treatment paradigm (Bertrand and Hobert, 2009; Zou et al., 2009). 24h after 6-OHDA exposure, we observed CED-1:GFP enrichment around rounded CEP somas (n=19/22) but not around non-rounded CEP somas (n=1/24) (Fig. 3 A). Thus, CED-1 is recruited around degenerating CEP neurons after 6-OHDA exposure.

This recruitment could be due to increased *ced-1* transcript or protein levels, or subcellular re-localization. We performed RT-qPCR in wild type N2 animals 24 hours after 6-OHDA exposure when significant engulfment is seen and found no significant change in *ced-1* transcript levels (Fig. 3 B). This argued against transcriptional upregulation of *ced-1* in response to 6-OHDA. CED-1 protein levels can be regulated by ubiquitin-mediated degradation, so we examined CED-1 protein levels (Yuan et al., 2022). However, western-blot analyses of CED-1:GFP transgenic animals exposed to 6-OHDA revealed no significant change in CED-1:GFP protein levels at either 24h or 40h post 6-OHDA exposure compared to non-exposed control animals (Fig. S2, F and G). These results, taken together with our in vivo localization results, lead us to infer that muscle and epithelial CED-1 is sub-cellularly recruited to the plasma membrane contacting degenerating CEP neurons, rather than being regulated at transcript or protein levels.

Necrotic-like PS exposure drives CEP degeneration

C. elegans CED-1 as well as its orthologs in *Drosophila* (Draper) and mammals (MEGF10) bind the phospholipid phosphatidylserine (PS) exposed on the surface of apoptotic cells as an "eat-me signal" (Iram et al., 2016; Li et al., 2015; MacDonald et al., 2006; Wang et al., 2010). To test if this was also true for dying CEP neurons, we generated transgenic animals expressing the PS-binding protein, secreted Annexin V (sAnxV),under the epithelial (P_{dpy-7}) promoter and examined CEP neuron corpses 24h after 6-OHDA exposure. We found that sAnxV marked rounded (dying) CEP neurons (n=8/28 CEPs with sAnxV enrichment) but not non-rounded (living) ones (n=1/30 CEPs with sAnxV enrichment) (Fig. 3 C). Thus, dying CEP neurons expose PS, which could sub-cellularly recruit CED-1 in phagocytic muscle/epithelia.

This result implied that other regulators of PS asymmetry should also impact CEP clearance. First, we probed mutations in the ATP-binding flippase TAT-1/ATP8A which maintains PS asymmetrically on the membrane inner leaflet (Darland-Ransom et al., 2008). Mutations in *tat-1* cause aberrant PS exposure on the outer leaflet , but this alone was insufficient to trigger CEP death or clearance (Fig. 3 D) (Chen et al., 2019; Darland-Ransom et al., 2008). However, *tat-1* mutants exhibited enhanced CEP degeneration after 6-OHDA exposure indicating that PS exposure in context of neurotoxic insult triggers clearance (Fig. 3 D). Next, CED-1 can bind PS either directly, or via opsonins like *C. elegans* TTR-52/Transthyretin (Mapes et al., 2012; Wang et al., 2010). Mutations in *ttr-52(tm2098)* animals exhibited reduced CEP degeneration after 6-OHDA treatment, albeit weaker than *ced-1*, revealing a minor role for TTR-52 in this process (Fig. 3 E).Next, we noted that PS exposure is executed via overlapping but distinct mechanisms in apoptosis and necrosis. Both pathways deploy the CED-7/ABCA1 transporter to aid PS-

exposure (Furuta et al., 2021; Li et al., 2015; Mapes et al., 2012). In contrast, the scramblase CED-8/Xkr8 is predominantly used by apoptotic cells to expose PS, while ANOH-1/TMEM16/Chloride channel is primarily used by necrotic cells to expose PS (Furuta et al., 2021). We found that *ced-7(n2094)* mutant animals exhibited reduced CEP degeneration and persistent rounded CEP neurons like *ced-1* mutants (Fig. 3 E). Unlike *ced-1* however, the persistent cells in *ced-7* mutants were "swollen", and resembled necrotic corpses (Fig. 3 F). Loss of *ced-8* had no effect on CEP degeneration, but loss of *anoh-1* reduced the degeneration of CEP neurons at 24h after 6-OHDA exposure, although this did not persist to 72 hours (Fig. 3 G). Taken together, we favor the conclusion that CEP degeneration occurs by a necrotic-like pathway, where PS-exposure via TAT-1/ATP8A, ANOH-1/TMEM16A, CED-7/ABCA1and TTR-52/Transthyretin drives engulfment by the rate-limiting CED-1/MEGF10.

Impact of CED-1 loss on dopamine neuron functions and downstream neural circuits

The "normal" CEP neurons in *ced-1* mutants led us to wonder how CEP degeneration impacts downstream circuit partners and functions. The mapped and invariant connectome in this animal indicated that CEP neurons are synaptic partners to twenty neurons (Cook et al., 2019; Sulston et al., 1983; White et al., 1986), of which we curated three for further analyses: RIC (post-synaptic to CEP), OLQ (gap junction to CEP) and OLL (gap-junction and pre-synaptic to CEP) (Fig. 4 A).We found no cell loss of any of these neurons in Day 3 adult animals 96 hours post-6-OHDA in either wild type animals (most CEP are eliminated at this stage) or in *ced-1* mutant animals with persistent corpses (Fig. 4 B). Thus, loss or persistence of CEP neurons post 6-OHDA does not alter survival of these cells in the circuit.

We next examined dopamine circuit function through two CEP-driven animal behaviors: **sw**imming **i**nduced **p**aralysis (SWIP) and **b**asal **s**lowing **r**esponse (BSR). In SWIP, animals swimming in water accumulate excess synaptic dopamine which triggers inhibitory cholinergic neurons and leads to muscle paralysis (McDonald et al., 2007). In a modified assay that tests for synaptic dopamine clearance, called DA-SWIP, exogenous dopamine is added to swimming animals to track the kinetics of paralysis in animals with impaired dopamine clearance (Clark et al., 2024). WT animals treated with 6-OHDA showed increased paralysis compared to non-treated controls in this assay suggesting reduced clearance of synaptic dopamine (Fig. 4, C and D)(Clark et al., 2024). In contrast, while initially paralyzed, *ced-1* mutant animals treated with 6-OHDA were better able to maintain synaptic dopamine clearance at extended time points (dark gray versus dark magenta, Fig. 4, C and D). BSR reports on mechanosensory function of dopamine neurons by monitoring how fed animals reduce their body bend frequency upon encountering the mechanosensory stimulus of a bacterial "food" lawn (Sawin et al., 2000). We found that WT and *ced-1* mutant animals exhibited normal BSR, while the positive control *cat-2* mutants (low dopamine) were defective as reported (Fig. 4 E) (Chase et al., 2004). After 6-OHDA exposure, both wild type animals and *ced-1* mutants exhibited defective BSR, consistent with loss of mechanosensation (Fig. 4 E). Thus, blocking dopamine neurodegeneration post 6-OHDA via *ced-1* mutants can reverse animal behavior defects regulated by synaptic dopamine levels but not those that rely on CEP's mechanosensory function.

CEPsh glia neurotoxicity is due to altered dopamine levels

While our studies above identified CED-1 as the phagocytic receptor in muscles and epithelia,

this left open the question of how CEPsh glia loss is neuroprotective (Fig. 1 J). CEPsh glia regulate levels of the neurotransmitter glutamate, and glutamate excitotoxicity is a feature of PD (Gibson et al., 2018; White et al., 1986). So, we first asked if the observed neuroprotection is impacted by impaired glutamate clearance. Prior work showed that CEPsh glia express the glutamate transporter GLT-1/EAAT2/SLC1A2 and loss of either the glia or *glt-1* causes glutamate spillover (Katz et al., 2019). We noted no CEP neuron loss in *glt-1* mutant animals indicating that excess glutamate is not innately neurotoxic. Further, rather than phenocopy the glia-ablations, *glt-1* mutant animals instead showed increased CEP neurodegeneration (Fig. S3 A). Loss of a second glutamate transporter *glt-3* did not further enhance *glt-1* mutant defects (Fig. S3 A). Finally, by RT-qPCR, CEPsh glia-ablated animals had higher *glt-1* transcript levels and not less, and no change in *glt-3* transcript levels (Fig. S3, B-C). We inferred this increase as compensatory up-regulation in non-glial cells where GLT-1 is also expressed. Further, wild-type animals showed no change in *glt-1* or glt-3 levels 24hr after 6-OHDA (Fig. S3, D-E). Taken together, we concluded that at least loss of GLT-1 from glia and resulting glutamate spillover is not the reason why loss of CEPsh glia is neuroprotective for CEP neurons.

In behavior studies, we had found that CEPsh glia-ablated animals exhibited SWIP like *dat-1* mutants, suggestive of elevated dopamine levels (Fig. 5, A and B). So, we asked if altered dopamine levels were causal to CEPsh glia effects by testing three conserved factors. Dopamine biosynthesis requires CAT-2/tyrosine hydroxylase, a rate-limiting enzyme that converts tyrosine to L-DOPA (Fig. 5 C) (Nass and Blakely, 2003). It is then packaged into synaptic vesicles by the vesicular monoamine transporter CAT-1/VMAT/SLC18A2 and cleared by the transporter DAT-1/SLC6A3 (Fig. 5 C) (Nass and Blakely, 2003). By RT-qPCR, we observed reduced transcript

levels of *cat-1*, no change for *dat-1*, and a trend toward 2-fold increase for *cat-2* (Fig. 5, D-F).

To test these as mechanistic possibilities, we first examined and found that CAT-1:GFP was diminished in CEP neurons of glia-ablated animals, corroborating the RT-qPCR (Fig. 5 G). However, *cat-1* mutant animals did not phenocopy CEPsh glia-ablation and instead showed increased degeneration, implying that reduced dopamine release was unlikely the causal mechanism (Fig. 5 H). Strikingly, loss of *cat-2* strongly suppressed the protection of glia-ablated animals, while over-expression of CAT-2 blocked CEP neurodegeneration as previously reported (Fig. 5 I and Fig. S3 F) (Masoudi et al., 2014). Importantly, SWIP behavior defects of CEPsh glia-ablated animals were also suppressed by mutations in *cat-2* (Fig. 5, A and B). Thus, taken together, these results reveal that CEPsh glia ablated animals have increased CAT-2/TH levels and thereby presumably L-DOPA/dopamine levels. This impairs dopamine-driven behaviors but protects the animals against 6-OHDA insult.

DISCUSSION

This study uncovers that multiple heterologous cell-types - glia, epithelia and muscle - modulate dopamine neurodegeneration across PD models. They each do so through distinct molecular mechanisms, with impact on associated dopamine-driven animal behavior.

Epithelia and muscle impact PD neurodegeneration

While PD has broad CNS and PNS involvement, and PD genes can be broadly expressed, roles of non-neuronal cells remain underexplored in PD. Our studies reveal epithelia and muscle as phagocytes for degenerating CEP neurons. While not yet implicated in PD, both cell types can

act as phagocytes in other contexts: both epithelia and muscle engulf axon debris post-injury and developmentally apoptotic cells in *C. elegans* (Chiu et al., 2018; Hsieh et al., 2012; Nichols et al., 2016; Reddien and Horvitz, 2004b); *Drosophila* muscle engulf presynaptic debris at the NMJ (Fuentes-Medel et al., 2009); and zebrafish skin Langerhans cells engulf axon debris (Peterman et al., 2023). In PD, skin epithelial α-synuclein levels are used as diagnostic biomarkers, and clinical and animal model studies show skeletal muscle atrophy and increased intramuscular α-synuclein (Gibbons et al., 2024; Yang et al., 2023). How either cell type accumulates α-synuclein or how this impacts PD progression in human patient context awaits inquiry.

CED-1/MEGF10 regulates neurodegeneration and corpse clearance in PD models

CED-1 orthologs Draper and MEGF10 engulf Aβ in Alzheimer's models in flies and cell culture and regulate glial pruning in development (Chung et al., 2013; Hong et al., 2016; Ray et al., 2017; Singh et al., 2010). However, phagocytic receptors that clear degenerating dopamine neurons in Parkinson's disease had not been identified (Tremblay et al., 2019). Our studies reveal the conserved CED-1/MEGF10/Draper as the phagocytic receptor in both 6-OHDA and α-synuclein *C .elegans* models of PD. Loss of *ced-1* blocks dopamine neurodegeneration after neurotoxic insult and protects some dopamine-driven animal behaviors. Our results also indicate that CED-1 driven phagocytosis may exacerbate neuron death by "assisted" suicide. While such a mechanism is not yet reported for PD to our knowledge, this is reminiscent of developmental apoptosis in *C. elegans* where engulfment similarly aids cell death (Hoeppner et al., 2001; Johnsen and Horvitz, 2016; Reddien et al., 2001).

How might CED-1 act? In innate immune signaling, *ced-1* loss can both protect animals against

pathogenic bacteria via PMK-1/MPK-1 signaling or enhance infection by downregulating the unfolded protein response (Haskins et al., 2008; Wan et al., 2021). CED-1 also has separable roles in axon debris clearance and regeneration (Chiu et al., 2018). Given these, we posit a two-step mechanism of action: CED-1 is first recruited by rate-limiting PS. Subsequent downstream signaling aids both the clearance of CEP corpses via engulfment and the facilitation of neuron-death by a separate unidentified pathway.

Our finding that over-expressing CED-1 exacerbates CEP degeneration implies it is tightly regulated in phagocytic cells. While Draper can transcriptionally self-regulate and CED-1 can be post-translationally regulated by ubiquitin-dependent degradation, our results suggest that CED-1 clustering around dying neurons with exposed PS may be the relevant step in our PD model contexts (Doherty et al., 2014; Lu et al., 2017; Yuan et al., 2022). Investigating how cells localize CED-1/MEGF10 will be an exciting avenue of future inquiry.

Our studies also identify roles for CED-7/ABCA1 transporter and ANOH-1/TMEM16F. This suggests a necrosis mode of PS-exposure consistent with prior studies that showed that caspases are irrelevant in CEP death in PD models (Nass et al., 2002). While ABCA1 is not yet directly implicated in human PD by GWAS, an AI-based drug repurposing screen identified an ABCA1 antagonist as a candidate blocker of PD pathology in a cell culture assay (Moskal et al., 2023). Independently, a missense mutation with enhanced TMEM16F scramblase function was identified in an Ashkenazi Jewish PD population, and TMEM16F lesions in cell culture exhibit reduced PS and α-synuclein spread (Cohen-Adiv et al., 2024). Thus, a potential model could be that ANOH-1-dependent PS exposure recruits CED-1 to trigger engulfment, thereby driving

spread of α-synuclein into the phagocytic cell.

Glial control of activity and degeneration of dopamine neurons

We found that *C. elegans* astrocyte-like CEPsh glia actively react to CEP neuron stress post 6-OHDA insult. They also regulate dopamine levels, primarily via the rate-limiting CAT-2/tyrosine hydroxylase, which impairs dopamine-related behavior but protects against neurotoxic insult. This provides mechanistic insight into how astrocyte-like glia respond to neurotoxic insult. In humans, both L-DOPA and glutamate modulation are therapeutic approaches, and glutamate imbalance can cause neurotoxicity in striatal neurons in PD, although roles for either neurotransmitter as protective versus toxic remains contentious (Lipski et al., 2011; Tambasco et al., 2018; Zhang et al., 2020, 2019a). Our results on a single glial cell reveal two mechanisms contributing to a multifaceted glial response (*glt-1* vs *cat-2)*, which may explain the challenge in understanding glial functions in PD in systems where reproducible single-cell and temporal resolution analyses are technically limiting. In summary, our findings provide a molecular and cellular framework to definitively tease apart contributions of glia, epithelia, and muscle cells in the degeneration and clearance of dopamine neurons in PD models.

ACKNOWLEDGEMENTS

We thank Lei Yuan and Hui Xiao for CED-1 western blot protocols; Zhen Zhou for plasmid pZZ615 ($P_{ced\text{-}1}$:NLS:GFP); and Nzinga Hendricks for help with generating reagents. We thank the Singhvi lab and Jihong Bai for discussions and comments. This work was supported in part by a grant to Fred Hutchinson Cancer Center and University of Washington from the Howard Hughes Medical Institute through the James H. Gilliam Fellowships for Advanced Study program (GT13626) to GR and AS. It was also supported by an NIH T32 Alzheimer's Disease Training Program Grant (5 T32 AG 52354-8) and a PHS Ruth L. Kirschstein National Research Service Award (5 T32 NS 099578-04) to GR. It was supported by a Simons Foundation/SFARI grant (488574), Esther A. & Joseph Klingenstein Fund and the Simons Foundation Award in Neuroscience (488574), Brain Research Foundation Seed Grant (BRFSG-2023-10), and NIH/NINDS funding (NS114222) to AS. This work was performed while AS was a Glenn Foundation for Medical Research and AFAR Junior Faculty Grant Awardee. AS thanks Fred Hutch Evergreen Funds and philanthropic donors for their generous support of the laboratory research program. Some work was performed at the Fred Hutch Shared Resources Core Facilities. Some strains were sourced from the CGC, funded by NIH 774 Office of Research Infrastructure Programs (P40 OD010440) and the International *C. elegans* 775 Gene Knockout Consortium (*C. elegans* Gene Knockout Facility at the Oklahoma Medical 776 Research Foundation, funded by the National Institutes of Health; and the *C. elegans* Reverse 777 Genetics Core Facility at the University of British Columbia, funded by the Canadian Institute for 778 Health Research, Genome Canada, Genome BC, the Michael Smith Foundation, and the National 779 Institutes of Health).

AUTHOR CONTRIBUTIONS

AS and GR conceptualized all experiments and co-write the manuscript. GR performed and analyzed all experiments except Western blots. SW and GR designed, performed, and analyzed SWIP and SWIP-DA experiments. SR designed, performed, and analyzed the western blot experiments. IT prepared strains and helped troubleshoot the BSR and western blot experiments.

MAIN FIGURE LEGENDS

Figure 1. Loss of CEPsh glia protects CEP dopamine neuron degeneration in PD models

(A-A'') Schematic showing anatomical positions of CEP neurons (CEPD and CEPV), CEPsh glia, GLR glia, body wall muscle, and epithelial cells in the head. **(A'-A'')** EM showing the positioning of dorsal CEP neuron somas, a GLRDR glial cell, dorsal body wall muscles, and dorsal epithelial cells; and ventral CEP neuron somas, ventral CEPsh glial cells, ventral body wall muscles, and ventral epithelial cells. Image source: N2T [MRC] N2T_1646 in *WormImage.* https://www.wormimage.org **(A')** and SW-Worm Viewer, Slice No. (85). 2024. Altun, Z.F., Crocker, C. and Hall, D.H. In *WormAtlas*. https://www.wormatlas.org/slidableworm.html) **(A'')**. **(B-B')** Micrograph (B) and schematic (B') of cell bodies of CEPD and CEPV neurons, and CEPshD and CEPshV glia in *nsIs105;otIs181* animals. Scale bar = 5µm. **(C)** Schematic of assay protocol, detailed in Methods. **(D)** Image of GFP-labeled dopaminergic CEP neurons of 50mM 6-OHDA or control treated *vtIs1* animals. White lines, CEPV and CEPD neurons. Scale bars, 3µm. **(D')** Single z-slice images of CEP neurons from **(D)** after control treatment (0) or after 6-OHDA treatment that appear (1) non-rounded, (2) rounded, or (3) missing. Scale bar, 1µm. **(E)** Quantification of CEP degeneration/clearance at time points noted (x-axis) and percent neurons (y-axis). Bar shades denote non-rounded cells (white), rounded (light gray), or missing (dark gray). 3+ biological replicates, 14-26 animals/replicate. Total n = 69-106 animals/timepoint. **(F)** Image of CEPsh glia in *nsIs105* animals 24 hours after control or 50mM 6-OHDA treatment. Dotted lines, CEPsh glia soma. Arrows, GFP aggregation in glia. **(G)** % CEPsh glia cells with GFP aggregates 24 and 72 hours after control or 6-OHDA treatment, n = 29-43 cells and 9-10 animals/condition. **(H)** Image of CEP neurons from L3 animals in *vtIs1* (WT) or *nsIs180;vtIs1* (CEPsh ablated) strains. White lines and numbers, labeled cell-soma around the brain neuropil.

Scale bars, 5µm. **(I)** CEPD neurons 72 hours after 50mM 6-OHDA in *vtIs1* (WT) or *nsIs180;vtIs1* (CEPsh ablated) animals, and CEPD neurons 72 hours after a control treatment in CEPsh ablated animals. 3 biological replicates, 21-26 animals/replicate. Total n = 68-77 animals/condition. **(J)** CEP neurons 72 hours after 50mM 6-OHDA treatment in WT*, mls-2(ns329)*, and *vab-3(ot276)* mutant animals in the *vtIs1* background. 4 biological replicates for wild type, 2 biological replicates for *mls*-2 and *vab-3* mutants, each with 26 animals/replicate. Total n = 52-104 animals **(K)** CEP neurons in Day 6 adults in WT or CEPsh ablated backgrounds overexpressing human α-synuclein in dopaminergic neurons (*erIs1).* 2-3 biological replicates, 5-10 animals/replicate. Total n = 28 for WT and 12 for CEPsh ablated animals. **(B, D, F, H)** Top = anterior of animal. Images are 60x magnification with max-z projection unless noted. Statistics for all graphs, unless noted otherwise: error bars = 95% confidence interval, n.s. $p>0.05$, *$p<0.05$, **$p<0.01$, ***$p<0.001$, ****$p<0.0001$ (Fisher's exact test).

Figure 1
Rojas et al., 2025

A
A'
A''
B
C
D
D'
E
F
G
H
I
J
K
Cuticle
Epithelia
Muscle
CEP neuron
CEPsh glia
GLR glia
A
D
V
P
L
R
Dorsal side
Ventral side
BwDL muscles
CEPDL
Epithelia
CEPDR
GLR DR
BwDR muscles
BwVL muscles
CEPshVL
CEPVL
Epithelia
CEPVR
CEPshVR
BwVR muscles
CEPshD
CEPV
CEPshV
CEPD
Filter synchronization
6-OHDA treatment
CEP neuron scoring
+0h
+24h
+48h
+72h
Control (+24h)
6-OHDA (+24h)
0
1
2
3
Control
Non-rounded
Rounded
Missing
CEP neurons with phenotype
100%
80%
60%
40%
20%
0%
Non-rounded
Rounded
Missing
+24h
+48h
+72h
+72h control
CEPsh glia
CEPsh glia with GFP aggregates
control
6-OHDA
**
p = 0.057
WT
CEPsh Ablated
CEPV?
4
5
6
****
CEPD neurons with phenotype
CEPsh glia:
6-OHDA:
p = 0.32
p = 0.18
CEPD
CEPV
WT
mls-2(n329)
vab-3(ot276)
P_{dat-1}:a-syn:
Day 6 Adults

Figure 2. CED-1 in muscle and epithelia drives degeneration and clearance of CEP neurons

(A, C, D) Quantification and statistics as in Fig. 1 E. **(A)** CEP neurons 72 hours after 50mM 6-OHDA in genotypes noted with *vtIs1* reporter. Total n = 66-78 animals/condition. **(B)** CEP neuron degeneration quantified in genotypes noted, plotted as Fig. 1 K. Same wild type data as Fig. 1K. Total n = 28 for WT and 31 for *ced-1* animals. **(C-D)** Effect of P_{myo-3}:CED-1 (C) or P_{dpy-7}:CED-1 (D) extrachromosomal array on CEPD and CEPV neurons 72 hours after 50mM 6-OHDA in WT and *ced-1(e1754)* animals with *vtIs1* reporter transgene. Total n = 70-78 animals/condition. **(E-F)** z-projection image of [P_{myo-3}:CED-1:SL2:mKate2]; *vtIs1* (E) or [P_{dpy-7}:CED-1:SL2:mKate2]; *vtIs1* (F) 24h after 6-OHDA or control treatment, as noted. Top, anterior of animal. CEP neurons, magenta (E, F); muscle, green (E); epithelia, gray (F). Scale bar, 10µm (40x magnification, single z-section). **(E'-F')** CEP neurons (magenta) either non-rounded (control treatment) or rounded (6-OHDA treatment) engulfed by dorsal body wall muscle (green, E') or ventral epithelia (gray, F'), as noted. Scale bars, 1µm (40x, single z-section).

A

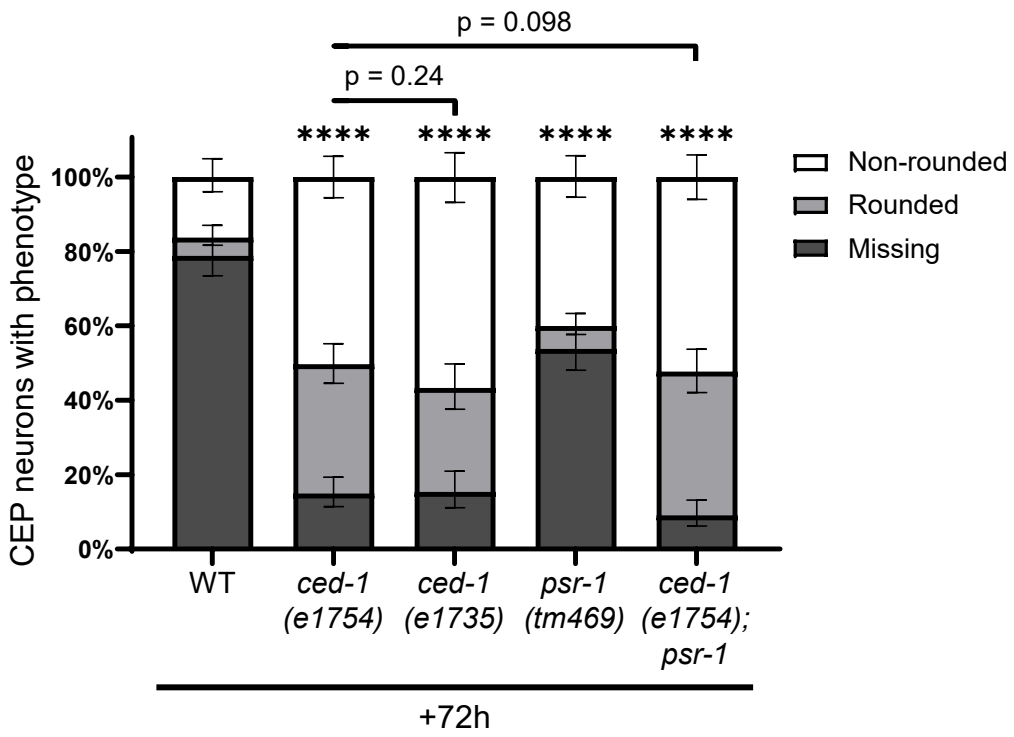
p = 0.098
p = 0.24
****
****
****
****
CEP neurons with phenotype
100%
80%
60%
40%
20%
0%
Non-rounded
Rounded
Missing
WT
ced-1 (e1754)
ced-1 (e1735)
psr-1 (tm469)
ced-1 (e1754); psr-1
+72h

B

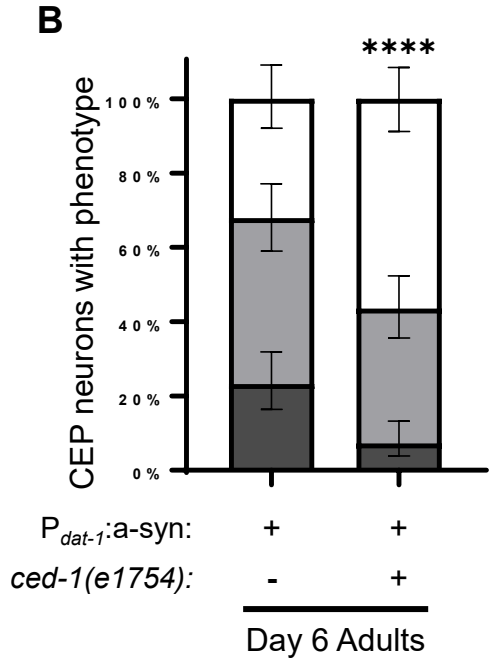
****
CEP neurons with phenotype
100 %
80 %
60 %
40 %
20 %
0 %
P dat-1 :a-syn: + +
ced-1(e1754): - +
Day 6 Adults

C

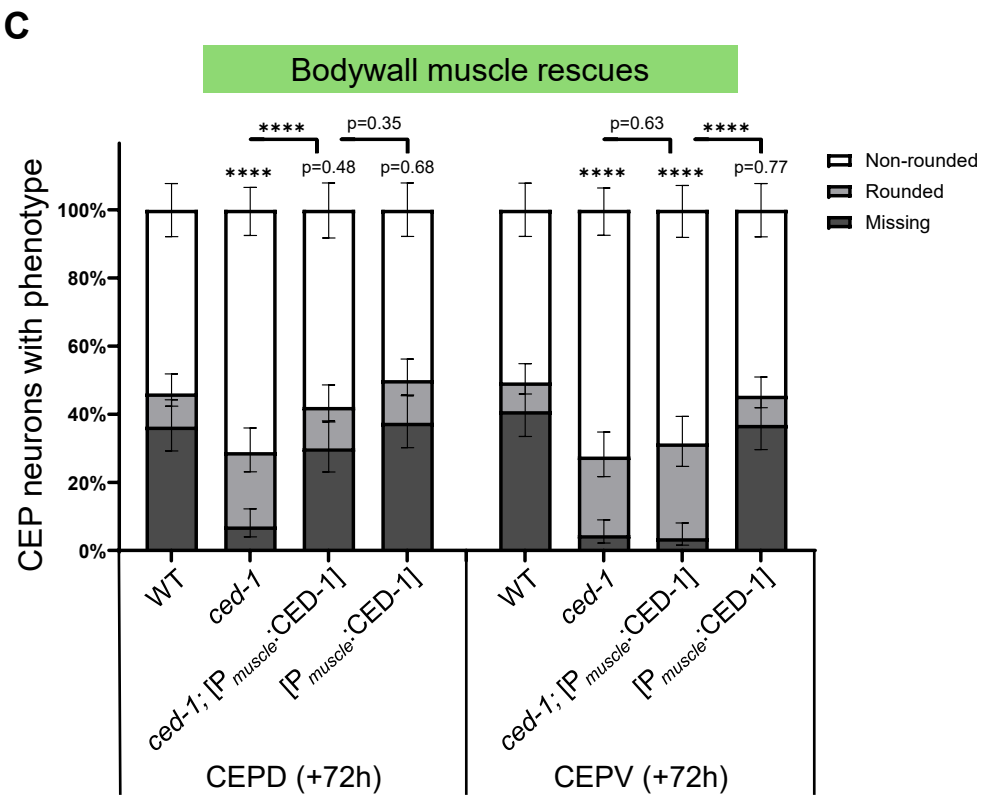
Bodywall muscle rescues
CEP neurons with phenotype
****
p=0.35
p=0.63
****
****
****
p=0.48
p=0.68
****
****
p=0.77
Non-rounded
Rounded
Missing
WT
ced-1
ced-1; [P muscle :CED-1]
[P muscle :CED-1]
CEPD (+72h)
CEPV (+72h)

D

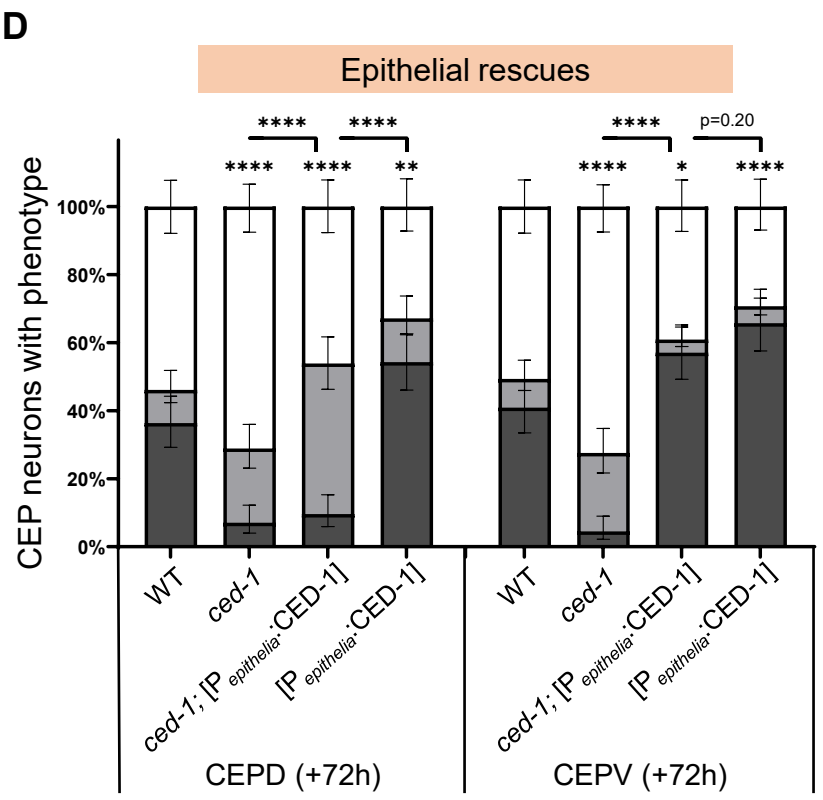
Epithelial rescues
CEP neurons with phenotype
****
****
****
****
**
****
*
p=0.20
****
WT
ced-1
ced-1; [P epithelia :CED-1]
[P epithelia :CED-1]
CEPD (+72h)
CEPV (+72h)

E

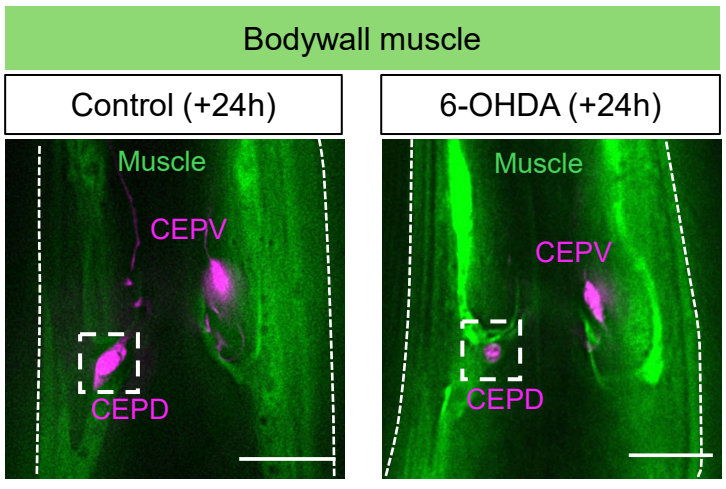
Bodywall muscle
Control (+24h)
6-OHDA (+24h)
Muscle
CEPV
CEPD

F

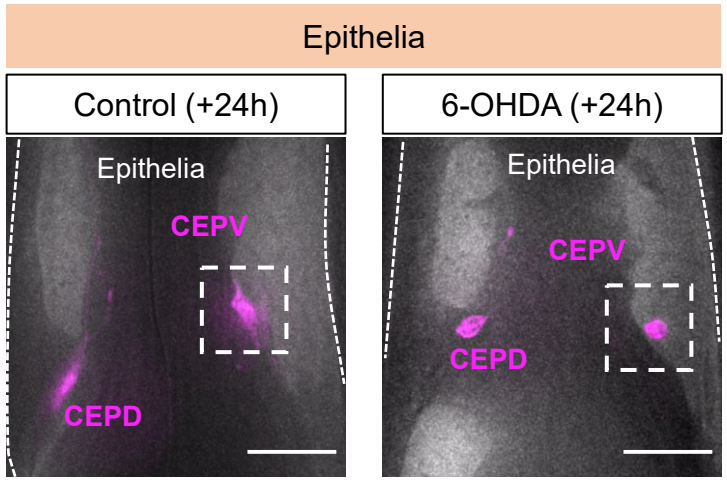
Epithelia
Control (+24h)
6-OHDA (+24h)
Epithelia
CEPV
CEPD

E'

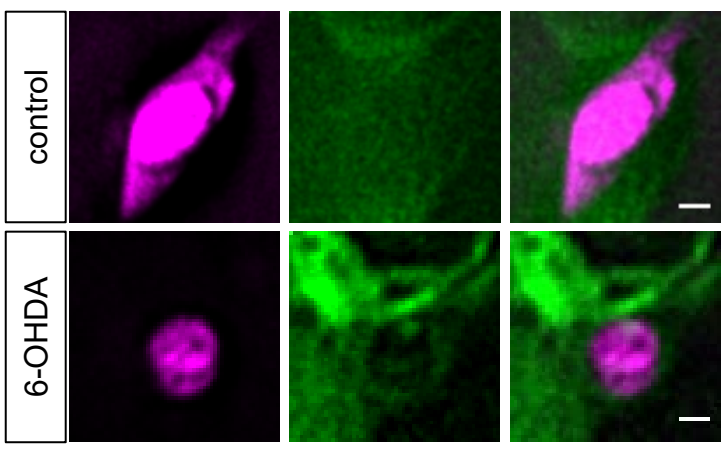
CEPD
BW muscle
MERGE
control
6-OHDA

F'

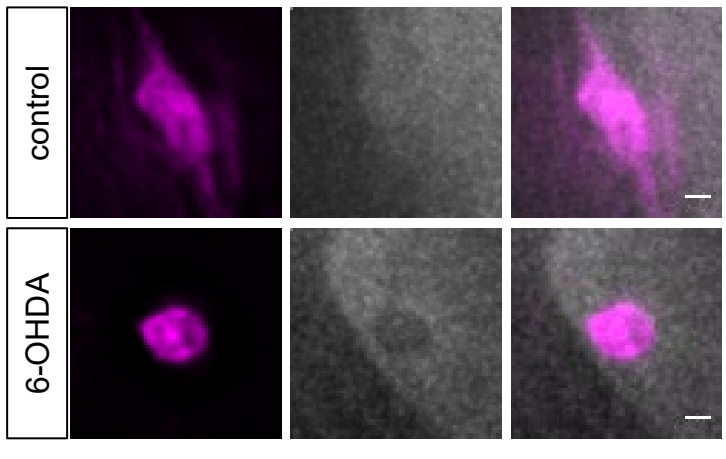
CEPV
Epithelia
MERGE
control
6-OHDA

Figure 3. CEP degeneration and engulfment is regulated by CED-1 recruitment and PS exposure

(A) Non-rounded or rounded CEP neurons (magenta) with CED-1 (green) clustering in *smIs34;otIs181* animals 24 hours after 6-OHDA treatment. Scale bar, 1µm. **(B)** Quantification of RT-qPCR for *ced-1* mRNA levels in control or 6-OHDA treated animals, 24 hours post-exposure, normalized to the control gene, *tba-1*. Means of 6 biological replicates plotted per condition. Error bars + SEM of 6 biological replicates (n.s. $p > 0.05$, unpaired two-tailed t-test). **(C)** Non-rounded or rounded CEP neuron (magenta) and secreted AnnexinV (sAnxV, cyan) localization in *vtIs1;*$P_{dpy\text{-}7}$:sAnnexinV:mScarlet animals 24 hours after 6-OHDA treatment. Scale bars, 1µm. **(D-E)** CEP neurons 72 hours after 50mM 6-OHDA treatment in genotypes noted. Quantification and statistics as in Fig. 1 E. **(D)** 2 biological replicates, 25-26 animals/replicate. Total n = 51-52 animals/condition. **(E)** 3-5 biological replicates, 23-26 animals/replicate. Total n = 73-130 animals/condition. **(F)** Fluorescence and DIC images of CEP neurons in wild type or *ced-7(n2094)* animals 24 hours after 6-OHDA exposure, in *vtIs1* reporter. White arrows, cell soma. Scale bars, 3µm. **(G)** CEP neurons 24 and 72 hours after 50mM 6-OHDA treatment in genotypes noted. Quantification and statistics as per Fig. 1 E. 3 biological replicates, 26-40 animals/replicate. Total n = 77-91 animals per condition. (A, C, F) Single z-slice presented, 60x magnification. Top of image, anterior of animal.

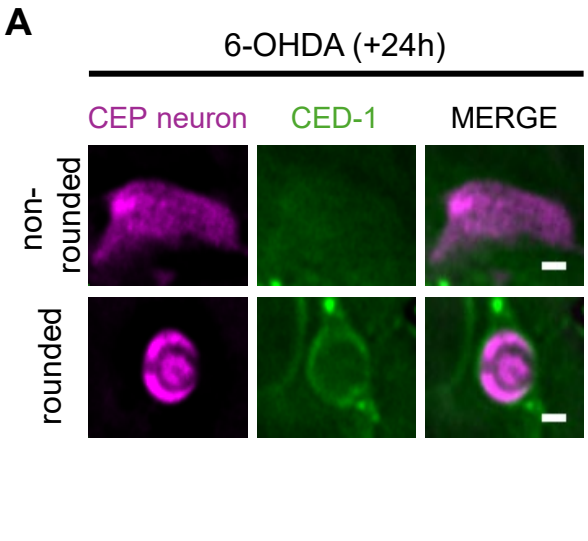
A
6-OHDA (+24h)
CEP neuron
CED-1
MERGE
non-rounded
rounded

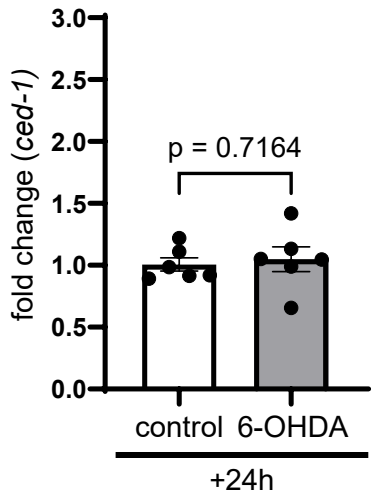
B
fold change (ced-1)
3.0
2.5
2.0
1.5
1.0
0.5
0.0
p = 0.7164
control
6-OHDA
+24h

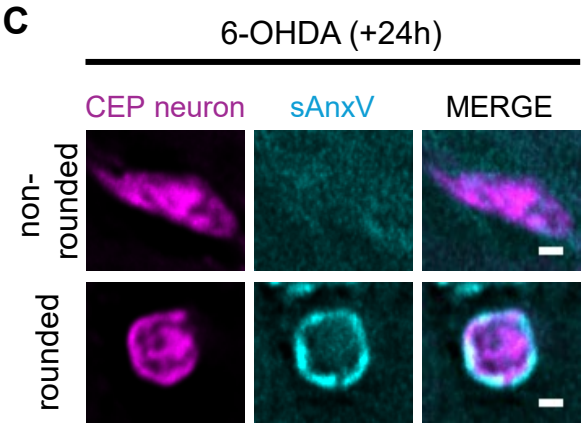
C
6-OHDA (+24h)
CEP neuron
sAnxV
MERGE
non-rounded
rounded

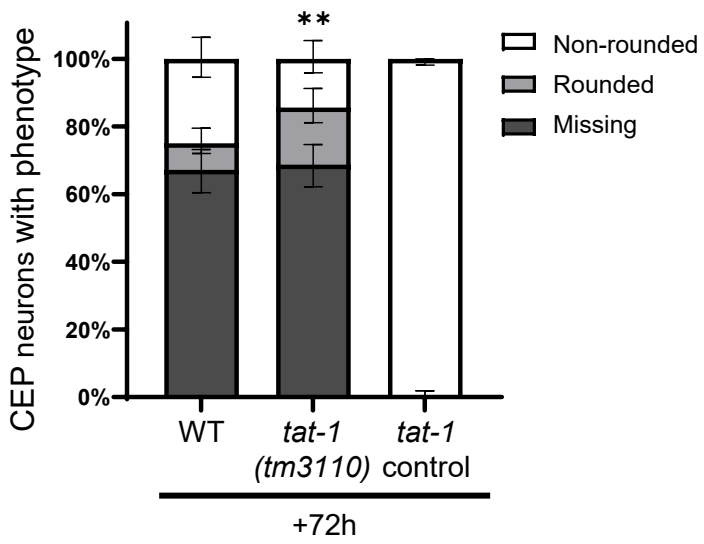
D
CEP neurons with phenotype
100%
80%
60%
40%
20%
0%
**
Non-rounded
Rounded
Missing
WT
tat-1 (tm3110)
tat-1 control
+72h

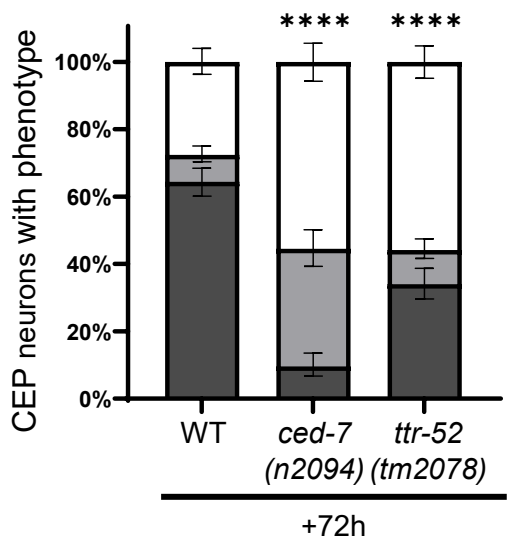
E
CEP neurons with phenotype
100%
80%
60%
40%
20%
0%
****
****
WT
ced-7 (n2094)
ttr-52 (tm2078)
+72h

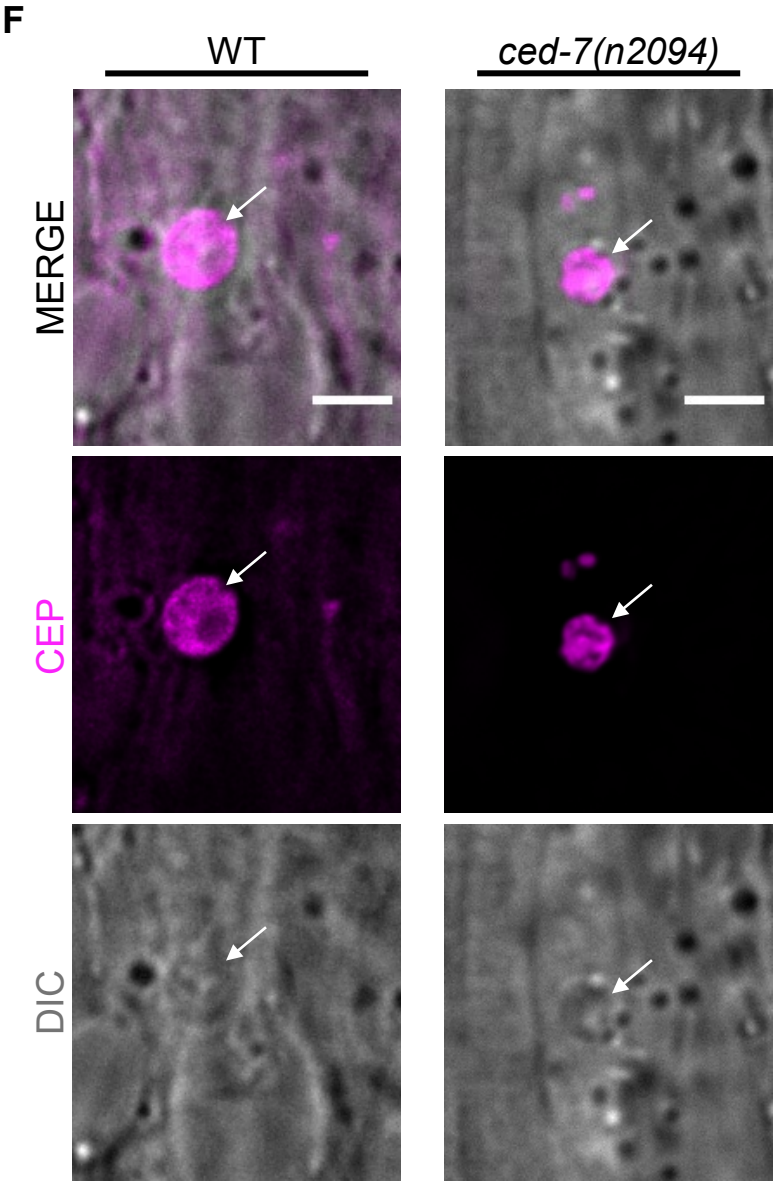
F
WT
ced-7(n2094)
MERGE
CEP
DIC

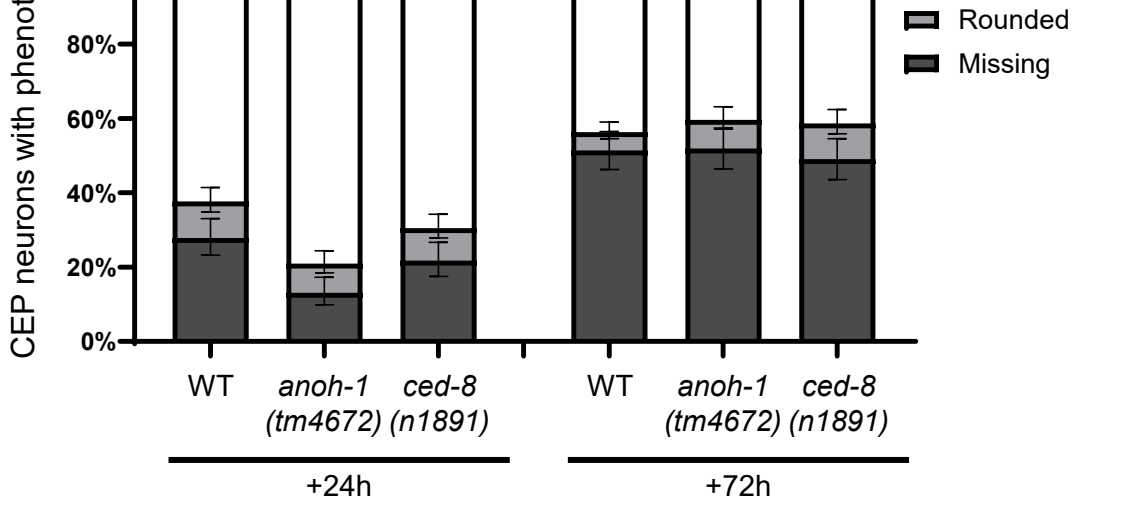
G
CEP neurons with phenotype
100%
80%
60%
40%
20%
0%
p=0.15
****
p=0.065
p=0.28
Non-rounded
Rounded
Missing
WT
anoh-1 (tm4672)
ced-8 (n1891)
WT
anoh-1 (tm4672)
ced-8 (n1891)
+24h
+72h

Figure 4. Loss of *ced-1* partially protects CEP functionality after 6-OHDA

(A) Schematic circuit with curated CEP synaptic partners: RIC, OLL, and OLQ. **(B)** RIC, OLL, and OLQ neurons in WT and *ced-1(e1754)* animals 96 hours after 6-OHDA treatment. Quantification as per Fig. 1 E. 2-3 biological replicates, 16-25 animals/replicate. Total n = 46-54 animals/condition. (**C-D**) Percent animals swimming in 300µm dopamine 72 hours after treatment (control or 6-OHDA) in genotypes as noted. *dat-1(ok157)* positive control had 2 biological replicates, 72 hours post-control treatment (n = 39 animals). Error bars, 95% confidence intervals, 4-8 biological replicates, 8-20 animals/replicate. Total n = 40-107 animals/timepoint. **(D)** Percent animals swimming at 15 min after control or 6-OHDA treatment. (****$p<0.0001$,**$p<0.01$, *$p<0.05$, n.s. $p>0.05$, Fisher's exact test). **(E)** Body bends per 20s of *vtIs1* and *vtIs1;ced-1(e1754)* animals 72 hours after 6-OHDA or control treatment in the presence or absence of HB101 bacteria. *cat-2(cer181)* animals 72 hours after control treatment were used as a positive control. The means and SD for 2 biological replicates each with 4-6 animals/replicate are plotted. Total n = 10-12 animals/condition (****$p<0.0001$, unpaired two-tailed t-test

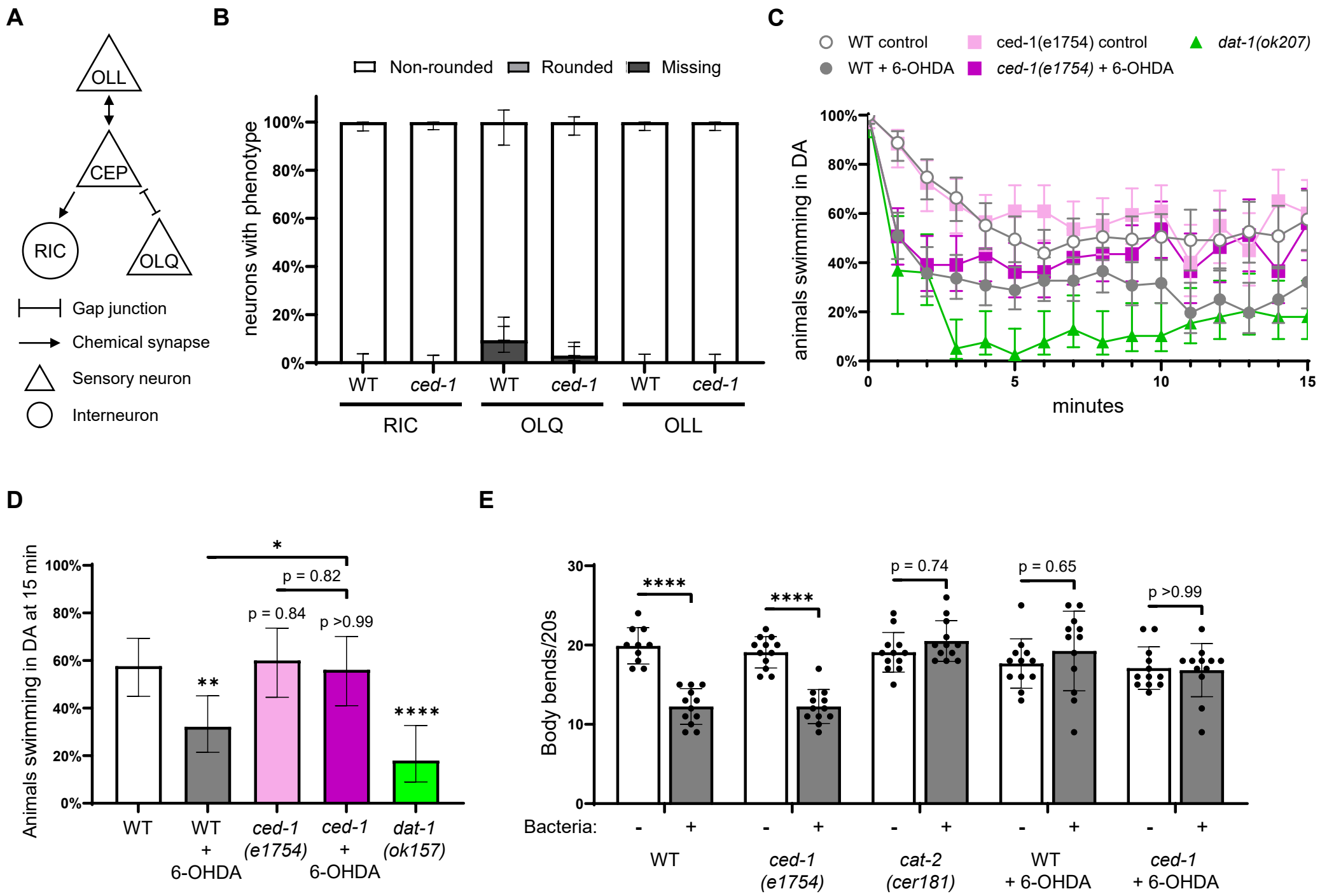
A
OLL
CEP
RIC
OLQ
Gap junction
Chemical synapse
Sensory neuron
Interneuron
B
Non-rounded
Rounded
Missing
neurons with phenotype
100%
80%
60%
40%
20%
0%
WT
ced-1
WT
ced-1
WT
ced-1
RIC
OLQ
OLL
C
WT control
ced-1(e1754) control
dat-1(ok207)
WT + 6-OHDA
ced-1(e1754) + 6-OHDA
animals swimming in DA
100%
80%
60%
40%
20%
0%
0
5
10
15
minutes
D
animals swimming in DA at 15 min
100%
80%
60%
40%
20%
0%
*
p = 0.82
p = 0.84
p >0.99
**
****
WT
WT + 6-OHDA
ced-1 (e1754)
ced-1 + 6-OHDA
dat-1 (ok157)
E
Body bends/20s
30
20
10
0
****
****
p = 0.74
p = 0.65
p >0.99
Bacteria: - + - + - + - + - +
WT
ced-1 (e1754)
cat-2 (cer181)
WT + 6-OHDA
ced-1 + 6-OHDA

Figure 5. Glial neurotoxicity is mediated by dopamine signaling

(A) Percentage of *vtIs1* (WT), *nsIs180;vtIs1* (CEPsh Ablated), *cat-2(cer181);nsIs180;vtIs1,* and *dat-1(ok207)* animals at the L4 stage swimming in deionized water for 20 min. Error bars = 95% confidence intervals. 2 biological replicates, 17-36 animals/replicate. Total n = 43-68 animals/timepoint. **(B)** Percentage of animals swimming at 20 min from (**A)** (****p<0.0001, n.s. p>0.05, Fisher's exact test). **(C)** Simplified schematic of dopamine biosynthesis and release pathway. **(D-F)** RT-qPCR quantification of *cat-2* (D), *dat-1* (E), or *cat-1* (F) mRNA levels in N2 and *nsIs180* L3 stage animals, normalized to the control gene, *tba-1*. The means and SEM of 3 biological replicates are plotted. (D-E) n.s. p>0.05, unpaired two-tailed t-test with welch's correction. (F) ***p<0.001, unpaired two-tailed t-test. **(G-H')** CAT-1:GFP in WT and CEPsh ablated animals. Boxed area in G-H, zoomed in G'-H', respectively. Scale bars, 10µm (60x magnification, max projection). Asterisk, CEP neurons (G-G'), missing in (H-H'). **(I)** CEP neurons 72 hours after 50mM 6-OHDA or control treatment in genotypes noted in *vtIs1* background. Error bars, 95% confidence intervals for 2 biological replicates, 33-36 animals/replicate. Total n = 66-69 animals per condition (****p<0.0001, **p<0.01, n.s. p>0.05, Fisher's exact test). **(J)** CEPD neurons 72 hours after 50mM 6-OHDA or control treatment in genotypes noted in the *vtIs1* background. *baIs4* animals (CAT-2 overexpression) were scored without *vtIs1* in the background. Error bars, 95% confidence intervals for 3-5 biological replicates, 19-26 animals/replicate. Total n = 71-130 animals per condition (****p<0.0001, **p<0.01, n.s. p>0.05, Fisher's exact test). **(K)** Model schematic: CEP neurons degenerate after 6-OHDA exposure. Epithelia and muscle cells engulf CEP neurons via CED-1. Loss of CED-1 prevents CEP neuron degeneration and clearance. Loss of glia prevents CEP neuron degeneration and increases dopamine signaling.

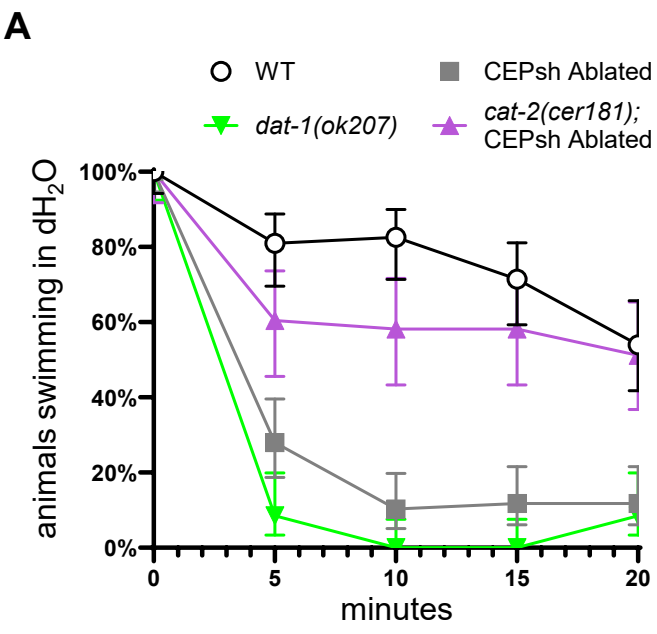
A
WT
CEPsh Ablated
dat-1(ok207)
cat-2(cer181); CEPsh Ablated
animals swimming in dH2O
100%
80%
60%
40%
20%
0%
0
5
10
15
20
minutes

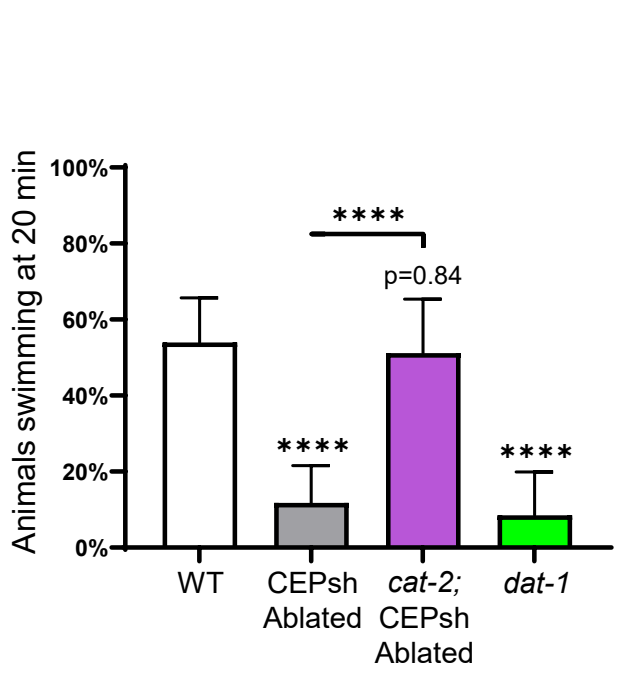
B
Animals swimming at 20 min
****
p=0.84
****
****
100%
80%
60%
40%
20%
0%
WT
CEPsh Ablated
cat-2; CEPsh Ablated
dat-1

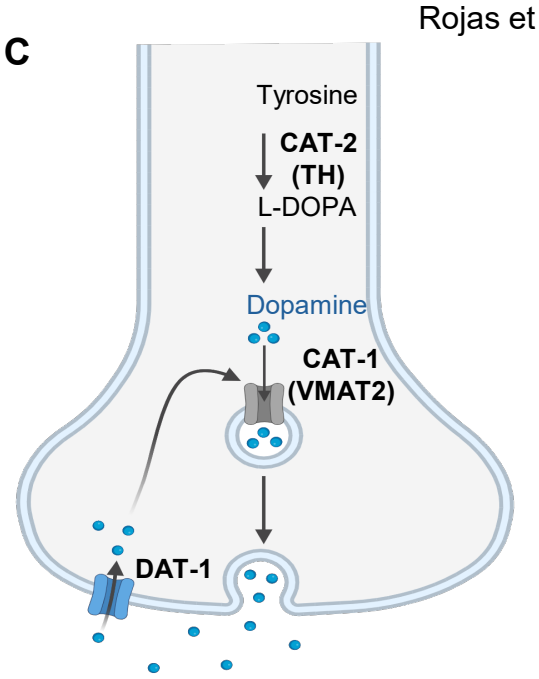
C
Tyrosine
CAT-2 (TH)
L-DOPA
Dopamine
CAT-1 (VMAT2)
DAT-1

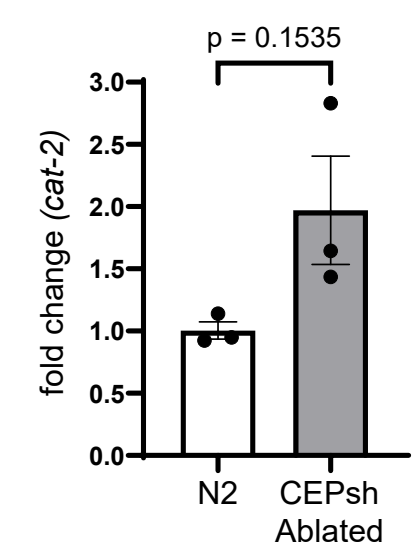
D
p = 0.1535
fold change (cat-2)
3.0
2.5
2.0
1.5
1.0
0.5
0.0
N2
CEPsh Ablated

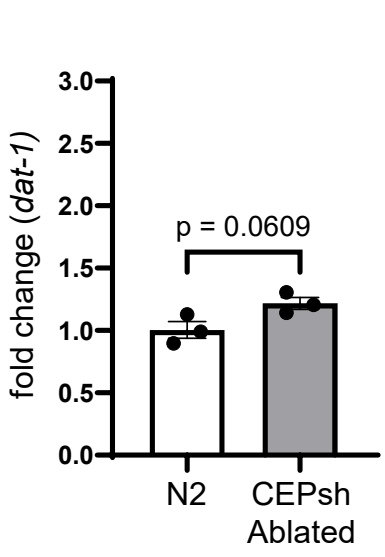
E
p = 0.0609
fold change (dat-1)
3.0
2.5
2.0
1.5
1.0
0.5
0.0
N2
CEPsh Ablated

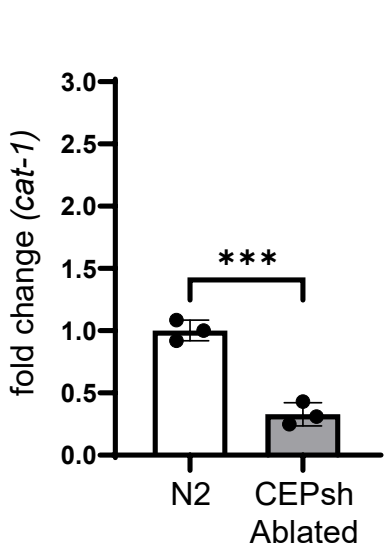
F
***
fold change (cat-1)
3.0
2.5
2.0
1.5
1.0
0.5
0.0
N2
CEPsh Ablated

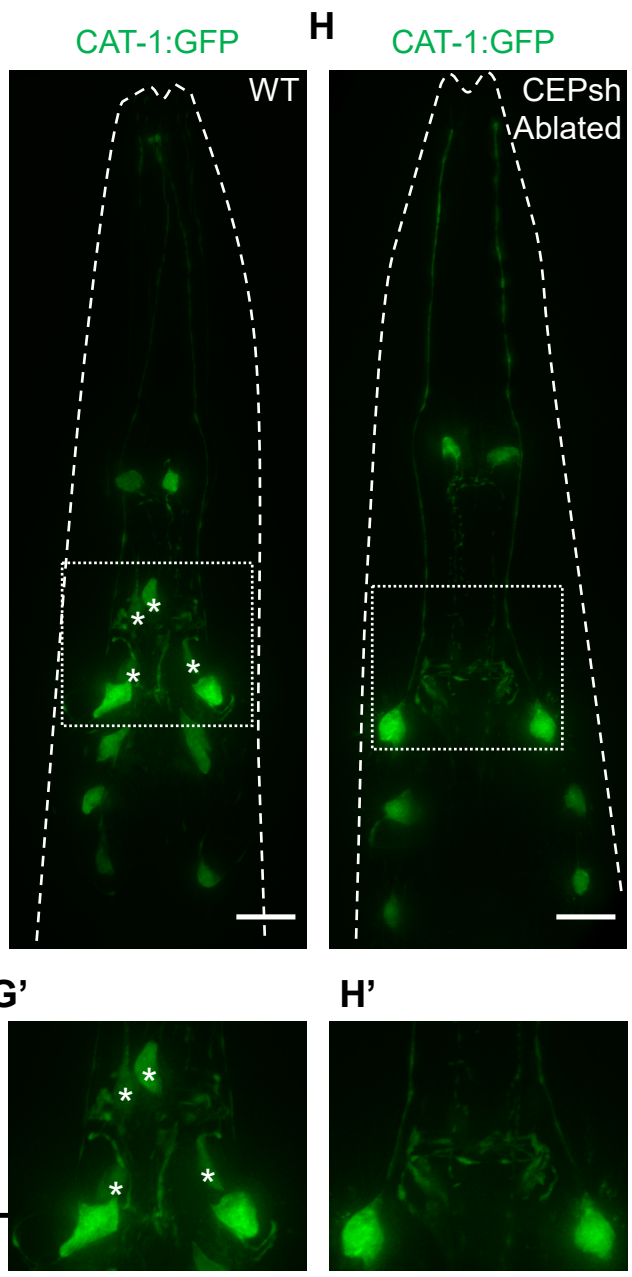
G
CAT-1:GFP
WT
H
CAT-1:GFP
CEPsh Ablated
G'
H'

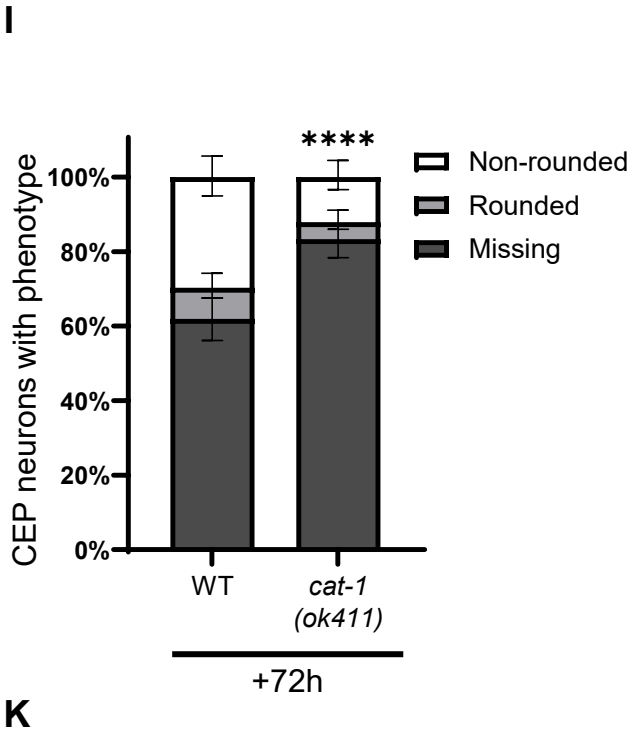
I
****
CEP neurons with phenotype
100%
80%
60%
40%
20%
0%
Non-rounded
Rounded
Missing
WT
cat-1 (ok411)
+72h

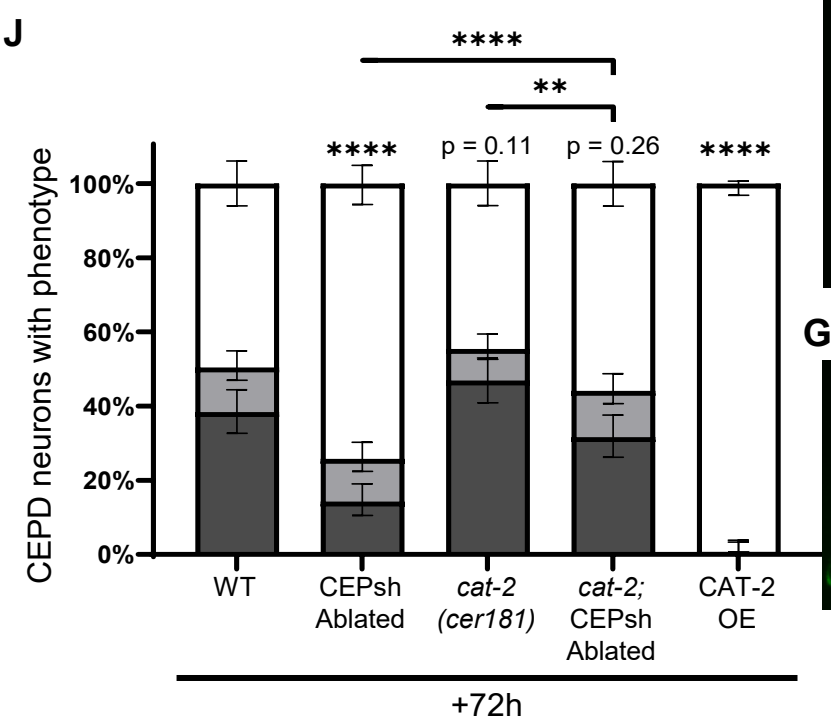
J
****
**
****
p = 0.11
p = 0.26
****
CEPD neurons with phenotype
100%
80%
60%
40%
20%
0%
WT
CEPsh Ablated
cat-2 (cer181)
cat-2; CEPsh Ablated
CAT-2 OE
+72h

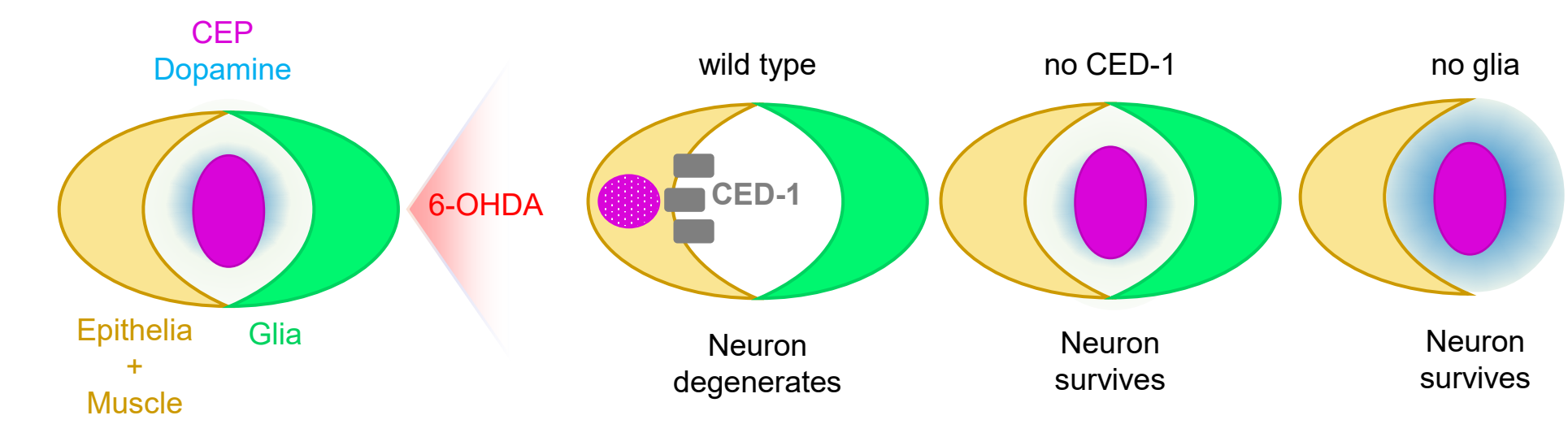
K
CEP
Dopamine
Epithelia
+
Muscle
Glia
6-OHDA
wild type
CED-1
Neuron degenerates
no CED-1
Neuron survives
no glia
Neuron survives

SUPPLEMENTAL FIGURE LEGENDS

Supplemental Figure 1. CEP degeneration quantified across conditions and genotypes

(A, B, D) Data quantification and statistics as per Figure 1E. **(A)** CEP phenotypes in L1 animals after 50mM 6-OHDA treatment at different time points as noted. 2+ biological replicates, 20-26 animals/replicate. Total n = 40-121 animals/timepoint. **(B)** CEP phenotypes in *otIs181* animals at timepoints noted after 50mM 6-OHDA treatment in L1 animals. 2+ biological replicates, 15-26 animals/replicate. Total n = 33-104 animals/timepoint. **(C)** Schematic of the known engulfment pathway. **(D)** CEP neurons 72 hours after 50mM 6-OHDA treatment in genotypes noted in *vtIs1* background. 3+ biological replicates, 13-26 animals/replicate. Total n = 65-102 animals/condition. **(E)** CED-1 domain structure with *(e1754)* and *(e1735)* lesions noted (both Q>Stop).

A

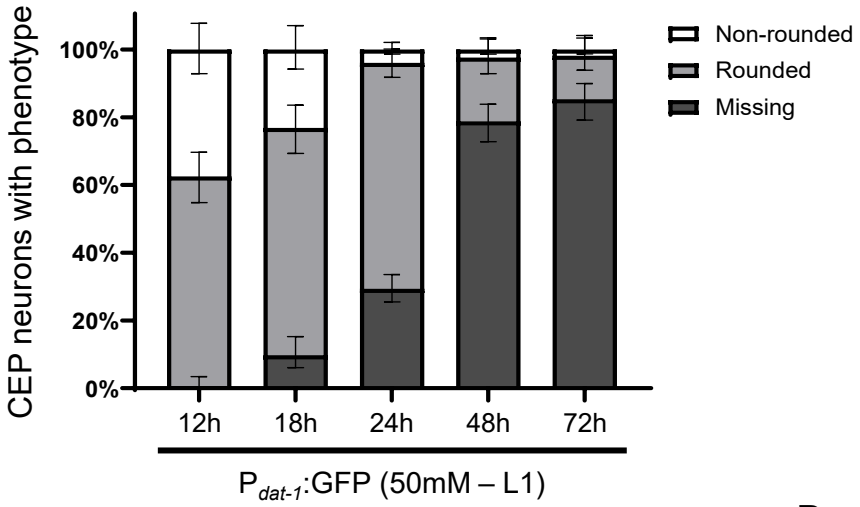
CEP neurons with phenotype
100%
80%
60%
40%
20%
0%
12h
18h
24h
48h
72h
Non-rounded
Rounded
Missing
P dat-1 :GFP (50mM – L1)

B

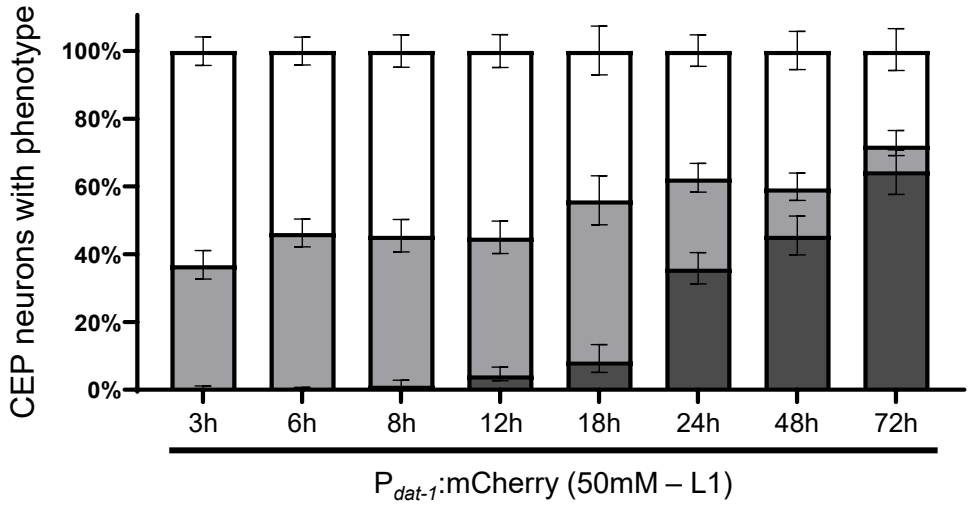
CEP neurons with phenotype
100%
80%
60%
40%
20%
0%
3h
6h
8h
12h
18h
24h
48h
72h
P dat-1 :mCherry (50mM – L1)

C

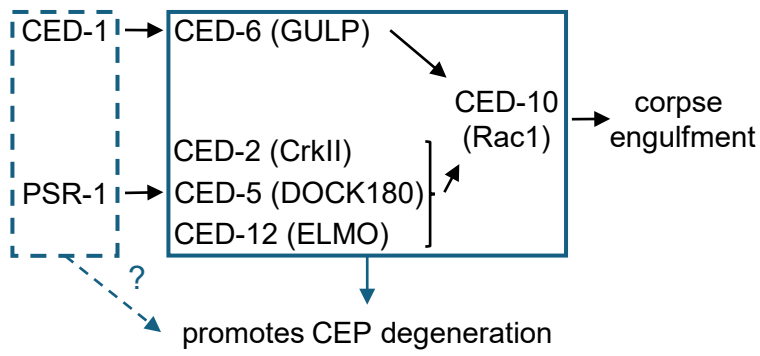
CED-1
PSR-1
CED-6 (GULP)
CED-10
(Rac1)
CED-2 (CrkII)
CED-5 (DOCK180)
CED-12 (ELMO)
corpse
engulfment
?
promotes CEP degeneration

D

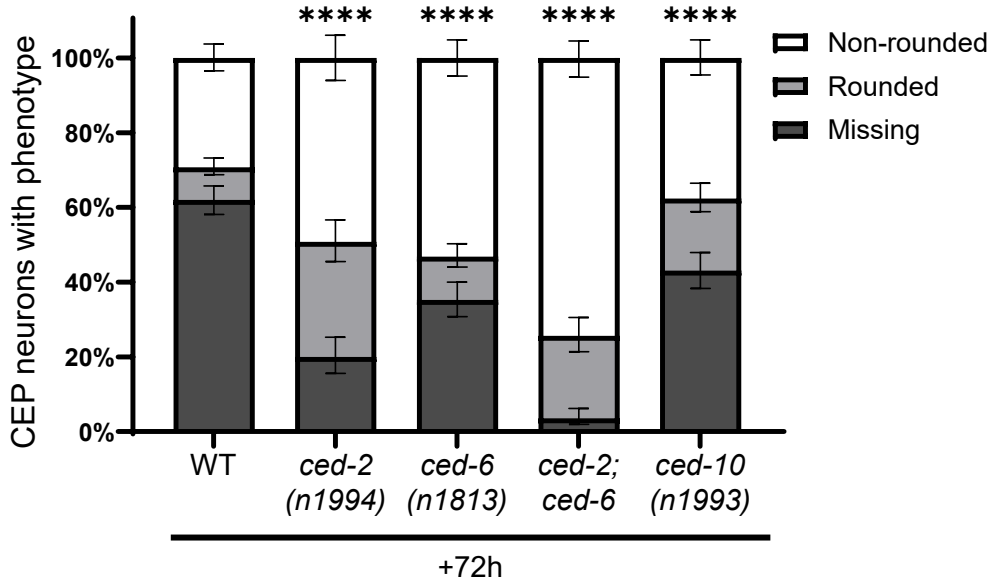
CEP neurons with phenotype
100%
80%
60%
40%
20%
0%
****
****
****
****
Non-rounded
Rounded
Missing
WT
ced-2
(n1994)
ced-6
(n1813)
ced-2;
ced-6
ced-10
(n1993)
+72h

E

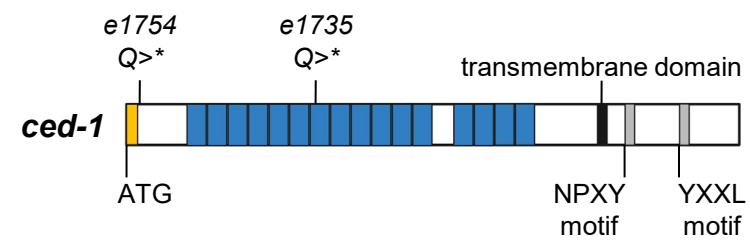
e1754
Q>*
e1735
Q>*
transmembrane domain
ced-1
ATG
NPXY
motif
YXXL
motif
signal sequence
16 atypical EGF-like repeats

Supplemental Figure 2. Gene and protein expression analysis of *ced-1*

(A) Quantification of *ced-1* mRNA levels by RT-qPCR in N2 and *nsIs180* L3 stage animals, normalized to the control gene, *tba-1*. Means and SEM of 2 biological replicates plotted (n.s. $p>0.05$, unpaired two-tailed t-test). **(B-C)** Effect of $P_{mir-228}$:CED-1 (B) or P_{nep-2s}:CED-1 (C) extrachromosomal arrays on CEPD and CEPV neurons 24 hours after 50mM 6-OHDA in *ced-1(e1754)* animals in the *vtIs1* background. Quantification as Figure 1E. (B) 3 biological replicates, 7-26 animals/replicate. Total n = 35-71 animals per condition. (C) 2-3 biological replicates each with 5-26 animals/replicate. Total n = 28-78 animals/condition (****$p<0.001$, n.s. $p>0.05$, Fisher's exact test). **(D-E)** Fluorescence imaging using split-GFP. Top, anterior of the animal. Dashed white line, animal outline. Scale bars, 10µm (40x magnification, single z-section). **(D)** P_{ced-1}:GFP(1-10) with P_{dpy-7}:GFP(11) for epithelia-specific expression and P_{dpy-7}:mScarlet to mark epithelia. Arrows, points of co-expression between GFP and mScarlet in epithelia. **(E)** P_{ced-1}:GFP(1-10) with P_{myo-3}:GFP(11) for muscle-specific expression. P_{myo-3}:mScarlet marks muscle. Arrows, points of co-expression between GFP and mScarlet in muscle. **(F-G)** Western blot (F) and quantification of CED-1:GFP in *smIs34* animals 24 and 40 hours after control or 6-OHDA treatment with an actin control for normalization. (G) Means and SEM of 2 biological replicates (24h samples) or 3 biological replicates (40h samples) plotted.

Supplemental Figure 2
Rojas et al., 2025

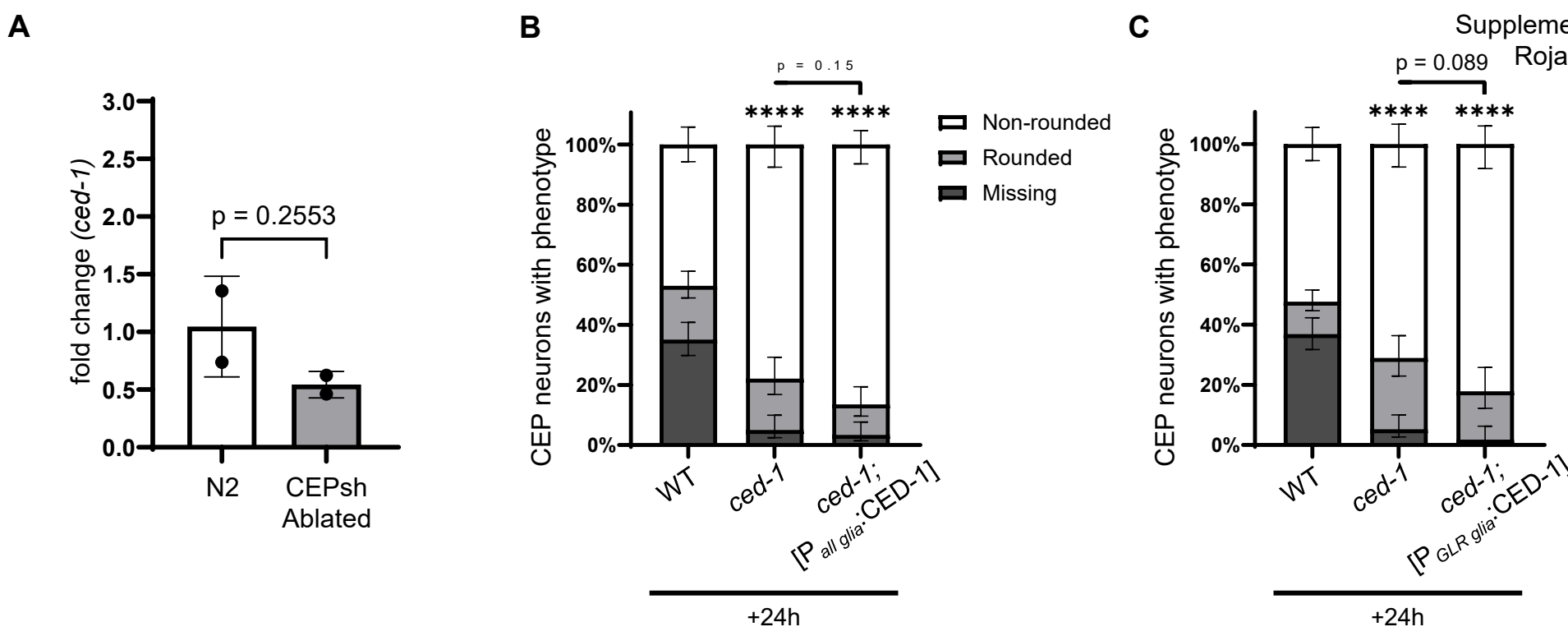

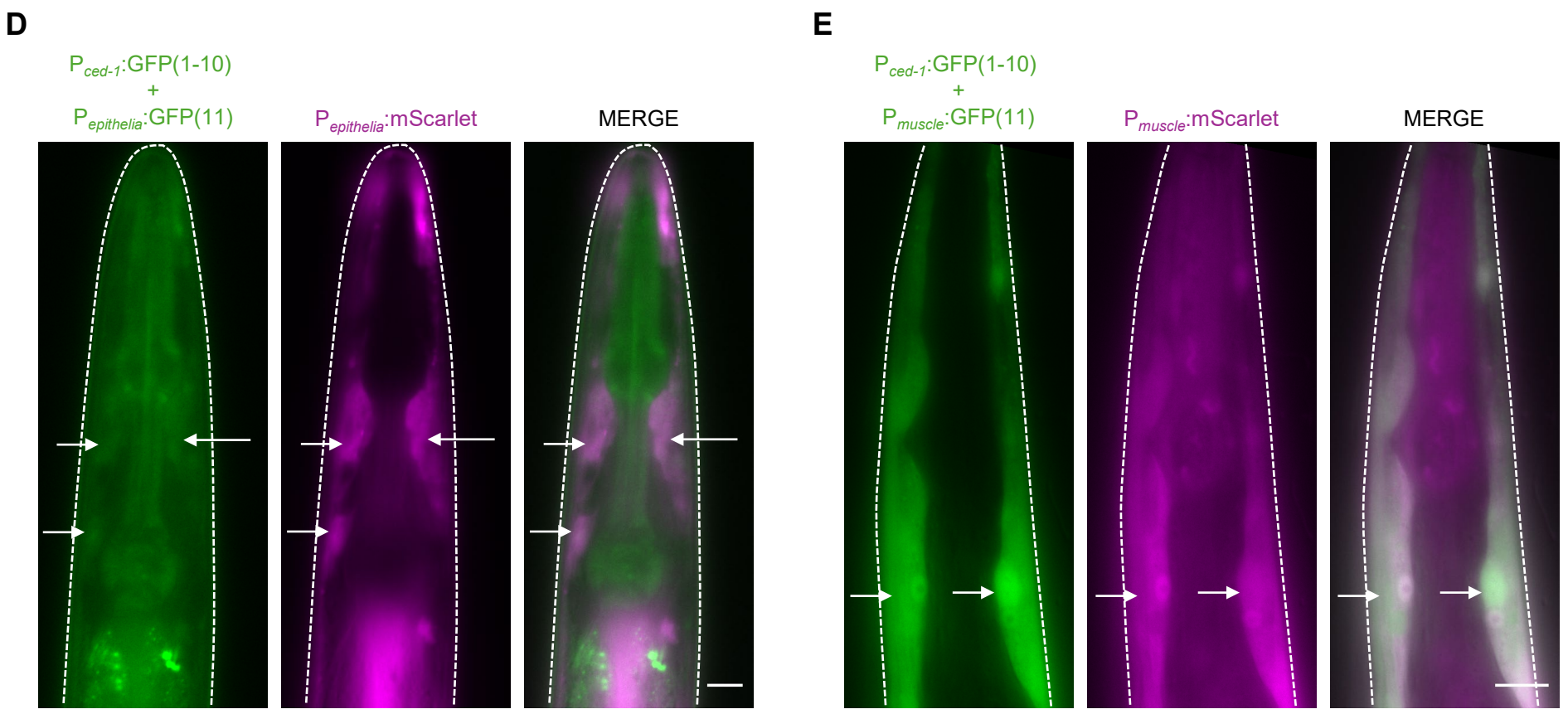

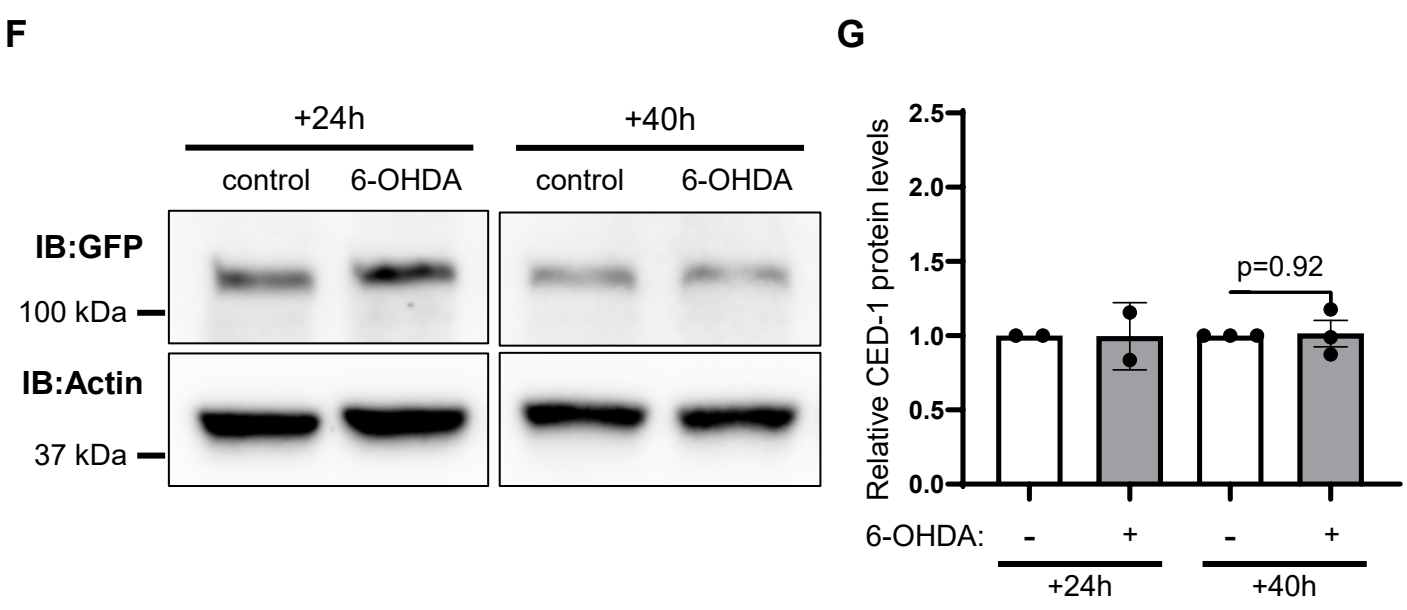

Supplemental Figure 3. Role of neurotransmitter regulators in CEP neurodegeneration

(A) CEP neurons 72 hours after 50mM 6-OHDA or control treatment in genotypes noted. Quantification as Figure 1E. 2-3 biological replicates each with 25-40 animals/replicate. Total n = 50-91 animals per condition (****p<0.0001, **p<0.01, n.s. p>0.05, Fisher's exact test). **(B-E)** *glt-1* (B) or *glt-3* (C) mRNA levels in N2 and *nsIs180* L3 stage animals, without (B, C) or 24h post-6-OHDA treatment (D-E), normalized to the control gene, *tba-1*. The means and SEM of 3 biological replicates are plotted (n.s. p>0.05, unpaired two-tailed t-test with welch's correction). **(F)** CEPD neurons 72 hours after 50mM 6-OHDA in genotypes noted, quantified as in Fig. 1 E. 3 biological replicates, 25-50 animals/replicate. Total n = 91-102 animals per condition (****p<0.0001, **p<0.01, n.s. p>0.05, Fisher's exact test).

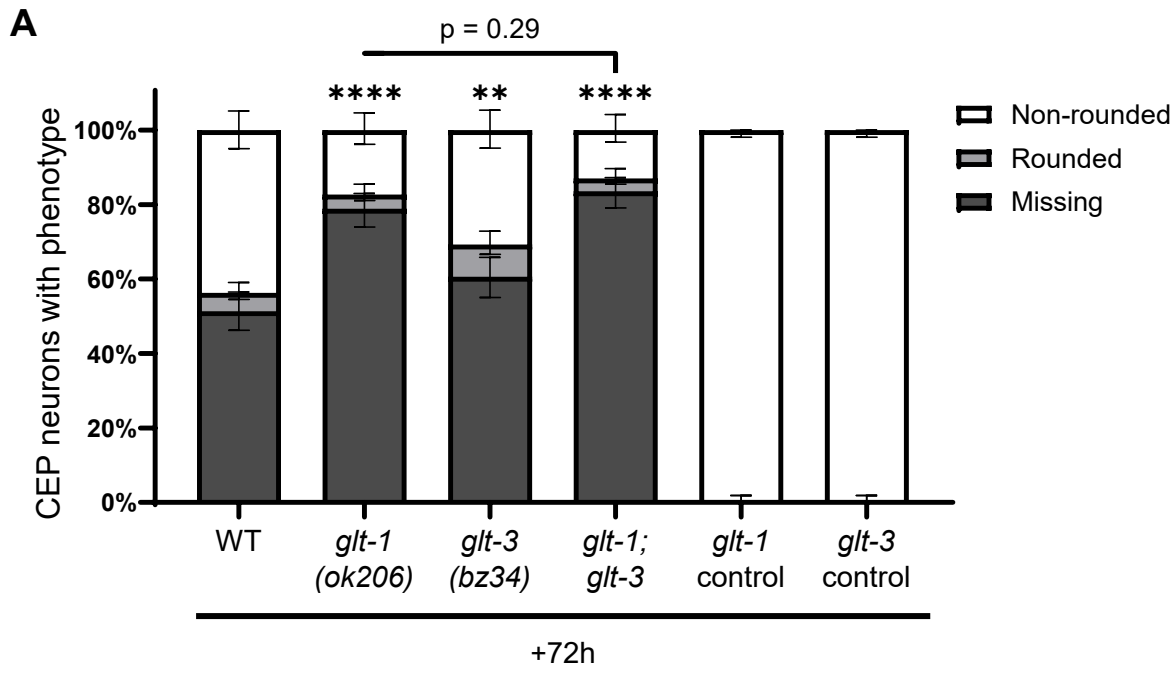
A
p = 0.29
****
**
****
CEP neurons with phenotype
100%
80%
60%
40%
20%
0%
Non-rounded
Rounded
Missing
WT
glt-1 (ok206)
glt-3 (bz34)
glt-1; glt-3
glt-1 control
glt-3 control
+72h

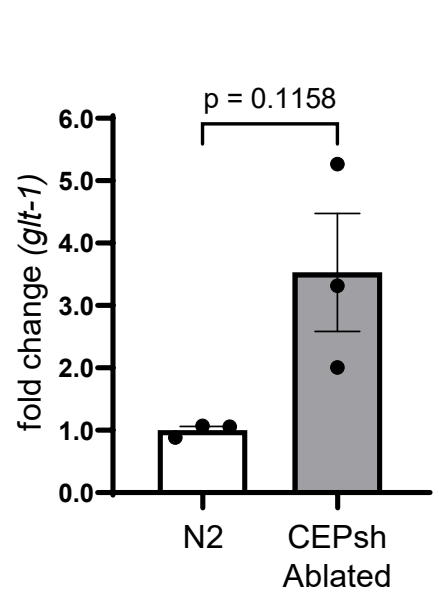
B
p = 0.1158
fold change (glt-1)
6.0
5.0
4.0
3.0
2.0
1.0
0.0
N2
CEPsh Ablated

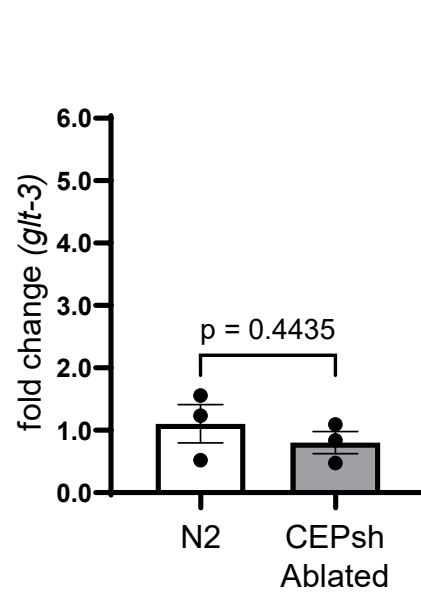
C
fold change (glt-3)
p = 0.4435
6.0
5.0
4.0
3.0
2.0
1.0
0.0
N2
CEPsh Ablated

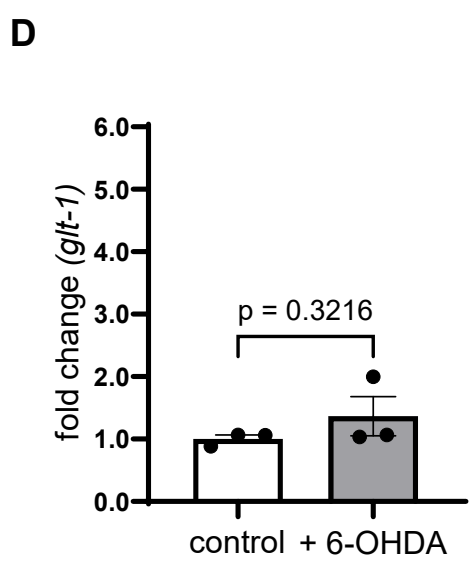
D
fold change (glt-1)
p = 0.3216
6.0
5.0
4.0
3.0
2.0
1.0
0.0
control
+ 6-OHDA

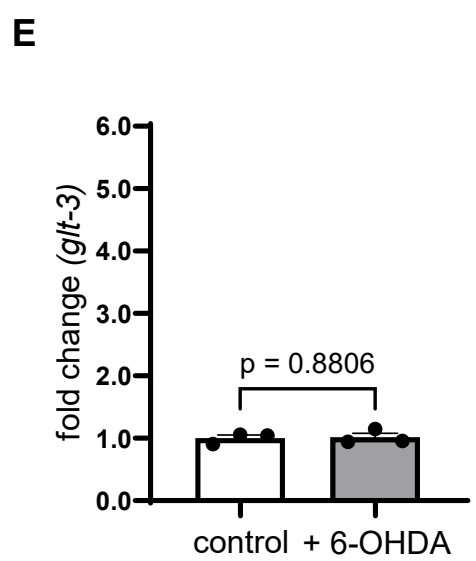
E
fold change (glt-3)
p = 0.8806
6.0
5.0
4.0
3.0
2.0
1.0
0.0
control
+ 6-OHDA

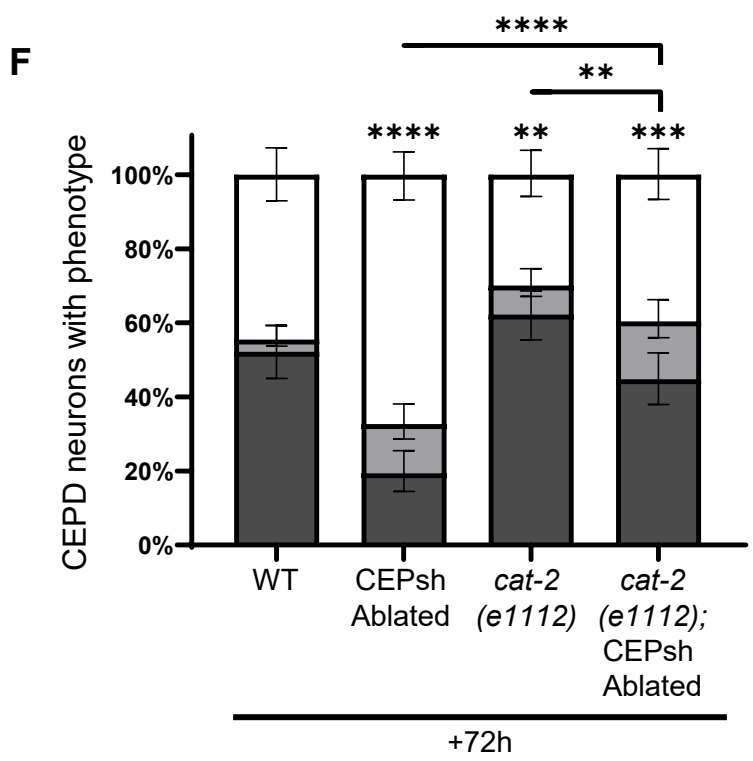
F
****
**
****
**
***
CEPD neurons with phenotype
100%
80%
60%
40%
20%
0%
WT
CEPsh Ablated
cat-2 (e1112)
cat-2 (e1112); CEPsh Ablated
+72h

EXPERIMENTAL PROCEDURES

C. elegans methods and strains

C. elegans were cultured as previously described (Brenner, 1974; Stiernagle, 2006). Bristol N2 strain was used as wild type. Animals were raised at 20ºC for two weeks without starvation. Germ-line transformations by micro-injection to generate unstable extra-chromosomal array transgenes were carried out using standard protocols (Mello et al., 1991). Strains used are listed below:

N2 Bristol

TG2435	*vtIs1 [dat-1p::GFP + rol-6(su1006)] V*
OS3549	*nsIs180 [Phlh-17:split-Caspase + coel:GFP]*
CB3261	*ced-1(e1754) I*
OH7193	*otIs181[dat-1::mCherry + ttx-3::mCherry] III; him-8(e1489) IV*
OH4254	*vtIs1[dat-1p::GFP + rol-6(su1006)] V; vab-3(ot266) X*
ASJ78	*ced-10(n1993) IV; vtIs1 V[dat-1p::GFP + rol-6(su1006)]*
ASJ207	*ced-1(e1754) I; psr-1(tm469) IV; vtIs1 [dat-1p::GFP + rol-6(su1006)] V*
ASJ208	*ced-1(e1754) I; vtIs1 [dat-1p::GFP + rol-6(su1006)] V*
ASJ209	*psr-1(tm469) IV; vtIs1 [dat-1p::GFP + rol-6(su1006)] V*
ASJ258	*nsIs180 [Phlh-17:split-Caspase + coel:GFP] IV; vtIs1 [dat-1p::GFP + rol-6(su1006)] V*
ASJ386	*nsIs105 [Phlh-17(1.9kb):GFP] I; otIs181 [dat-1::mCherry + ttx-3::mCherry] III*
ASJ397	*ced-6(n1813) III; vtIs1 [dat-1p::GFP + rol-6(su1006)] V*
ASJ475	*ced-7(n2094) III; ntIs1 V*
ASJ482	*ttr-52(tm2078) III; vtIs1 [dat-1p::GFP + rol-6(su1006)] V*
ASJ483	*ced-2(n1994) IV; vtIs1 [dat-1p::GFP + rol-6(su1006)] V*
ASJ484	*otIs181[dat-1::mCherry + ttx-3::mCherry] III; smIs34[ced-1p::ced-1::GFP + rol-6(su1006)]*
ASJ633	*dnaEx168[Pmir-228:CED-1:SL2:mKate2 + coel:RFP]; ced-1(e1754) I; vtIs1 V*
ASJ637	*dnaEx192[Pdpy-7:CED-1:SL2:mKate + coel:RFP]; vtIs1 V*

ASJ638	*dnaEx192[Pdpy-7:CED-1:SL2:mKate + coel:RFP]; ced-1(e1754) I; vtIs1 [dat-1p::GFP + rol-6(su1006)] V*
ASJ648	*ced-6(n1813) III; ced-2(n1994) IV; vtIs1 [dat-1p::GFP + rol-6(su1006)] V*
ASJ978	*ced-1(e1754) I; dnaEx249[Pnep-2s:CED-1:SL2:mKate2 + coel:RFP]; vtIs1 V*
ASJ1051	*otIs181[dat-1::mCherry + ttx-3::mCherry] III*
ASJ1511	*dnaEx483[Pmyo-3:CED-1:SL2:mKate2 + coel:RFP]; vtIs1 V*
ASJ1066	*dnaEx483[Pmyo-3:CED-1:SL2:mKate2 + coel:RFP]; ced-1(e1754) I; vtIs1 V*
ASJ1069	*dnaEx485[Pdpy-7:annexin V:mscarlet + coel:RFP]; vtIs1*
ASJ1471	*vtIs1[dat-1p::GFP + rol-6(su1006)] V; mls-2(ns329) X*
ASJ1505	*nsIs107 [tbh-1:GFP + lin-15(+)] III; vtIs1 [dat-1p::GFP + rol-6(su1006)] V*
ASJ1507	*vtIs1 [dat-1p::GFP + rol-6(su1006)] V; otIs138 [ser-2(prom3)::GFP + rol-6(su1006)] X*
ASJ1508	*ced-1(e1754) I; vtIs1 [dat-1p::GFP + rol-6(su1006)] V; otIs138 [ser-2(prom3)::GFP + rol-6(su1006)] X*
ASJ1510	*ced-1 (e1754) I; nsIs107 [tbh-1:GFP + lin-15(+)] III; vtIs1 [dat-1p::GFP + rol-6(su1006)] V*
ASJ1527	*vtIs1 [dat-1p::GFP + rol-6(su1006)] V; glt-1(ok206) X*
ASJ1528	*glt-3(bz34) IV; vtIs1 [dat-1p::GFP + rol-6(su1006)] V; glt-1(ok206) X*
ASJ1529	*glt-3(bz34) IV; vtIs1 [dat-1p::GFP + rol-6(su1006)] V*
ASJ1548	*anoh-1(tm4762) III; vtIs1 [dat-1p::GFP + rol-6(su1006)] V*
ASJ1563	*vtIs1 [dat-1p::GFP + rol-6(su1006)] V; ced-8(n1891) X*
UA57	*baIs4 [dat-1p::GFP + dat-1p::CAT-2]*
ASJ1564	*ced-1 (e1754) I; baIs4 [dat-1p::GFP + dat-1p::CAT-2] IV*
ASJ1610	*cat-2(cer181[cat-2p::GFP::H2B 1-3]) II; vtIs1 [dat-1p::GFP + rol-6(su1006)] V*
ASJ1612	*cat-2(cer181[cat-2p::GFP::H2B 1-3]) II; nsIs180 [Phlh-17:split-Caspase + coel:GFP] IV; vtIs1 [dat-1p::GFP + rol-6(su1006)] V*
ASJ1554	*cat-2 (e1112) II; vtIs1 [dat-1p::GFP + rol-6(su1006)] V*
ASJ1556	*cat-2 (e1112) II; nsIs180 [Phlh-17:split-Caspase + coel:GFP] IV; vtIs1 [dat-1p::GFP + rol-6(su1006)] V*
ASJ1613	*dnaEx712[Pced-1:spGFP(1-10) + Pmyo-3:spGFP(11) + Pmyo-3:mScarlet]*
ASJ1614	*dnaEx713[Pced-1:spGFP(1-10) + Pdpy-7:spGFP(11) + Pdpy-7:mScarlet]*

ASJ1686	*ced-1(e1754) I; eraIs1 [dat-1p::mCherry + dat-1p::hSNCA::Venus]*
ERS100	*eraIs1 [dat-1p::mCherry + dat-1p::hSNCA::Venus]*
ASJ1863	*nsIs180 [Phlh-17:split-Caspase + coel:GFP] IV; eraIs1 [dat-1p::mCherry + dat-1p::hSNCA::Venus]*
ASJ1063	*dnaEx481[Pdpy-7:annexin V:mscarlet + coel RFP]; vtIs1*
TL9	*bam-2(cy7) I; cyIs4 [cat-1p::cat-1::GFP + rol-6(su1006)]*
ASJ	*nsIs180 [Phlh-17:split-Caspase + coel:GFP] IV; cyIs4 [cat-1p::cat-1::GFP + rol-6(su1006)]; bam-2(cy7)?*
ASJ	*kyEx581 [ocr-4::GFP + lin-15(+)];ced-1(e1754) I; vtIs1 [dat-1p::GFP + rol-6(su1006)] V*
ASJ	*kyEx581 [ocr-4::GFP + lin-15(+)]; vtIs1 [dat-1p::GFP + rol-6(su1006)] V*

Plasmids

Cell-specific CED-1: cDNA for the CED-1A isoform was PCR amplified from a mixed stage cDNA library and cloned into ASJ54 ($P_{mir\text{-}228}$:SL2:mKate2) using *Xma1*/*Nhe1* sites to generate the pan-glial CED-1 rescue construct ASJ154/pGR3 ($P_{mir\text{-}228}$:CED-1A:SL2:mKate2); ASJ154 was injected into N2 worms at 15ng/µL with 20ng/µL of $P_{unc\text{-}122}$:RFP(Miyabayashi et al., 1999) as a co-injection marker. To generate the GLR CED-1 rescue construct, the truncated $P_{nep\text{-}2s}$ promoter was digested from ASJ27/pGR1 ($P_{nep\text{-}2s}$:GFP) and cloned into ASJ154 using *SphI*/*NotI* restriction sites to generate ASJ165/ASJ166 ($P_{nep\text{-}2s}$:CED-1A:SL2:mKate2); ASJ165 was injected into N2 worms at 20ng/µL with 20ng/µL of $P_{unc\text{-}122}$:RFP as a co-injection marker (Yamada et al., 2010). To generate the epithelial CED-1 rescue construct, the $P_{dpy\text{-}7}$ promoter was digested and cloned into ASJ154 using *SphI*/*NotI* restriction sites to generate ASJ157/ASJ158 ($P_{dpy\text{-}7}$:CED-1A:SL2:mKate2); ASJ157 was injected into N2 worms at 20ng/µL with 20ng/µL of $P_{unc\text{-}122}$:RFP as a co-injection marker. To generate the body wall muscle CED-1 rescue construct, the $P_{myo\text{-}3}$ promoter was cloned into ASJ54 using Gibson cloning to generate ASJ356 ($P_{myo\text{-}3}$:CED-

1A:SL2:mKate2); ASJ356 was injected at 20ng/µL with 20ng/µL of $P_{unc-122}$:RFP as a co-injection marker directly into *ced-1(e1754)* mutant animals carrying the vtIs1 transgene.

P_{dpy-7}:sAnnexinV:mScarlet: The *dpy-7* promoter (~350bp) from ASJ157 (P_{dpy-7}:CED-1A:SL2:mKate2) was restriction digested using *Sph1* and *Not1* enzymes and ligated with the sAnnexinV:mScarlet sequence from ASJ45 ($P_{F53F4.13}$:AnnexinV:mScarlet) to make ASJ387/388.

Cell-specific split-GFP: To generate epithelial- or muscle-specific expression of split GFP, fragment spGFP(1-10) was expressed under the P_{ced-1} promoter and fragment spGFP(11) was expressed under either P_{dpy-7} (epithelia) or P_{myo-3} (muscle) (Feinberg et al., 2008). spGFP(1-10) was PCR amplified from a plasmid containing P_{ace-4}:CD4-2:spGFP1-10 with *MscI* and *EcoRI* restriction sites added to the 5' and 3' ends, respectively (Feinberg et al., 2008). spGFP(11) was PCR amplified from a plasmid containing P_{rig-3}:CD4-2:mCherry:spGFP11 with *XbaI* and *EcoRI* restriction sites added to the 5' and 3' ends, respectively (Feinberg et al., 2008). To generate P_{ced-1}:spGFP1-10, the *ced-1* promoter was restriction digested from pZZ615 using *SphI* and *MscI* enzymes and ligated together with spGFP1-10 into the pSM:GFP vector backbone was restriction digested with *Sph1* and *EcoRI* enzymes to make ASJ457/458 (McCarroll et al., 2005). To generate P_{dpy-7}:spGFP11, spGFP11 cDNA was restriction digested with *XbaI* and *EcoRI* enzymes and ligated into ASJ157 (P_{dpy-7}:CED-1A:SL2:mKate2) to make ASJ459/460. To generate P_{myo-3}:spGFP11, spGFP11 cDNA was restriction digested with *XbaI* and *EcoRI* enzymes and ligated into ASJ356 (P_{myo-3}:CED-1A:SL2:mKate2) to make ASJ461/462. All constructs were injected at 30ng/µL into N2 animals.

6-hydroxydopamine treatment

Treatment with 6-hydroxydopamine was done as previously described with modifications (Nass et al., 2002; Offenburger et al., 2018b). Worms were washed off a mixed population 6cm plate using M9 buffer, and specific larval stages were synchronized and enriched using sieves of different sizes (15 µm = L1, 20 µm = L2/L3). While on the filters, worms were washed with M9 buffer 3x. They were then collected in 1.7mL Eppendorf tubes and allowed to settle to the bottom of the tube. 30µL of worms were added to a 96-well plate with 10µL of 200mM L-ascorbic acid (Sigma CAS #50-81-7) and then 10µL of a 5x 6-OHDA stock (Sigma CAS #28094-15-7) was added to a final volume of 50 µL (or L-Ascorbic acid alone as control). The plate was shaken on a horizontal shaker for 1hr at 500 RPM, after which 150µL of M9 was added to each well to oxidize the 6-OHDA and stop the reaction. Worms were then transferred using a glass pipette to an OP50 seeded plate and left uncovered for 5-10 minutes in a fume hood to dry. Plates were then covered and incubated at 20ºC. In all paradigms, we exposed staged animals to a given concentration of 6-OHDA for 1 hour and examined CEP neurons via fluorescent reporters for changes in morphology as a basis for degeneration. CEP neurons were then scored for clearance 24 hours, 48 hours, and 72 hours after 50mM 6-OHDA treatment. CEP neurons were visualized using the *vtIs1* or *otIs181* transgenes expressing GFP or mCherry under the *dat-1* promoter, respectively, as noted (Bertrand and Hobert, 2009; Nass et al., 2002). CEP neurons were scored for intact and visible cell bodies. CEP neurons were scored as (1) non-rounded if the cell body was visible and maintained its gross shape, (2) rounded if the cell body was visible but looked rounded or spherical, or (3) missing if there was no cell body visible or detectable fluorescent signal. Percent CEP neurons visible were calculated against total number of CEP neurons expected (4 per animal).

Microscopy

Worms were immobilized on 2% agar pads using 1% tetramisole hydrochloride (Sigma CAS #16595-80-5) dissolved in M9 buffer. Images were acquired on a Deltavision Elite RoHS wide-field deconvolution system with Ultimate Focus (GE), a PlanApo 60×/1.42 NA or OLY 100×/1.40 NA oil-immersion objective and a DV Elite CMOS Camera. Images were processed using ImageJ, FIJI.

Alpha synuclein degeneration assay

eraIs1 worms expressing human α-synuclein tagged with mVenus under the *dat-1* promoter (Vozdek et al., 2022b) in WT, *ced-1(e1754),* and *nsIs180* background were synchronized by picking L4 worms from a mixed stage plate and culturing them at 20ºC. Animals were transferred daily to segregate from newly molted adults. The 4 CEP neurons were monitored on Adult Day 6 for neurodegeneration. The CEP neurons were scored for intact and visible cell bodies like in the 6-OHDA scoring protocol.

Behavior assays

Swimming induced paralysis (SWIP): Animals were examined for swimming induced paralysis in deionized water as previously described (Hardaway et al., 2015; McDonald et al., 2007). In brief, L4 animals were picked from a mixed-stage plate and placed in 20µL of deionized water on a glass coverslip. Animals were monitored for body bends every 5 minutes for 20 minutes. Animals that performed a full body bend were labeled “swimming” whereas animals that could not perform a full body bend were labeled “not-swimming.”

Swimming induced paralysis in dopamine (SWIP-DA): Animals were examined for swimming induced paralysis with the addition of exogenous dopamine as previously described (Clark et al., 2024). In brief, L3 animals underwent either a 1h 6-OHDA (50mM) or control treatment and allowed to recover for 72h. 8-10 animals were then placed in 20µL of a 300µM solution of dopamine-hydrochloride (Sigma CAS #62-31-7) in deionized water on a glass coverslip. Animals were monitored for body bends every minute for 15 minutes. Animals that performed a full body bend were labeled "swimming" whereas animals that could not perform a full body bend were labeled "not-swimming."

Basal slowing response: Animals were examined for the basal slowing response as previously described (Petratou et al., 2024; Sawin et al., 2000). In brief, L3 animals underwent either a 1h 6-OHDA (50mM) or control treatment and allowed to recover for 72h. 5-7 animals were then picked and transferred through three 20µL drops of M9 on a coverslip to remove any bacteria on their body. Washed worms were then placed onto unseeded and seeded NGM plates with HB101. Worms were allowed to recover for 2 minutes before taking 5-minute videos of their locomotion. Videos were manually scored for body bends over a continuous 20 second period. Each worm was only counted once. A body bend is considered complete when the head area moves to the opposite direction (Petratou et al., 2024). Body bends were counted for both forward and backward locomotion. On NGM plates with HB101, body bend counts were done only on animals that had entered the bacterial lawn.

RTq-PCR

To evaluate changes in *ced-1* expression after 6-OHDA exposure, N2 L3 worms were treated with 50mM 6-OHDA or without 6-OHDA for 1 hour and then prepped for RNA isolation 24 hours later. To evaluate changes in *glt-1, glt-3, ced-1, cat-2, cat-1,* and *dat-1* expression in CEPsh ablated animals, L3 N2 and CEPsh ablated animals were isolated from a mixed stage 6 cm plate using filters. For all experiments, RNA for at least three independent biological replicates was isolated using TRIzol and Direct-zol RNA extraction kit protocols, with modifications. Briefly, worms were incubated in TRIzol at room temperature for 10 minutes and occasionally vortexed. Worms were then flash frozen in liquid nitrogen, thawed at 37ºC on a heat block and then vortexed for 1 min. Thaw/freeze/vortex cycle was repeated 5x. Worms were then placed at -80°C before all biological replicate samples were ready for RNA extraction. RNA was purified via the Direct-zol RNA extraction kit, quantified via nanodrop, normalized to 100ng, and transcribed into cDNA using QuantiTect RT kit. RT-qPCR was performed in three technical replicates on each biological sample using TaqMan primers. A no template control was run alongside each biological replicate.

Statistical Analysis

All statistical analysis was performed using GraphPad Prism 11. To evaluate changes in CEP neurodegeneration, a Fisher's Exact Test was used. To compare changes in fluorescence intensities, a two-tailed t-test was used unless otherwise stated. To compare changes in gene expression from RT-qPCR data, RQ values were averaged for each condition and compared using a two-tailed t-test with or without Welch's correction depending on the standard deviation.

Western Blot

Immunoblotting was done as reported with modifications (Yuan et al., 2022). L3 *smIs34* worms underwent a 1h 50mM 6-OHDA or control treatment and allowed to recover for 24h or 40h before being cleaned and collected in M9 buffer and stored at -80^{O}C. After thawing, worms were resuspended in RIPA lysis buffer (25 mM Tris–HCl, pH 7.4, 150 mM NaCl, 1% sodium deoxycholate, 0.1% SDS) containing the HALT protease inhibitor cocktail (Thermo Fisher Scientific ref. 78441), homogenized completely with a mechanical mortar and pestle, and centrifuged at 15,000 × *g* at 4°C for 20 min to remove debris. Protein samples were quantified by the BCA method, then 20–30 µg samples containing 1×SDS loading buffer with 5% 2-mercaptoethanol were boiled at 100°C for 5 min. Protein samples were loaded onto a 10% Tris-Glycine gel and transferred onto mini 0.2 µm PVDF membranes using the Trans-Blot Turbo system (Bio-Rad ref. 1704156), probed with the mouse anti-GFP primary antibody (Santa Cruz Biotechnologies, ref. sc-9996)(1:1000) and a goat anti-mouse HRP-conjugated secondary antibody (Thermo Fisher ref. AB_2533947) (1:250), and developed with the Clarity Max™ Western ECL substrate (Biorad ref. 1705062).

REFERENCES

Abbott, N.J., 2002. Astrocyte–endothelial interactions and blood–brain barrier permeability. J. Anat. 200, 629–638. https://doi.org/10.1046/j.1469-7580.2002.00064.x

Allen, N.J., Eroglu, C., 2017. Cell Biology of Astrocyte-Synapse Interactions. Neuron 96, 697–708. https://doi.org/10.1016/j.neuron.2017.09.056

Barcomb, K., Ford, C.P., 2023. Alterations in neurotransmitter co-release in Parkinson's disease. Exp. Neurol. 370, 114562. https://doi.org/10.1016/j.expneurol.2023.114562

Bertrand, V., Hobert, O., 2009. Linking Asymmetric Cell Division to the Terminal Differentiation Program of Postmitotic Neurons in *C. elegans*. Dev. Cell 16, 563–575. https://doi.org/10.1016/j.devcel.2009.02.011

Bigdai, E.V., Samoilov, V.O., 2022. Role of Neurotransmitters in the Functioning of Olfactory Sensory Neurons. J. Evol. Biochem. Physiol. 58, 865–874. https://doi.org/10.1134/S0022093022030206

Blum, D., Torch, S., Lambeng, N., Nissou, M.-F., Benabid, A.-L., Sadoul, R., Verna, J.-M., 2001. Molecular pathways involved in the neurotoxicity of 6-OHDA, dopamine and MPTP: contribution to the apoptotic theory in Parkinson's disease. Prog. Neurobiol. 65, 135–172. https://doi.org/10.1016/S0301-0082(01)00003-X

Braak, H., Del Tredici, K., Rüb, U., de Vos, R.A.I., Jansen Steur, E.N.H., Braak, E., 2003. Staging of brain pathology related to sporadic Parkinson's disease. Neurobiol. Aging 24, 197–211. https://doi.org/10.1016/s0197-4580(02)00065-9

Brenner, S., 1974. The Genetics of CAENORHABDITIS ELEGANS. Genetics 77, 71–94.

Chalazonitis, A., Rao, M., Sulzer, D., 2022. Similarities and differences between nigral and enteric dopaminergic neurons unravel distinctive involvement in Parkinson's disease. Npj Park. Dis. 8, 1–16. https://doi.org/10.1038/s41531-022-00308-9

Chang, K.-H., Chen, C.-M., 2020. The Role of Oxidative Stress in Parkinson's Disease. Antioxidants 9, 597. https://doi.org/10.3390/antiox9070597

Chase, D.L., Pepper, J.S., Koelle, M.R., 2004. Mechanism of extrasynaptic dopamine signaling in Caenorhabditis elegans. Nat. Neurosci. 7, 1096–1103. https://doi.org/10.1038/nn1316

Chelur, D.S., Chalfie, M., 2007. Targeted cell killing by reconstituted caspases. Proc. Natl. Acad. Sci. U. S. A. 104, 2283–2288. https://doi.org/10.1073/pnas.0610877104

Chen, Y.-Z., Klöditz, K., Lee, E.-S., Nguyen, D.P., Yuan, Q., Johnson, J., Lee-yow, Y., Hall, A., Mitani, S., Xia, N.-S., Fadeel, B., Xue, D., 2019. Structure and function analysis of the *C. elegans* aminophospholipid translocase TAT-1. J. Cell Sci. 132, jcs227660. https://doi.org/10.1242/jcs.227660

Chisholm, A.D., Horvitz, H.R., 1995. Patterning of the Caenorhabditis elegans head region by the Pax-6 family member vab-3. Nature 377, 52–55. https://doi.org/10.1038/377052a0

Chiu, H., Zou, Y., Suzuki, N., Hsieh, Y.-W., Chuang, C.-F., Wu, Y.-C., Chang, C., 2018. Engulfing cells promote neuronal regeneration and remove neuronal debris through distinct biochemical functions of CED-1. Nat. Commun. 9, 4842. https://doi.org/10.1038/s41467-018-07291-x

Chung, W.-S., Clarke, L.E., Wang, G.X., Stafford, B.K., Sher, A., Chakraborty, C., Joung, J., Foo, L.C., Thompson, A., Chen, C., Smith, S.J., Barres, B.A., 2013. Astrocytes mediate synapse elimination through MEGF10 and MERTK pathways. Nature 504, 394–400. https://doi.org/10.1038/nature12776

Clairembault, T., Leclair-Visonneau, L., Coron, E., Bourreille, A., Le Dily, S., Vavasseur, F., Heymann, M.-F., Neunlist, M., Derkinderen, P., 2015. Structural alterations of the intestinal epithelial barrier in Parkinson's disease. Acta Neuropathol. Commun. 3, 12. https://doi.org/10.1186/s40478-015-0196-0

Clark, A.S., Huayta, J., Morton, K.S., Meyer, J.N., San-Miguel, A., 2024. Morphological hallmarks of dopaminergic neurodegeneration are associated with altered neuron function in Caenorhabditis elegans. Neurotoxicology 100, 100–106. https://doi.org/10.1016/j.neuro.2023.12.005

Cohen-Adiv, S., Amer-Sarsour, F., Berdichevsky, Y., Boxer, E., Goldstein, O., Gana-Weisz, M., Tripathi, U., Rike, W.A., Prag, G., Gurevich, T., Giladi, N., Stern, S., Orr-Urtreger, A., Friedmann-Morvinski, D., Ashkenazi, A., 2024. TMEM16F regulates pathologic α-synuclein secretion and spread in cellular and mouse models of Parkinson's disease. Aging Cell e14387. https://doi.org/10.1111/acel.14387

Conradt, B., Wu, Y.-C., Xue, D., 2016. Programmed Cell Death During Caenorhabditis elegans Development. Genetics 203, 1533–1562. https://doi.org/10.1534/genetics.115.186247

Cook, S.J., Jarrell, T.A., Brittin, C.A., Wang, Y., Bloniarz, A.E., Yakovlev, M.A., Nguyen, K.C.Q., Tang, L.T.-H., Bayer, E.A., Duerr, J.S., Bülow, H.E., Hobert, O., Hall, D.H., Emmons, S.W., 2019. Whole-animal connectomes of both Caenorhabditis elegans sexes. Nature 571, 63–71. https://doi.org/10.1038/s41586-019-1352-7

Coutinho-Budd, J., Freeman, M.R., Ackerman, S., 2024. Glial Regulation of Circuit Wiring, Firing, and Expiring in the Drosophila Central Nervous System. Cold Spring Harb. Perspect. Biol. 16, a041347. https://doi.org/10.1101/cshperspect.a041347

Damier, P., Hirsch, E.C., Agid, Y., Graybiel, A.M., 1999. The substantia nigra of the human brain. II. Patterns of loss of dopamine-containing neurons in Parkinson's disease. Brain J. Neurol. 122 (Pt 8), 1437–1448. https://doi.org/10.1093/brain/122.8.1437

Darland-Ransom, M., Wang, X., Sun, C.-L., Mapes, J., Gengyo-Ando, K., Mitani, S., Xue, D., 2008. Role of *C. elegans* TAT-1 protein in maintaining plasma membrane phosphatidylserine asymmetry. Science 320, 528–531. https://doi.org/10.1126/science.1155847

Day, J.O., Mullin, S., 2021. The Genetics of Parkinson's Disease and Implications for Clinical Practice. Genes 12, 1006. https://doi.org/10.3390/genes12071006

de Ceglia, R., Ledonne, A., Litvin, D.G., Lind, B.L., Carriero, G., Latagliata, E.C., Bindocci, E., Di Castro, M.A., Savtchouk, I., Vitali, I., Ranjak, A., Congiu, M., Canonica, T., Wisden, W., Harris, K., Mameli, M., Mercuri, N., Telley, L., Volterra, A., 2023. Specialized astrocytes mediate glutamatergic gliotransmission in the CNS. Nature 622, 120–129. https://doi.org/10.1038/s41586-023-06502-w

Derk, J., Jones, H.E., Como, C., Pawlikowski, B., Siegenthaler, J.A., 2021. Living on the Edge of the CNS: Meninges Cell Diversity in Health and Disease. Front. Cell. Neurosci. 15. https://doi.org/10.3389/fncel.2021.703944

Dias, V., Junn, E., Mouradian, M.M., 2013. The Role of Oxidative Stress in Parkinson's Disease. J. Park. Dis. 3, 461. https://doi.org/10.3233/JPD-130230

Dickson, D.W., Braak, H., Duda, J.E., Duyckaerts, C., Gasser, T., Halliday, G.M., Hardy, J., Leverenz, J.B., Del Tredici, K., Wszolek, Z.K., Litvan, I., 2009. Neuropathological assessment of Parkinson's disease: refining the diagnostic criteria. Lancet Neurol. 8, 1150–1157. https://doi.org/10.1016/S1474-4422(09)70238-8

Doherty, J., Sheehan, A.E., Bradshaw, R., Fox, A.N., Lu, T.-Y., Freeman, M.R., 2014. PI3K Signaling and Stat92E Converge to Modulate Glial Responsiveness to Axonal Injury. PLOS Biol. 12, e1001985. https://doi.org/10.1371/journal.pbio.1001985

Dorsey, E.R., Sherer, T., Okun, M.S., Bloem, B.R., n.d. The Emerging Evidence of the Parkinson Pandemic. J. Park. Dis. 8, S3–S8. https://doi.org/10.3233/JPD-181474

Fearnley, J.M., Lees, A.J., 1991. Ageing and Parkinson's disease: substantia nigra regional selectivity. Brain J. Neurol. 114 (Pt 5), 2283–2301. https://doi.org/10.1093/brain/114.5.2283

Feinberg, E.H., Vanhoven, M.K., Bendesky, A., Wang, G., Fetter, R.D., Shen, K., Bargmann, C.I., 2008. GFP Reconstitution Across Synaptic Partners (GRASP) defines cell contacts and synapses in living nervous systems. Neuron 57, 353–363. https://doi.org/10.1016/j.neuron.2007.11.030

Fuentes-Medel, Y., Logan, M.A., Ashley, J., Ataman, B., Budnik, V., Freeman, M.R., 2009. Glia and Muscle Sculpt Neuromuscular Arbors by Engulfing Destabilized Synaptic Boutons and Shed Presynaptic Debris. PLoS Biol. 7, e1000184. https://doi.org/10.1371/journal.pbio.1000184

Fullard, M.E., Morley, J.F., Duda, J.E., 2017. Olfactory Dysfunction as an Early Biomarker in Parkinson's Disease. Neurosci. Bull. 33, 515–525. https://doi.org/10.1007/s12264-017-0170-x

Furuta, Y., Pena-Ramos, O., Li, Z., Chiao, L., Zhou, Z., 2021. Calcium ions trigger the exposure of phosphatidylserine on the surface of necrotic cells. PLoS Genet. 17, e1009066. https://doi.org/10.1371/journal.pgen.1009066

Gaeta, A.L., Caldwell, K.A., Caldwell, G.A., 2019. Found in Translation: The Utility of *C. elegans* A-synuclein Models of Parkinson's Disease. Brain Sci. 9, 73. https://doi.org/10.3390/brainsci9040073

Gibbons, C.H., Levine, T., Adler, C., Bellaire, B., Wang, N., Stohl, J., Agarwal, P., Aldridge, G.M., Barboi, A., Evidente, V.G.H., Galasko, D., Geschwind, M.D., Gonzalez-Duarte, A., Gil, R., Gudesblatt, M., Isaacson, S.H., Kaufmann, H., Khemani, P., Kumar, R., Lamotte, G., Liu, A.J., McFarland, N.R., Miglis, M., Reynolds, A., Sahagian, G.A., Saint-Hillaire, M.-H., Schwartzbard, J.B., Singer, W., Soileau, M.J., Vernino, S., Yerstein, O., Freeman, R., 2024. Skin Biopsy Detection of Phosphorylated α-Synuclein in Patients With Synucleinopathies. JAMA 331, 1298–1306. https://doi.org/10.1001/jama.2024.0792

Gibson, C.L., Balbona, J.T., Niedzwiecki, A., Rodriguez, P., Nguyen, K.C.Q., Hall, D.H., Blakely, R.D., 2018. Glial loss of the metallo β-lactamase domain containing protein, SWIP-10, induces age- and glutamate-signaling dependent, dopamine neuron degeneration. PLoS Genet. 14, e1007269. https://doi.org/10.1371/journal.pgen.1007269

Gilleard, J.S., Barry, J.D., Johnstone, I.L., 1997. cis Regulatory Requirements for Hypodermal Cell-Specific Expression of the Caenorhabditis elegans Cuticle Collagen Gene dpy-7. Mol. Cell. Biol. 17, 2301–2311. https://doi.org/10.1128/MCB.17.4.2301

Gómez-Benito, M., Granado, N., García-Sanz, P., Michel, A., Dumoulin, M., Moratalla, R., 2020. Modeling Parkinson's Disease With the A-synuclein Protein. Front. Pharmacol. 11, 356. https://doi.org/10.3389/fphar.2020.00356

Goudeau, J., Sharp, C.S., Paw, J., Savy, L., Leonetti, M.D., York, A.G., Updike, D.L., Kenyon, C., Ingaramo, M., 2021. Split-wrmScarlet and split-sfGFP: tools for faster, easier

fluorescent labeling of endogenous proteins in Caenorhabditis elegans. Genetics 217, iyab014. https://doi.org/10.1093/genetics/iyab014
Gulbransen, B.D., Sharkey, K.A., 2012. Novel functional roles for enteric glia in the gastrointestinal tract. Nat. Rev. Gastroenterol. Hepatol. 9, 625–632. https://doi.org/10.1038/nrgastro.2012.138
Hardaway, J.A., Sturgeon, S.M., Snarrenberg, C.L., Li, Z., Xu, X.Z.S., Bermingham, D.P., Odiase, P., Spencer, W.C., Miller, D.M., Carvelli, L., Hardie, S.L., Blakely, R.D., 2015. Glial Expression of the Caenorhabditis elegans Gene swip-10 Supports Glutamate Dependent Control of Extrasynaptic Dopamine Signaling. J. Neurosci. 35, 9409–9423. https://doi.org/10.1523/JNEUROSCI.0800-15.2015
Haskins, K.A., Russell, J.F., Gaddis, N., Dressman, H.K., Aballay, A., 2008. Unfolded Protein Response Genes Regulated by CED-1 are Required for Caenorhabditis elegans Innate Immunity. Dev. Cell 15, 87–97. https://doi.org/10.1016/j.devcel.2008.05.006
Hernandez-Baltazar, D., Zavala-Flores, L.M., Villanueva-Olivo, A., 2017. The 6-hydroxydopamine model and parkinsonian pathophysiology: Novel findings in an older model. Neurol. Barc. Spain 32, 533–539. https://doi.org/10.1016/j.nrl.2015.06.011
Hoeppner, D.J., Hengartner, M.O., Schnabel, R., 2001. Engulfment genes cooperate with ced-3 to promote cell death in Caenorhabditis elegans. Nature 412, 202–206. https://doi.org/10.1038/35084103
Hong, S., Beja-Glasser, V.F., Nfonoyim, B.M., Frouin, A., Li, S., Ramakrishnan, S., Merry, K.M., Shi, Q., Rosenthal, A., Barres, B.A., Lemere, C.A., Selkoe, D.J., Stevens, B., 2016. Complement and microglia mediate early synapse loss in Alzheimer mouse models. Science 352, 712–716. https://doi.org/10.1126/science.aad8373
Hsieh, H.-H., Hsu, T.-Y., Jiang, H.-S., Wu, Y.-C., 2012. Integrin α PAT-2/CDC-42 signaling is required for muscle-mediated clearance of apoptotic cells in Caenorhabditis elegans. PLoS Genet. 8, e1002663. https://doi.org/10.1371/journal.pgen.1002663
Iovino, L., Tremblay, M.E., Civiero, L., 2020. Glutamate-induced excitotoxicity in Parkinson's disease: The role of glial cells. J. Pharmacol. Sci. 144, 151–164. https://doi.org/10.1016/j.jphs.2020.07.011
Iram, T., Ramirez-Ortiz, Z., Byrne, M.H., Coleman, U.A., Kingery, N.D., Means, T.K., Frenkel, D., El Khoury, J., 2016. Megf10 Is a Receptor for C1Q That Mediates Clearance of Apoptotic Cells by Astrocytes. J. Neurosci. 36, 5185–5192. https://doi.org/10.1523/JNEUROSCI.3850-15.2016
Jiang, Y., Horner, V., Liu, J., 2005. The HMX homeodomain protein MLS-2 regulates cleavage orientation, cell proliferation and cell fate specification in the *C. elegans*postembryonic mesoderm. Development 132, 4119–4130. https://doi.org/10.1242/dev.01967
Johnsen, H.L., Horvitz, H.R., 2016. Both the apoptotic suicide pathway and phagocytosis are required for a programmed cell death in Caenorhabditis elegans. BMC Biol. 14, 39. https://doi.org/10.1186/s12915-016-0262-5
Kam, T.-I., Park, H., Chou, S.-C., Van Vranken, J.G., Mittenbühler, M.J., Kim, H., A, M., Choi, Y.R., Biswas, D., Wang, J., Shin, Y., Loder, A., Karuppagounder, S.S., Wrann, C.D., Dawson, V.L., Spiegelman, B.M., Dawson, T.M., 2022. Amelioration of pathologic α-synuclein-induced Parkinson's disease by irisin. Proc. Natl. Acad. Sci. 119, e2204835119. https://doi.org/10.1073/pnas.2204835119

Katz, M., Corson, F., Iwanir, S., Biron, D., Shaham, S., 2018. Glia Modulate a Neuronal Circuit for Locomotion Suppression during Sleep in *C. elegans*. Cell Rep. 22, 2575–2583. https://doi.org/10.1016/j.celrep.2018.02.036

Katz, M., Corson, F., Keil, W., Singhal, A., Bae, A., Lu, Y., Liang, Y., Shaham, S., 2019. Glutamate spillover in *C. elegans* triggers repetitive behavior through presynaptic activation of MGL-2/mGluR5. Nat. Commun. 10, 1882. https://doi.org/10.1038/s41467-019-09581-4

Khakh, B.S., Sofroniew, M.V., 2015. Diversity of astrocyte functions and phenotypes in neural circuits. Nat. Neurosci. 18, 942–952. https://doi.org/10.1038/nn.4043

Langen, U.H., Ayloo, S., Gu, C., 2019. Development and Cell Biology of the Blood-Brain Barrier. Annu. Rev. Cell Dev. Biol. 35, 591–613. https://doi.org/10.1146/annurev-cellbio-100617-062608

Lee, K.H., Cha, M., Lee, B.H., 2021. Crosstalk between Neuron and Glial Cells in Oxidative Injury and Neuroprotection. Int. J. Mol. Sci. 22, 13315. https://doi.org/10.3390/ijms222413315

Li, Z., Venegas, V., Nagaoka, Y., Morino, E., Raghavan, P., Audhya, A., Nakanishi, Y., Zhou, Z., 2015. Necrotic Cells Actively Attract Phagocytes through the Collaborative Action of Two Distinct PS-Exposure Mechanisms. PLoS Genet. 11, e1005285. https://doi.org/10.1371/journal.pgen.1005285

Lipski, J., Nistico, R., Berretta, N., Guatteo, E., Bernardi, G., Mercuri, N.B., 2011. l-DOPA: A scapegoat for accelerated neurodegeneration in Parkinson's disease? Prog. Neurobiol. 94, 389–407. https://doi.org/10.1016/j.pneurobio.2011.06.005

Liu, K.E., Raymond, M.H., Ravichandran, K.S., Kucenas, S., 2022. Clearing Your Mind: Mechanisms of Debris Clearance After Cell Death During Neural Development. Annu. Rev. Neurosci. 45, 177–198. https://doi.org/10.1146/annurev-neuro-110920-022431

Lu, T.-Y., MacDonald, J.M., Neukomm, L.J., Sheehan, A.E., Bradshaw, R., Logan, M.A., Freeman, M.R., 2017. Axon degeneration induces glial responses through Draper-TRAF4-JNK signalling. Nat. Commun. 8, 14355. https://doi.org/10.1038/ncomms14355

MacDonald, J.M., Beach, M.G., Porpiglia, E., Sheehan, A.E., Watts, R.J., Freeman, M.R., 2006. The Drosophila cell corpse engulfment receptor Draper mediates glial clearance of severed axons. Neuron 50, 869–881. https://doi.org/10.1016/j.neuron.2006.04.028

Mapes, J., Chen, Y.-Z., Kim, A., Mitani, S., Kang, B.-H., Xue, D., 2012. CED-1, CED-7, and TTR-52 Regulate Surface Phosphatidylserine Expression on Apoptotic and Phagocytic Cells. Curr. Biol. 22, 1267–1275. https://doi.org/10.1016/j.cub.2012.05.052

Martin, C.G., Bent, J.S., Hill, T., Topalidou, I., Singhvi, A., 2024. Epithelial UNC-23 limits mechanical stress to maintain glia-neuron architecture in *C. elegans*. Dev. Cell 59, 1668-1688.e7. https://doi.org/10.1016/j.devcel.2024.04.005

Martin-Lopez, E., Vidyadhara, D.J., Liberia, T., Meller, S.J., Harmon, L.E., Hsu, R.M., Spence, N., Brennan, B., Han, K., Yücel, B., Chandra, S.S., Greer, C.A., 2023. α-Synuclein Pathology and Reduced Neurogenesis in the Olfactory System Affect Olfaction in a Mouse Model of Parkinson's Disease. J. Neurosci. Off. J. Soc. Neurosci. 43, 1051–1071. https://doi.org/10.1523/JNEUROSCI.1526-22.2022

Masoudi, N., Ibanez-Cruceyra, P., Offenburger, S.-L., Holmes, A., Gartner, A., 2014. Tetraspanin (TSP-17) protects dopaminergic neurons against 6-OHDA-induced neurodegeneration in *C. elegans*. PLoS Genet. 10, e1004767. https://doi.org/10.1371/journal.pgen.1004767

McCarroll, S.A., Li, H., Bargmann, C.I., 2005. Identification of Transcriptional Regulatory Elements in Chemosensory Receptor Genes by Probabilistic Segmentation. Curr. Biol. 15, 347–352. https://doi.org/10.1016/j.cub.2005.02.023

McDonald, P.W., Hardie, S.L., Jessen, T.N., Carvelli, L., Matthies, D.S., Blakely, R.D., 2007. Vigorous motor activity in Caenorhabditis elegans requires efficient clearance of dopamine mediated by synaptic localization of the dopamine transporter DAT-1. J. Neurosci. Off. J. Soc. Neurosci. 27, 14216–14227. https://doi.org/10.1523/JNEUROSCI.2992-07.2007

Mello, C.C., Kramer, J.M., Stinchcomb, D., Ambros, V., 1991. Efficient gene transfer in C.elegans: extrachromosomal maintenance and integration of transforming sequences. EMBO J. 10, 3959–3970. https://doi.org/10.1002/j.1460-2075.1991.tb04966.x

Miyabayashi, T., Palfreyman, M.T., Sluder, A.E., Slack, F., Sengupta, P., 1999. Expression and Function of Members of a Divergent Nuclear Receptor Family in *Caenorhabditis elegans*. Dev. Biol. 215, 314–331. https://doi.org/10.1006/dbio.1999.9470

Morales, I., Sanchez, A., Rodriguez-Sabate, C., Rodriguez, M., 2017. Striatal astrocytes engulf dopaminergic debris in Parkinson's disease: A study in an animal model. PloS One 12, e0185989. https://doi.org/10.1371/journal.pone.0185989

Moskal, N., Visanji, N.P., Gorbenko, O., Narasimhan, V., Tyrrell, H., Nash, J., Lewis, P.N., McQuibban, G.A., 2023. An AI-guided screen identifies probucol as an enhancer of mitophagy through modulation of lipid droplets. PLoS Biol. 21, e3001977. https://doi.org/10.1371/journal.pbio.3001977

Murphy, K.T., Lynch, G.S., 2023. Impaired skeletal muscle health in Parkinsonian syndromes: clinical implications, mechanisms and potential treatments. J. Cachexia Sarcopenia Muscle 14, 1987–2002. https://doi.org/10.1002/jcsm.13312

Nass, R., Blakely, R.D., 2003. The Caenorhabditis elegans Dopaminergic System: Opportunities for Insights into Dopamine Transport and Neurodegeneration. Annu. Rev. Pharmacol. Toxicol. 43, 521–544. https://doi.org/10.1146/annurev.pharmtox.43.100901.135934

Nass, R., Hall, D.H., Miller, D.M., Blakely, R.D., 2002. Neurotoxin-induced degeneration of dopamine neurons in Caenorhabditis elegans. Proc. Natl. Acad. Sci. 99, 3264–3269. https://doi.org/10.1073/pnas.042497999

Nichols, A.L.A., Meelkop, E., Linton, C., Giordano-Santini, R., Sullivan, R.K., Donato, A., Nolan, C., Hall, D.H., Xue, D., Neumann, B., Hilliard, M.A., 2016. The Apoptotic Engulfment Machinery Regulates Axonal Degeneration in *C. elegans* Neurons. Cell Rep. 14, 1673–1683. https://doi.org/10.1016/j.celrep.2016.01.050

Offenburger, S.-L., Ho, X.Y., Tachie-Menson, T., Coakley, S., Hilliard, M.A., Gartner, A., 2018a. 6-OHDA-induced dopaminergic neurodegeneration in Caenorhabditis elegans is promoted by the engulfment pathway and inhibited by the transthyretin-related protein TTR-33. PLoS Genet. 14. https://doi.org/10.1371/journal.pgen.1007125

Offenburger, S.-L., Jongsma, E., Gartner, A., 2018b. Mutations in Caenorhabditis elegans neuroligin-like glit-1, the apoptosis pathway and the calcium chaperone crt-1 increase dopaminergic neurodegeneration after 6-OHDA treatment. PLoS Genet. 14. https://doi.org/10.1371/journal.pgen.1007106

Peterman, E., Quitevis, E.J.A., Black, E.C., Horton, E.C., Aelmore, R.L., White, E., Sagasti, A., Rasmussen, J.P., 2023. Zebrafish cutaneous injury models reveal that Langerhans cells engulf axonal debris in adult epidermis. Dis. Model. Mech. 16, dmm049911. https://doi.org/10.1242/dmm.049911

Pierce, M.L., Weston, M.D., Fritzsch, B., Gabel, H.W., Ruvkun, G., Soukup, G.A., 2008. MicroRNA-183 family conservation and ciliated neurosensory organ expression. Evol. Dev. 10, 106–113. https://doi.org/10.1111/j.1525-142X.2007.00217.x

Poewe, W., Seppi, K., Tanner, C.M., Halliday, G.M., Brundin, P., Volkmann, J., Schrag, A.-E., Lang, A.E., 2017. Parkinson disease. Nat. Rev. Dis. Primer 3, 1–21. https://doi.org/10.1038/nrdp.2017.13

Purice, M.D., Quitevis, E.J.A., Manning, R.S., Severs, L.J., Tran, N.-T., Sorrentino, V., Setty, M., Singhvi, A., 2023. Molecular heterogeneity of *C. elegans* glia across sexes. BioRxiv Prepr. Serv. Biol. 2023.03.21.533668. https://doi.org/10.1101/2023.03.21.533668

Purice, M.D., Severs, L.J., Singhvi, A., 2024. Glia in Invertebrate Models: Insights from Caenorhabditis elegans, in: Blanco-Suarez, E., Farhy-Tselnicker, I. (Eds.), Astrocyte-Neuron Interactions in Health and Disease. Springer Nature Switzerland, Cham, pp. 19–49. https://doi.org/10.1007/978-3-031-64839-7_2

Raiders, S., Black, E.C., Bae, A., MacFarlane, S., Klein, M., Shaham, S., Singhvi, A., 2021a. Glia actively sculpt sensory neurons by controlled phagocytosis to tune animal behavior. eLife 10, e63532. https://doi.org/10.7554/eLife.63532

Raiders, S., Han, T., Scott-Hewitt, N., Kucenas, S., Lew, D., Logan, M.A., Singhvi, A., 2021b. Engulfed by Glia: Glial Pruning in Development, Function, and Injury across Species. J. Neurosci. 41, 823. https://doi.org/10.1523/JNEUROSCI.1660-20.2020

Rapti, G., Li, C., Shan, A., Lu, Y., Shaham, S., 2017. Glia initiate brain assembly through non-canonical Chimaerin/Furin axon guidance in *C. elegans*. Nat. Neurosci. 20, 1350. https://doi.org/10.1038/nn.4630

Ray, A., Speese, S.D., Logan, M.A., 2017. Glial Draper Rescues Aβ Toxicity in a Drosophila Model of Alzheimer's Disease. J. Neurosci. Off. J. Soc. Neurosci. 37, 11881–11893. https://doi.org/10.1523/JNEUROSCI.0862-17.2017

Reddien, P.W., Cameron, S., Horvitz, H.R., 2001. Phagocytosis promotes programmed cell death in *C. elegans*. Nature 412, 198–202. https://doi.org/10.1038/35084096

Reddien, P.W., Horvitz, H.R., 2004. The engulfment process of programmed cell death in caenorhabditis elegans. Annu. Rev. Cell Dev. Biol. 20, 193–221. https://doi.org/10.1146/annurev.cellbio.20.022003.114619

Reemst, K., Noctor, S.C., Lucassen, P.J., Hol, E.M., 2016. The Indispensable Roles of Microglia and Astrocytes during Brain Development. Front. Hum. Neurosci. 10, 566. https://doi.org/10.3389/fnhum.2016.00566

Rueda-Carrasco, J., Sokolova, D., Lee, S., Childs, T., Jurčáková, N., Crowley, G., De Schepper, S., Ge, J.Z., Lachica, J.I., Toomey, C.E., Freeman, O.J., Hardy, J., Barnes, S.J., Lashley, T., Stevens, B., Chang, S., Hong, S., 2023. Microglia-synapse engulfment via PtdSer-TREM2 ameliorates neuronal hyperactivity in Alzheimer's disease models. EMBO J. 42, e113246. https://doi.org/10.15252/embj.2022113246

Sawin, E.R., Ranganathan, R., Horvitz, H.R., 2000. *C. elegans* locomotory rate is modulated by the environment through a dopaminergic pathway and by experience through a serotonergic pathway. Neuron 26, 619–631. https://doi.org/10.1016/s0896-6273(00)81199-x

Schober, A., 2004. Classic toxin-induced animal models of Parkinson's disease: 6-OHDA and MPTP. Cell Tissue Res. 318, 215–224. https://doi.org/10.1007/s00441-004-0938-y

Singh, T.D., Park, S.-Y., Bae, J., Yun, Y., Bae, Y.-C., Park, R.-W., Kim, I.-S., 2010. MEGF10 functions as a receptor for the uptake of amyloid-β. FEBS Lett. 584, 3936–3942. https://doi.org/10.1016/j.febslet.2010.08.050
Singhvi, A., Shaham, S., Rapti, G., 2024. Glia Development and Function in the Nematode Caenorhabditis elegans. Cold Spring Harb. Perspect. Biol. a041346. https://doi.org/10.1101/cshperspect.a041346
Stiernagle, T., 2006. Maintenance of *C. elegans*, in: WormBook: The Online Review of C. Elegans Biology [Internet]. WormBook.
Sulston, J., Dew, M., Brenner, S., 1975. Dopaminergic neurons in the nematode Caenorhabditis elegans. J. Comp. Neurol. 163, 215–226. https://doi.org/10.1002/cne.901630207
Sulston, J.E., Schierenberg, E., White, J.G., Thomson, J.N., 1983. The embryonic cell lineage of the nematode Caenorhabditis elegans. Dev. Biol. 100, 64–119. https://doi.org/10.1016/0012-1606(83)90201-4
Tambasco, N., Romoli, M., Calabresi, P., 2018. Levodopa in Parkinson's Disease: Current Status and Future Developments. Curr. Neuropharmacol. 16, 1239–1252. https://doi.org/10.2174/1570159X15666170510143821
Tremblay, M.-E., Cookson, M.R., Civiero, L., 2019. Glial phagocytic clearance in Parkinson's disease. Mol. Neurodegener. 14, 16. https://doi.org/10.1186/s13024-019-0314-8
Vilalta, A., Brown, G.C., 2018. Neurophagy, the phagocytosis of live neurons and synapses by glia, contributes to brain development and disease. FEBS J. 285, 3566–3575. https://doi.org/10.1111/febs.14323
Vozdek, R., Pramstaller, P.P., Hicks, A.A., 2022. Functional Screening of Parkinson's Disease Susceptibility Genes to Identify Novel Modulators of α-Synuclein Neurotoxicity in Caenorhabditis elegans. Front. Aging Neurosci. 14, 806000. https://doi.org/10.3389/fnagi.2022.806000
Wadsworth, W.G., Bhatt, H., Hedgecock, E.M., 1996. Neuroglia and pioneer neurons express UNC-6 to provide global and local netrin cues for guiding migrations in *C. elegans*. Neuron 16, 35–46. https://doi.org/10.1016/s0896-6273(00)80021-5
Wan, J., Yuan, L., Jing, H., Zheng, Q., Xiao, H., 2021. Defective apoptotic cell clearance activates innate immune response to protect Caenorhabditis elegans against pathogenic bacteria. Virulence 12, 75–83. https://doi.org/10.1080/21505594.2020.1857982
Wang, X., Li, W., Zhao, D., Liu, B., Shi, Y., Chen, B., Yang, H., Guo, P., Geng, X., Shang, Z., Peden, E., Kage-Nakadai, E., Mitani, S., Xue, D., 2010. *C. elegans* transthyretin-like protein TTR-52 mediates recognition of apoptotic cells by the CED-1 phagocyte receptor. Nat. Cell Biol. 12, 655–664. https://doi.org/10.1038/ncb2068
Wang, X., Wu, Y.-C., Fadok, V.A., Lee, M.-C., Gengyo-Ando, K., Cheng, L.-C., Ledwich, D., Hsu, P.-K., Chen, J.-Y., Chou, B.-K., Henson, P., Mitani, S., Xue, D., 2003. Cell corpse engulfment mediated by *C. elegans* phosphatidylserine receptor through CED-5 and CED-12. Science 302, 1563–1566. https://doi.org/10.1126/science.1087641
White, J.G., Southgate, E., Thomson, J.N., Brenner, S., 1986. The structure of the nervous system of the nematode Caenorhabditis elegans. Philos. Trans. R. Soc. Lond. B. Biol. Sci. 314, 1–340. https://doi.org/10.1098/rstb.1986.0056
Yamada, K., Hirotsu, T., Matsuki, M., Butcher, R.A., Tomioka, M., Ishihara, T., Clardy, J., Kunitomo, H., Iino, Y., 2010. Olfactory plasticity is regulated by pheromonal signaling in Caenorhabditis elegans. Science 329, 1647–1650. https://doi.org/10.1126/science.1192020

Yang, H., Chen, Y.-Z., Zhang, Y., Wang, X., Zhao, X., Godfroy, J.I., Liang, Q., Zhang, M., Zhang, T., Yuan, Q., Ann Royal, M., Driscoll, M., Xia, N.-S., Yin, H., Xue, D., 2015. A lysine-rich motif in the phosphatidylserine receptor PSR-1 mediates recognition and removal of apoptotic cells. Nat. Commun. 6, 5717. https://doi.org/10.1038/ncomms6717

Yang, Q., Wang, Y., Zhao, C., Pang, S., Lu, J., Chan, P., 2023. α-Synuclein aggregation causes muscle atrophy through neuromuscular junction degeneration. J. Cachexia Sarcopenia Muscle 14, 226–242. https://doi.org/10.1002/jcsm.13123

Yoshimura, S., Murray, J.I., Lu, Y., Waterston, R.H., Shaham, S., 2008. mls-2 and vab-3 Control glia development, hlh-17/Olig expression and glia-dependent neurite extension in *C. elegans*. Dev. Camb. Engl. 135, 2263–2275. https://doi.org/10.1242/dev.019547

Yuan, L., Li, P., Jing, H., Zheng, Q., Xiao, H., 2022. trim-21 promotes proteasomal degradation of CED-1 for apoptotic cell clearance in *C. elegans*. eLife 11, e76436. https://doi.org/10.7554/eLife.76436

Zhang, X., Zhang, R., Nisa Awan, M.U., Bai, J., 2022. The Mechanism and Function of Glia in Parkinson's Disease. Front. Cell. Neurosci. 16, 903469. https://doi.org/10.3389/fncel.2022.903469

Zhang, Y., Meng, X., Jiao, Z., Liu, Y., Zhang, X., Qu, S., 2020. Generation of a Novel Mouse Model of Parkinson's Disease via Targeted Knockdown of Glutamate Transporter GLT-1 in the Substantia Nigra. ACS Chem. Neurosci. 11, 406–417. https://doi.org/10.1021/acschemneuro.9b00609

Zhang, Zhu, Zhang, S., Fu, P., Zhang, Zhang, Lin, K., Ko, J.K.-S., Yung, K.K.-L., 2019. Roles of Glutamate Receptors in Parkinson's Disease. Int. J. Mol. Sci. 20, 4391. https://doi.org/10.3390/ijms20184391

Zhao, C., Wang, C., Zhang, H., Yan, W., 2023. A mini-review of the role of vesicular glutamate transporters in Parkinson's disease. Front. Mol. Neurosci. 16, 1118078. https://doi.org/10.3389/fnmol.2023.1118078

Zhou, Z., Hartwieg, E., Horvitz, H.R., 2001. CED-1 is a transmembrane receptor that mediates cell corpse engulfment in *C. elegans*. Cell 104, 43–56. https://doi.org/10.1016/s0092-8674(01)00190-8

Zou, W., Lu, Q., Zhao, D., Li, W., Mapes, J., Xie, Y., Wang, X., 2009. Caenorhabditis elegans Myotubularin MTM-1 Negatively Regulates the Engulfment of Apoptotic Cells. PLOS Genet. 5, e1000679. https://doi.org/10.1371/journal.pgen.1000679

Zuchero, J.B., Barres, B.A., 2015. Glia in mammalian development and disease. Dev. Camb. Engl. 142, 3805. https://doi.org/10.1242/dev.129304

Chapter 3

ADDITIONAL EXPERIMENTS

In this chapter, I summarize experiments I performed but were not included in the published manuscript. At the end, I also include the methods and strains used in this chapter.

CED-1 and CED-10 regulate CEP corpse clearance in L1-arrested animals

I previously showed that loss of *ced-1* protects CEP neurons from degeneration and prevents CEP corpse clearance after treatment in well-fed L3 animals. However, I also examined the role of *ced-1, psr-1,* and *ced-10* in CEP corpse clearance when L1-arrested animals are treated with 6-OHDA. In brief, adult gravid animals were allowed to lay eggs in M9 in a 96 well plate overnight (between 18-30hr). The eggs would hatch overnight and would arrest at L1 because there was no food present. The next day, these L1-arrested animals were treated with 6-OHDA for 1h and then placed onto an OP50-seeded plate and allowed to recover at 20^{o}C. These animals were examined for CEP clearance 24, 48, and 72 hours later.

I found that *ced-1* mutant animals showed less missing CEP neurons at all time points; however, by 72 hours, over 70% of CEP neurons are missing in *ced-1* mutants which is in stark contrast to L3-treated animals (Figure 1 A-C). Loss of *psr-1* had a mild effect on CEP clearance at 48h and 72h after 6-OHDA treatment and no effect at 24h (Figure 1 A-C). Finally, loss of *ced-10* seemed to protect CEP neurons from degeneration at 24h and mildly at 48h (Figure 1 A-C). These results suggest that *ced-1* is only partially necessary for CEP corpse clearance in this paradigm and another mechanism is employed to remove the corpses.

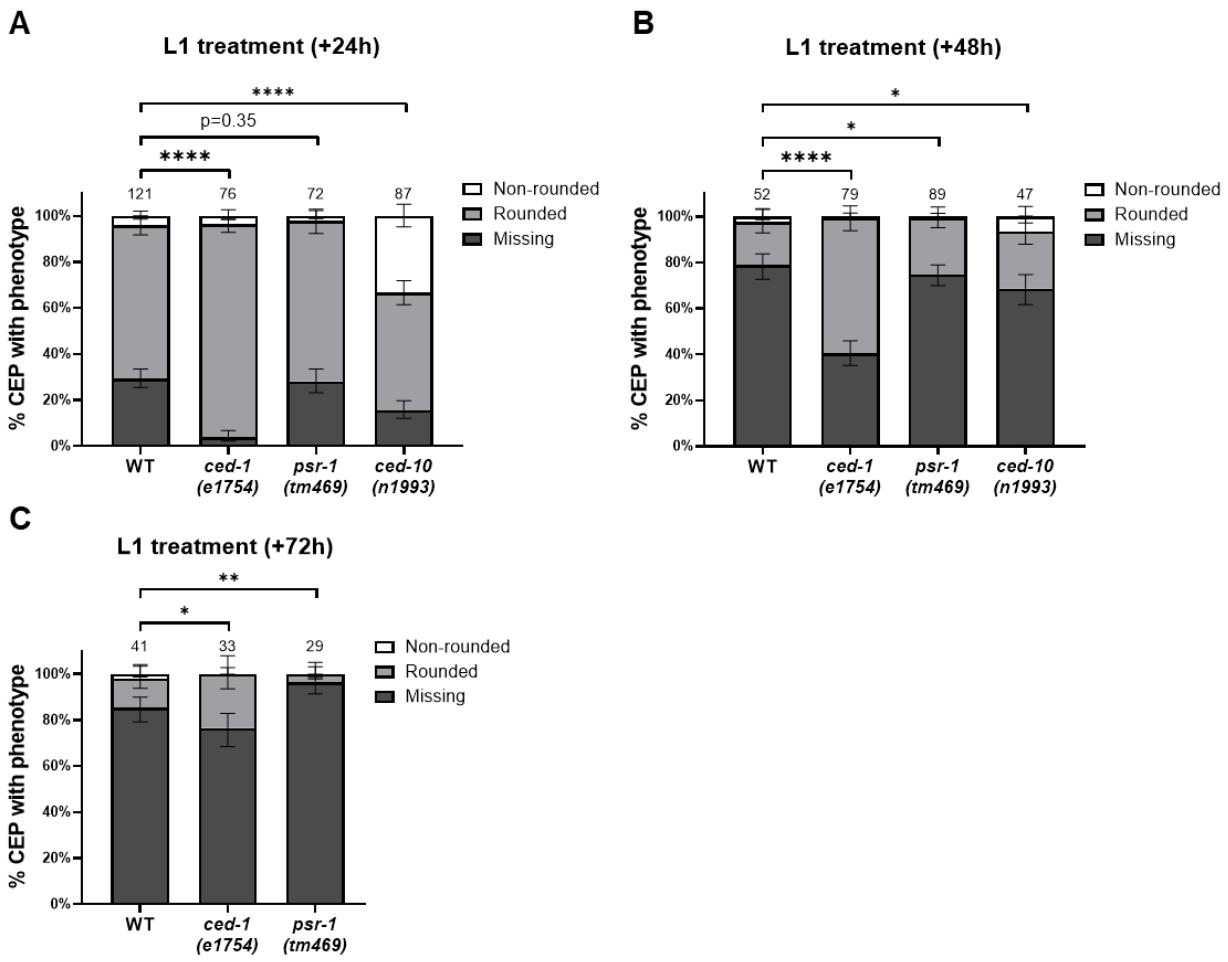

Figure 1: *ced-1, psr-1,* and *ced-10* mutants after 6-OHDA exposure

(A-C) Percentage of CEP neurons 24 hours (A), 48 hours (B), or 72 hours (C) after 50mM 6-OHDA exposure in L1-arrested WT, *ced-1(e1754)*, *psr-1(tm469)*, or *ced-10(n1993)* animals expressing the transgene *vtIs1*. Error bars = 95% confidence intervals for 2-5 biological replicates each with 10-26 animals per condition. Total animals examined is indicated above each bar. (*p<0.05, **p<0.01, ****p<0.0001, Fisher's exact test).

One possibility is that the GFP is quenched faster in younger animals because of the smaller size of the neurons in earlier larval stages. One way to mitigate this would be to examine CEP neurons using Normaski microscopy techniques which relies on the difference in contrast of dying cells compared to living cells (Lu et al., 2009). Another possibility is that the persistent CEP corpses disintegrate. Early studies on the CED genes suggested that cell corpses in embryos and early larva are more fragile than living cells and are prone to bursting before being engulfed (Ellis et al., 1991). Nonetheless, ced-1 mutants alter the clearance of CEP neurons in L1-treated animals.

The lack of CEP protection seen in *ced-1* mutants in L1 animals was also surprising given the protective role I see when treating L3 animals. One possibility is that 50mM exposure may be too high of a dose which overrides any protection that may occur in *ced-1* mutants. To determine this, future studies could use lower concentrations of 6-OHDA. Finally, another possibility is that L1-arrested animals are already protected against 6-OHDA, possibly through the same mechanism as *ced-1.* When L1-arrested animals are fed again and resume development, they upregulate ER and UPR stress genes that help them recover from their starved states (Roux et al., 2016). Indeed, a recent study found that L1-arrested animals were more resistant to 6-OHDA compared to unstarved L1 animals (Offenburger et al., 2018b). To determine if starvation is impacting *ced-1* protection against 6-OHDA, filtered L1 animals need to be tested in the assay, instead of using L1-arrested animals.

DYN-1 protects against 6-OHDA degeneration

It has been previously shown that the CED-1 engulfment pathway includes the large GTPase dynamin (DYN-1) (Yu et al., 2006). DYN-1 works downstream of CED-1 and CED-6 to

promote both pseudopod extension and phagosome maturation (Yu et al., 2006). Thus, DYN-1 is necessary for both corpse internalization and degradation. I asked whether DYN-1 was involved in the clearance of CEP corpses. To test this, I examined the heat-sensitive *dyn-1(ky51)* mutant after 6-OHDA exposure. In brief, WT and *dyn-1(ky51)* animals were raised at 20ºC, treated with 6-OHDA at L3 for 1h, and then allowed to recover on OP50 plates at 25ºC. The *dyn-51(ky51)* mutant is sensitive to higher temperatures and is unable to function at 25ºC. Loss of *dyn-1* enhanced CEP neuron degeneration at 24, 48, and 72 hours, and most neurons appeared to have degenerated within the first 24 hours (Figure 2A). This result was surprising since loss of *ced-1* prevents CEP clearance and degeneration. DYN-1 is known to have roles in axonal regeneration, so one possibility is that DYN-1 functions in CEP neurons to protect them or help them recover from 6-OHDA toxicity (Vijayaraghavan et al., 2023). It was also surprising that *dyn-1* mutants did not inhibit the removal of CEP corpses. However, when looking at previously published expression datasets, DYN-1 appears to be expressed highly in neurons (including CEP) but not in epithelial or muscle cells in larval and adult animals (Clark et al., 1997). In addition, although *dyn-1* loss has been shown to cause engulfment defects during *C. elegans* embryogenesis, *dyn-1(ky51)* mutants show no engulfment defects in embryos (Yu et al., 2006).

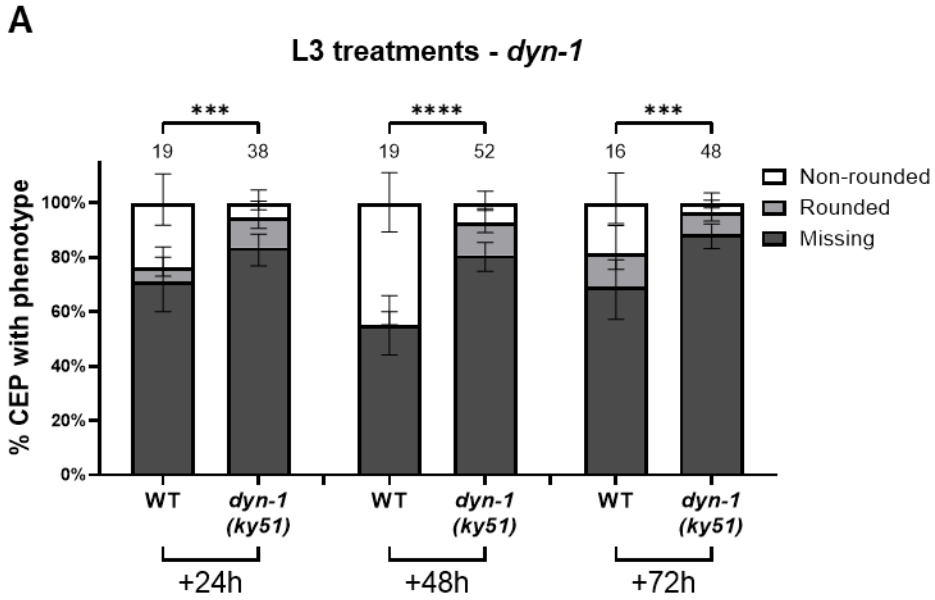

Figure 2. *dyn-1(ky51)* mutants increase CEP degeneration

(A) Percentage of CEP neurons 24 hours, 48 hours, or 72 hours after 50mM 6-OHDA exposure in L3 WT or dyn-1(ky51) animals expressing the transgene *vtIs1*. Error bars = 95% confidence intervals. 2 biological replicates each with 12-26 animals were measured for dyn-1 animals. Only one biological replicate for WT was measured. Total animals examined is indicated above each bar. (***p<0.001, ****p<0.0001, Fisher's exact test).

Interestingly, *dyn-1* also plays a role in synaptic vesicle recycling (Wu et al., 2014). Thus, the effect we are seeing could be due to its role in synaptic vesicle recycling. Indeed, *dyn-1(ky51)* mutants show almost immediate locomotory defects when shifted to higher temperatures, but they are also able to recover when shifted back down (Clark et al., 1997). This suggests a role in disrupted synaptic signaling like in *unc-13* mutants which are unable to release synaptic vesicles. Thus, these results suggest that DYN-1 may be neuroprotective against 6-OHDA by regulating synaptic vesicle release.

MEK-1 and SEK-1 protect while KGB-1 promotes CEP degeneration

Previous work has shown that JNK signaling is necessary for proper engulfment of axonal debris via CED-1 (Chiu et al., 2018). In addition, loss of function mutations in *kgb-1* and *mek-1* attenuated degeneration of CEP and ADE neurons after 6-OHDA treatment in hypersensitive *ttr-3* mutants, but not in WT animals (Offenburger et al., 2018). To determine if JNK signaling is necessary for CEP corpse engulfment, I examined *kgb-1* and *mek-1* mutant strains after 6-OHDA exposure. Loss of *kgb-1* seemed to protect CEP neurons from degeneration, but did not prevent CEP corpse engulfment (Figure 3). In contrast, loss of *mek-1* sensitized CEP neurons to 6-OHDA but also did not prevent the clearance of CEP neurons (Figure 3). *mek-1* (MAPKK) is known to act upstream of *kgb-1* (MAPK) in response to heavy metal stress or axon injury, so it is interesting to see a difference in responses to 6-OHDA. However, this mutant strain of *mek-1* is known to be tightly linked with a partial loss of function mutation in *sek-1,* another MAPKK. *sek-1* is known to be important for protection against oxidative stress and bacterial infections (Andrusiak and Jin, 2016). Thus, the increased susceptibility to 6-OHDA I see in *mek-1(ks54)* mutants could be due to the tightly linked *sek-1* mutation. Nonetheless, my studies confirmed prior findings that MAPK signaling regulates 6-OHDA toxicity in CEP neurons, as measured by my assay on corpse clearance.

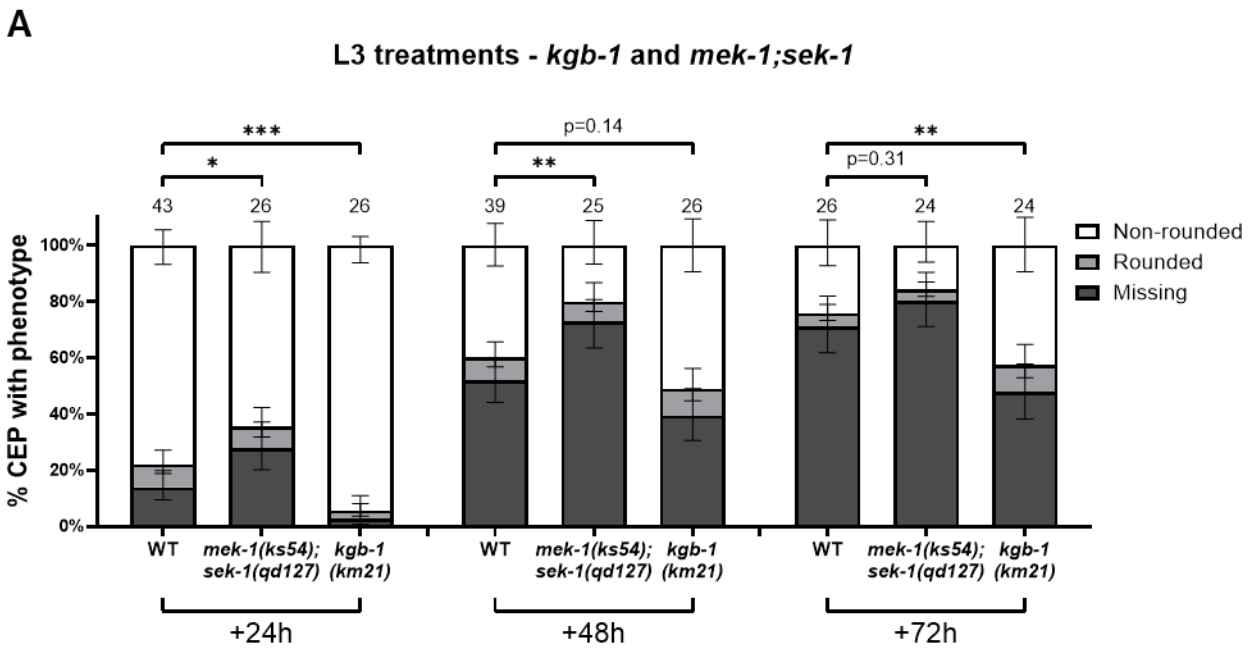

Figure 3. *kgb-1* and *mek-1;sek-1* mutants in 6-OHDA

(A) Percentage of CEP neurons 24 hours, 48 hours, or 72 hours after 50mM 6-OHDA exposure in L3 WT, *kgb-1(km21),* or *mek-1(ks54);sek-1(qd127)* animals expressing the transgene *vtIs1*. Error bars = 95% confidence intervals. 2 biological replicates, each with 14-26 animals were measured for WT animals for the 24h and 48h scores. Only one biological replicate was measured for *kgb-1* and *mek-1;sek-1* animals and 72h WT animals. Total animals examined is indicated above each bar. (n.s. $p>0.05$, *$p<0.05$, **$p<0.01$, ***$p<0.001$, Fisher's exact test).

Human MEGF10 expression does not rescue *ced-1* mutant defects

CED-1 an ortholog of human MEGF10 and MEGF11 (Suzuki and Nakayama, 2007). Previous work has shown that MEGF10 expression in *C. elegans* can partially rescue engulfment defects in *ced-1* mutant animals (Hamon et al., 2006). To determine if MEGF10 can rescue the *ced-1(e1754)* engulfment defects of CEP corpses after 6-OHDA exposure, I expressed human MEGF10 under an epithelial and muscle specific promoter, *dpy-7* and *myo-3,* respectively.

Expression of MEGF10 under either promoter was statistically non-significant compared to *ced-1(e1754)* mutants (Figure 4 A-B). Thus, human MEGF10 expression failed to rescue the *ced-1(e1754)* CEP corpse clearance defects (Figure 4 A-B).

One possibility is that human MEGF10 is unable to recognize phosphatidylserine without the help of the complement component C1q which acts as an opsonin for MEGF10 during synapse engulfment in mammals (Iram et al., 2016). *C. elegans* does not have orthologs for the complement system. Indeed, a previous study found that MEGF10 could only partially rescue *ced-1* engulfment defects in *C. elegans* embryos (Hamon et al., 2006). In addition, while their MEGF10:GFP fusion protein localized to cell surfaces, they also saw a punctate expression pattern intracellularly suggesting an inability to efficiently localize MEGF10 to the outer plasma membrane (Hamon et al., 2006). Thus, while MEGF10 and CED-1 are orthologs, both may require species-specific chaperones for their correct localization and function.

A limitation of this experiment is that the human MEGF10 construct I used was not codon-optimized to *C. elegans*, so it is possible that the expression of MEGF10 was very low.

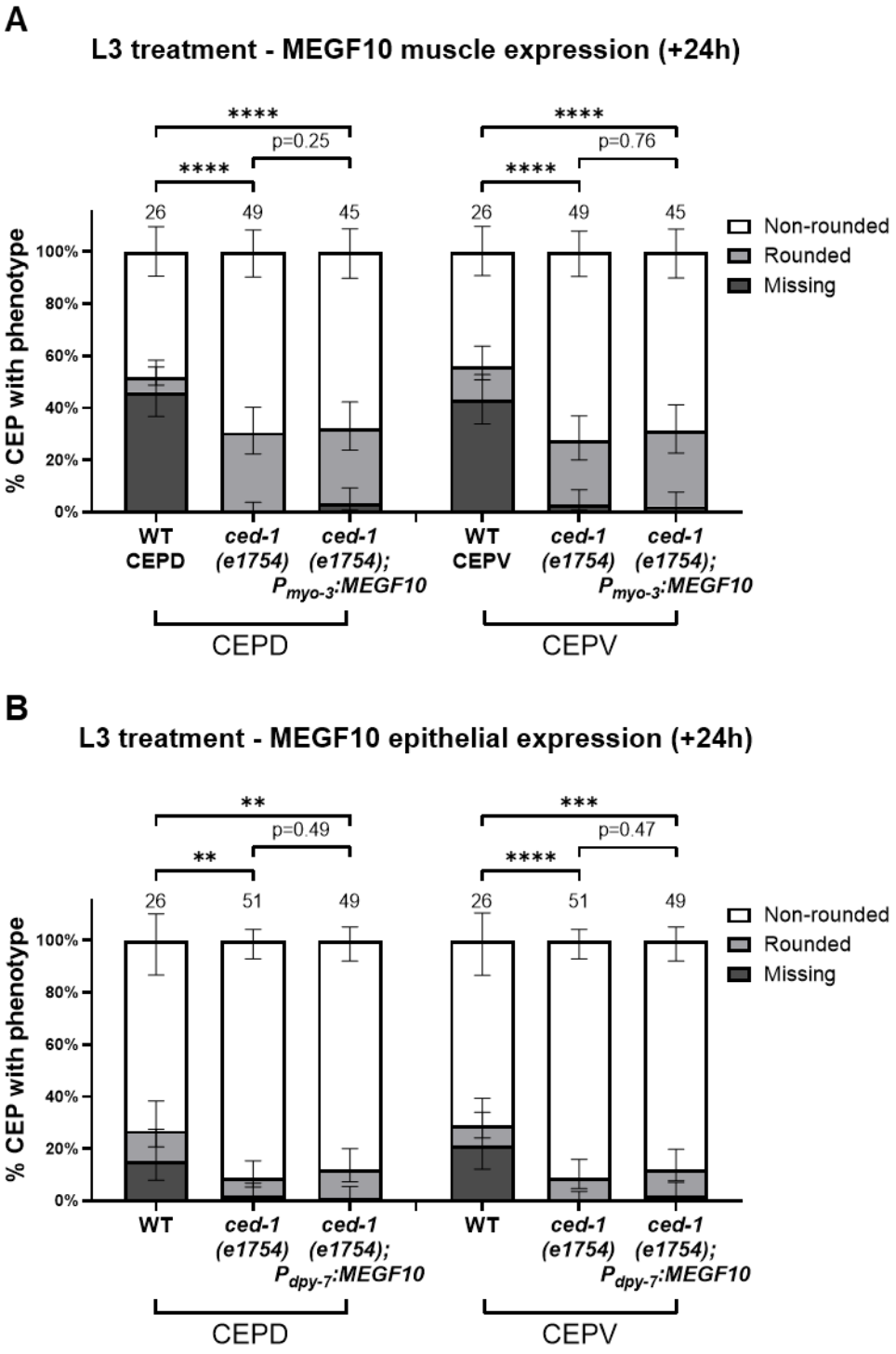
A
L3 treatment - MEGF10 muscle expression (+24h)
****
p=0.25
****
****
p=0.76
****
26
49
45
26
49
45
% CEP with phenotype
100%
80%
60%
40%
20%
0%
Non-rounded
Rounded
Missing
WT CEPD
ced-1 (e1754)
ced-1 (e1754); Pmyo-3:MEGF10
WT CEPV
ced-1 (e1754)
ced-1 (e1754); Pmyo-3:MEGF10
CEPD
CEPV
B
L3 treatment - MEGF10 epithelial expression (+24h)
**
p=0.49
**
***
p=0.47
****
26
51
49
26
51
49
% CEP with phenotype
Non-rounded
Rounded
Missing
WT
ced-1 (e1754)
ced-1 (e1754); Pdpy-7:MEGF10
WT
ced-1 (e1754)
ced-1 (e1754); Pdpy-7:MEGF10
CEPD
CEPV

Figure 4. Epithelial and muscle MEGF10 do not rescue in *ced-1(e1754)* mutants

(A) Percentage of CEP neurons 24 hours after 50mM 6-OHDA exposure in L3 WT, *ced-1(e1754),* and *ced-1(e1754);Ex[P_{myo-3}:MEGF10]* animals expressing the transgene *vtIs1.* Error bars = 95% confidence intervals. Only one biological replicate for WT was measured. 2 biological replicates were measured for all other animals with 21-25 animals per replicate. Total animals examined is indicated above each bar. (n.s. $p>0.05$, ****$p<0.0001$, Fisher's exact test).

(B) Percentage of CEP neurons 24 hours after 50mM 6-OHDA exposure in L3 WT, *ced-1(e1754),* and *ced-1(e1754);Ex[P_{dpy-7}:MEGF10]* animals expressing the transgene *vtIs1.* Error bars = 95% confidence intervals. Only one biological replicate for WT was measured. 2 biological replicates were measured for all other animals with 23-26 animals per replicate. Total animals examined is indicated above each bar. (n.s. $p>0.05$, **$p<0.01$, ***$p<0.001$, ****$p<0.0001$, Fisher's exact test).

CED-1 expresses on PDE dopamine neurons

While examining the expression pattern of CED-1:GFP around mCherry-labeled CEP neurons, I noticed that both PDE neurons showed CED-1:GFP expression around their somas and projections (Figure 5 A-B). I saw this expression in animals without 6-OHDA exposure, so it was not a response to degeneration or stress. Previous studies in mice have identified several neurons that express MEGF10 in the central nervous system (Fujita et al., 2017). In the retina, star amacrine cells express MEGF10 for proper positioning during development (Kozlowski et al., 2024). Glutamatergic and cholinergic neurons in the cortex, hippocampus, and substantia nigra also express MEGF10, but its function remains unclear (Fujita et al., 2017). The role of CED-1 in PDE neurons is unknown and would be an interesting topic for future study.

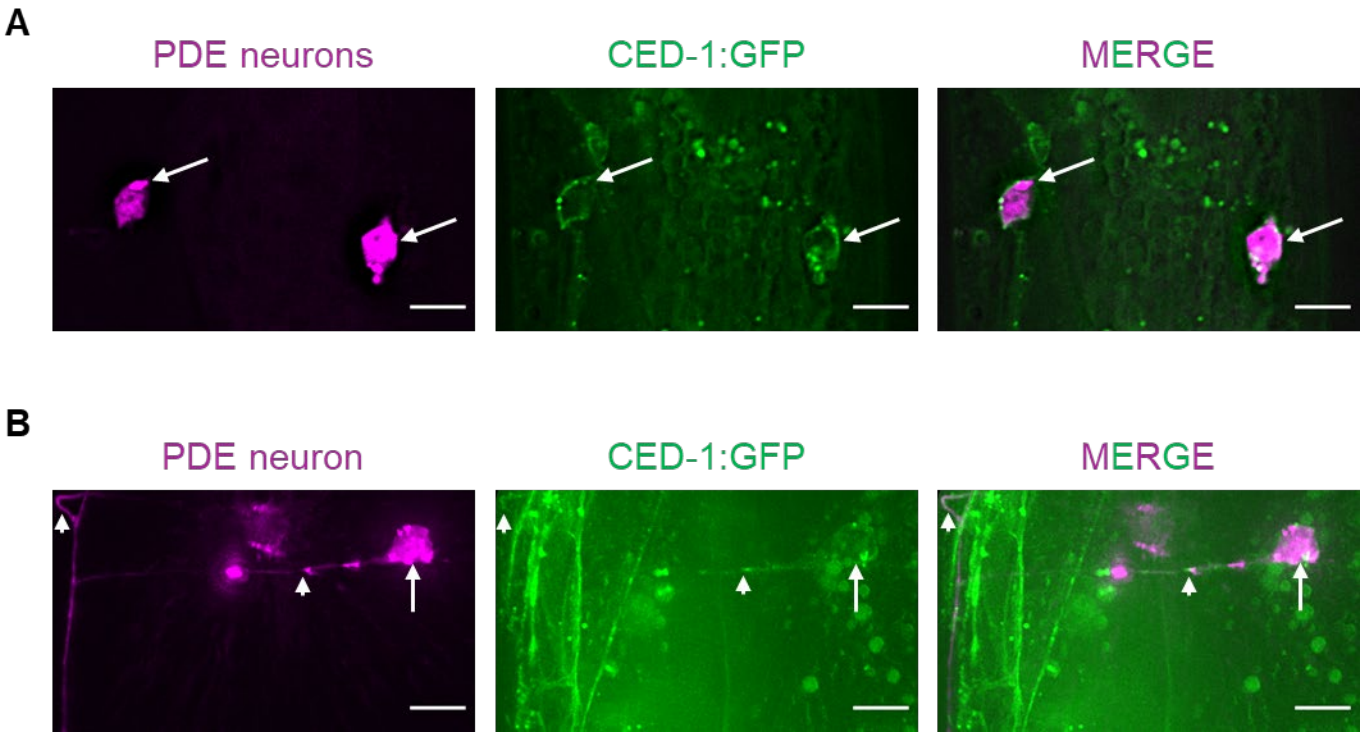

Figure 5. CED-1 localizes to PDE somas and projections

(A-B) Images of cytosolic mCherry-labeled dopaminergic PDE neurons (magenta) and CED-1:GFP (green) in *smIs34;otIs181* animals. Scale bars, 5 µm. **(A)** CED-1:GFP localizing around both PDE neurons in an L4 animal. Arrows indicate PDE cell somas. 100x magnification, single-z slice. **(B)** CED-1:GFP localizing around a single PDE neuron and along its projection in an L4 animal. Arrow indicates the PDE cell soma. Arrowheads indicate areas of colocalization along PDE neuron projection. 100x magnification, max z-projection.

CEPsh ablation protects CEP neurons in L1-arrested animals after 6-OHDA exposure

I previously showed that CEPsh glia ablation protects CEPD neurons after 6-OHDA treatment in L3 animals. I also found that CEPD neurons in L1-arrested animals treated with 6-OHDA are also protected against 6-OHDA (Figure 6 A). Thus, CEPsh glia ablation is protective across different animal stages.

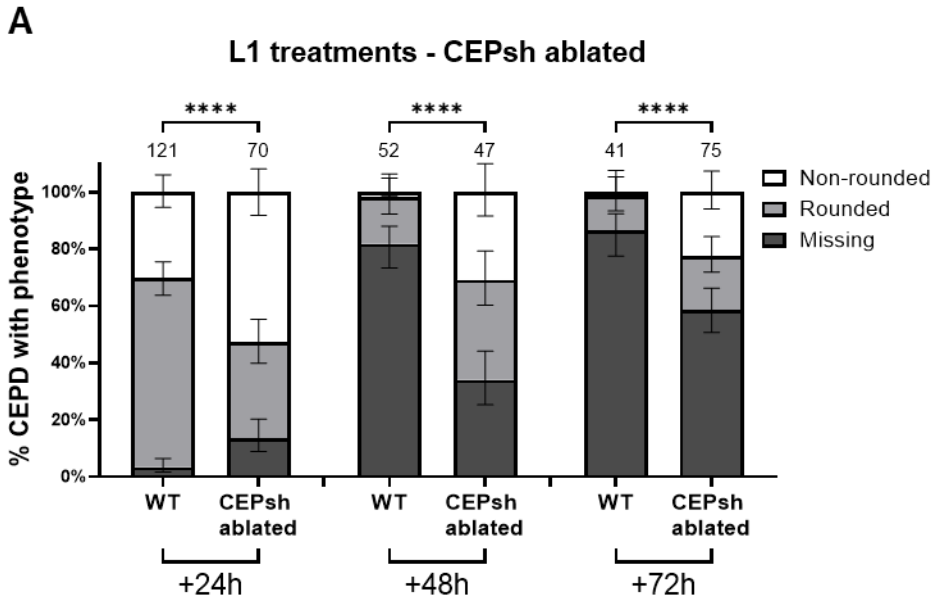

Figure 6. CEPsh glia ablation protects CEP neurons in L1-arrested animals

(A) Percentage of CEPD neurons 24 hours, 48 hours, or 72 hours after 50mM 6-OHDA exposure in L1 WT or *nsIs180* (CEPsh ablated) animals expressing the transgene *vtIs1*. Error bars = 95% confidence intervals for 2-5 biological replicates each with 10-26 animals per condition. Total animals examined is indicated above each bar. (****$p<0.0001$, Fisher's exact test). The WT for these experiments is shared with the WT in Figure 1.

KCC-3 protects against 6-OHDA degeneration

KCC-3 is a K+/CL- co-transporter expressed in many sheath glia including the CEPsh glia (Purice et al., 2023; Ray et al., 2024; Singhvi et al., 2016). To understand how CEPsh glia

ablation protects CEP neurons, I wondered if KCC-3 played a role in this process. Interestingly, loss of *kcc-3* slightly protects CEP neurons from 6-OHDA exposure (Figure 7 A). The function of KCC-3 in the CEPsh glia remains unknown; however, KCC-3 in the amphid sheath glia is known to regulate both chemosensory and thermosensory behaviors (Ray et al., 2024; Singhvi et al., 2016). Thus, one possibility is that KCC-3 in CEPsh glia may also function to regulate CEP neuron function, and disrupting CEP function could drive either protection or sensitivity to 6-OHDA.

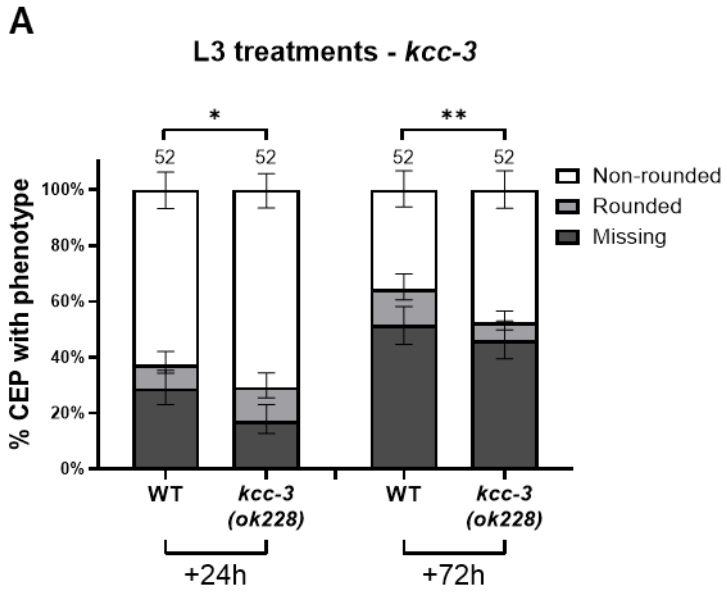

Figure 7. Loss of *kcc-3* slightly protects against 6-OHDA treatment

(A) Percentage of CEP neurons 24 hours or 72 hours after 50mM 6-OHDA exposure in L3 WT or *kcc-3* animals expressing the transgene *vtIs1*. Error bars = 95% confidence intervals for 2 biological replicates with 26 animals per replicate. Total animals examined is indicated above each bar. (*p<0.05, **p<0.01, Fisher's exact test).

UNC-13 protects CEP neurons while UNC-31 promotes CEP degeneration

The causal relationship between synaptic dysfunction in dopamine neurons and PD remains unknown. To test how synaptic vesicle and dense-core vesicle release impacts 6-OHDA toxicity, I examined animals mutants for *unc-13* and *unc-31* which are necessary for synaptic vesicle and dense-core vesicle release, respectively. I hypothesized that loss of either gene would protect CEP neurons from 6-OHDA toxicity by reducing neuronal activity. While loss of *unc-31* protects CEP neurons from degeneration, loss of *unc-13* sensitizes CEP neurons to 6-OHDA exposure (Figure 8 A). These results suggest that proper synaptic vesicle release is necessary for neuronal health. Thus, the synaptic dysfunction seen in PD could be a driver of degeneration rather than a compensatory mechanism for neuronal loss. Little is known about dense-core vesicle release and its impact on Parkinson's disease; however, my work suggests that dense-core vesicles may carry signals that can promote neurotoxicity. Interestingly, dopamine can be released in both synaptic vesicles and dense-core vesicles. How synaptic vesicles and dense-core vesicles impact Parkinson's disease will be an interesting and important topic of study.

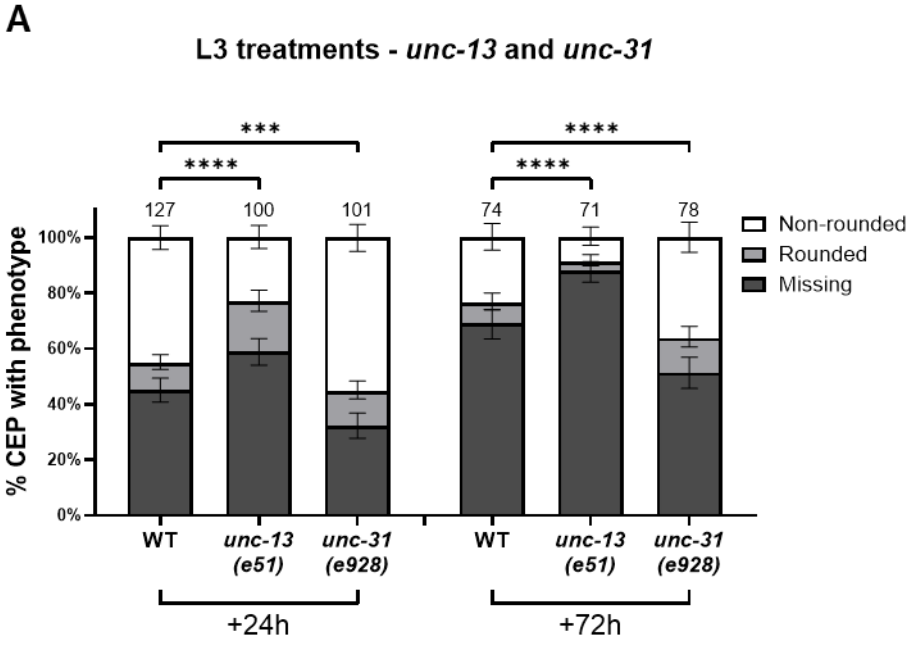

Figure 8. *unc-13* protects while *unc-31* promotes 6-OHDA degeneration

(A) Percentage of CEP neurons 24 hours or 72 hours after 50mM 6-OHDA exposure in L3 WT, *unc-13*, or *unc-31* animals expressing the transgene *vtIs1*. Error bars = 95% confidence intervals for 3-5 biological replicates with 22-26 animals per replicate. Total animals examined is indicated above each bar. (***p<0.001, ****p<0.0001, Fisher's exact test).

DYF-11 promotes CEP degeneration

CEP dendrite endings are comprised of cilia that pass through a channel made by the CEPsh glia and CEP socket glia before embedding into the cuticle at the nose-tip of the animal (Figure 9 A-A'). I noticed that in CEPsh ablated animals, CEP dendrites do not embed correctly into the cuticle (Figure 9 B-B'). In addition, while each neuron maintains a cilia, it appears misshapen (Figure 9 B'). To test if CEP cilia are necessary for 6-OHDA toxicity, I examined animals mutants for *dyf-11,* a gene important for proper cilia function. *dyf-11(mn392)* animals appear to have shortened and misshapen CEP cilia (Figure 9 C-C'). When exposed to 6-OHDA, *dyf-11(mn392)* animals showed protection against 6-OHDA as most CEP neurons maintained their non-rounded morphology (Figure 9 D). One possibility is that CEP neurons with disrupted cilia compensate by altering *dat-1* expression. A recent study found that loss of the ciliary protein BBS-1 reduced DAT-1 expression and protects against 6-OHDA exposure (Refai et al., 2024). Thus, loss of ciliary function in *dyf-11* mutants is neuroprotective against 6-OHDA toxicity possibly by altering DAT-1 expression levels.

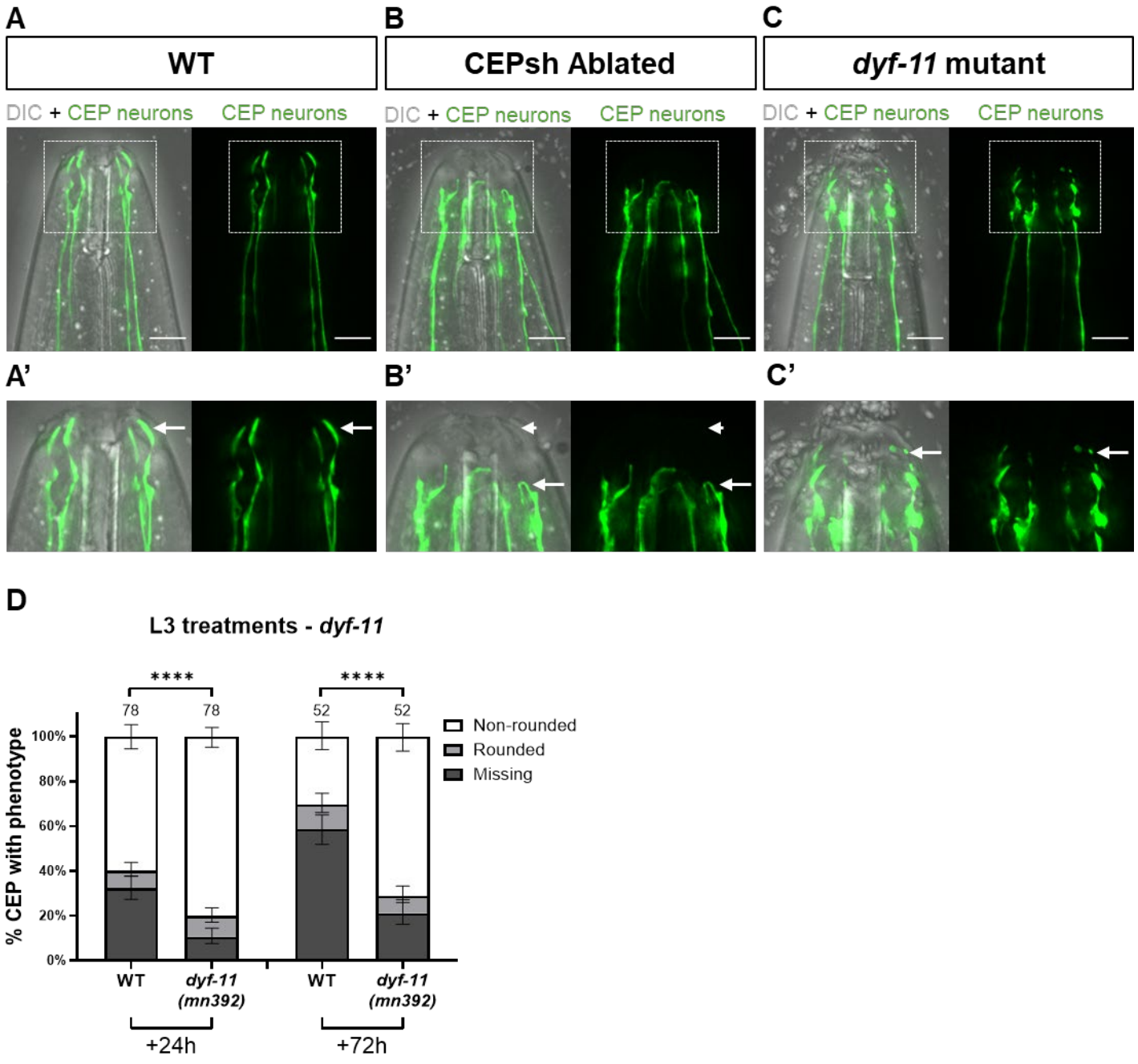

Figure 9. Role of cilia on CEP degeneration

(A-C) Images of CEP neuron dendrites in **(A)** WT, **(B)** CEPsh Ablated, and **(C)** *dyf-11(mn329)* animals expressing the *vtIs1[dat-1p::GFP + rol-6(su1006)]* transgene. Scale bar, 5µm. 60x magnification, max z-projection. **(A'-C')** Insets from (A-C) showing the cilia of the CEP

dendrites. Arrows point to a single CEP dendrite cilia. **(A')** Cilia in WT animals correctly extend and embed into the cuticle at the nose tip of the animal. **(B')** Cilia in CEPsh glia do not extend into the cuticle. Arrowheads indicate the area where cilia would normally embed into the cuticle. **(C')** Cilia in *dyf-11* mutants can extend into the cuticle but are shorter or appear punctate. **(D)** Percentage of CEP neurons 24 hours or 72 hours after 50mM 6-OHDA exposure in L3 WT or *dyf-11* animals expressing the transgene *vtIs1.* Error bars = 95% confidence intervals for 2-3 biological replicates with 26 animals per replicate. Total animals examined is indicated above each bar. (****p<0.01, Fisher's exact test).

dat-1 promoter expression is reduced in CEPsh ablated animals

6-OHDA enters dopamine neurons through the dopamine transporter DAT-1 to cause neurotoxicity (Nass et al., 2002). When examining CEP neurons in CEPsh ablated animals using the *vtIs1[*$P_{dat\text{-}1}$*:GFP]* transgene, I noticed that their CEP neurons appeared dimmer when compared to WT animals (Figure 10 A-B). Indeed, when measuring the GFP expression in CEPD neurons of WT and CEPsh ablated animals, CEPsh ablated CEPD neurons have reduced GFP expression when compared to WT CEPD neurons (Figure 10 C). Whether this reduction in dat-1 promoter activity leads to reduced levels of DAT-1 protein is unclear and would be an important follow-up experiment that can be tested with a western blot or quantitative fluorescence imaging.

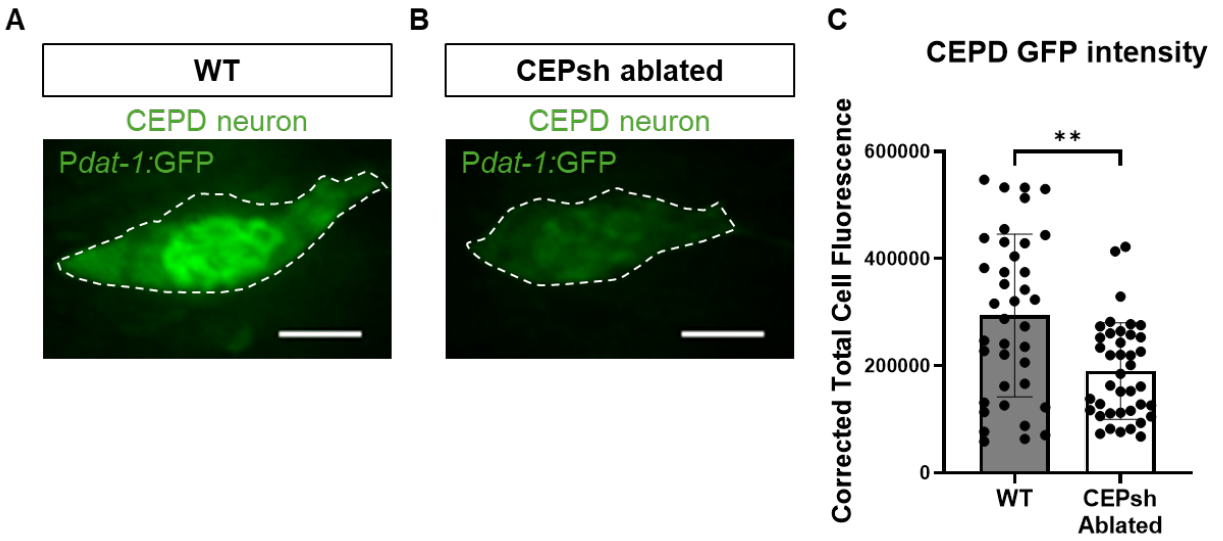

Figure 10. Decrease in P_{dat-1}:GFP expression in CEPsh ablated animals

(A-B) Images of CEPD neuron somas in **(A)** WT and **(B)** CEPsh Ablated animals expressing the *vtIs1[dat-1p::GFP + rol-6(su1006)]* transgene. Scale bar, 2µm. 60x magnification, max z-projection. **(C)** The Corrected Total Cell Fluorescence was measured from CEPD neurons in **(A)** WT and **(B)** CEPsh ablated animals. Mean + SD plotted for 19 (WT) and 20 (CEPsh Ablated) animals – both CEPD from each animal were measured and plotted (**p<0.01, Mann-Whitney Test).

C. elegans methods and strains

C. elegans were cultured as previously described (Brenner, 1974; Stiernagle, 2006). Bristol N2 strain was used as wild type. Animals were raised at 20ºC for two weeks without starvation. Germ-line transformations by micro-injection to generate unstable extra-chromosomal array transgenes were carried out using standard protocols (Mello et al., 1991). Strains used in this chapter are listed below:

N2 Bristol	WT strain
TG2435	*vtIs1 [dat-1p::GFP + rol-6(su1006)] V*
ASJ964	*vtIs1 V; dyf-11(mn392) X*
ASJ208	*ced-1(e1754) I; vtIs1 [dat-1p::GFP + rol-6(su1006)] V*
ASJ209	*psr-1(tm469) IV; vtIs1 [dat-1p::GFP + rol-6(su1006)] V*
ASJ78	*ced-10(n1993) IV; vtIs1[dat-1p::GFP + rol-6(su1006)] V*
ASJ257	*vtIs1[dat-1p::GFP + rol-6(su1006)] V; dyn-1(ky51) X*
ASJ258	*nsIs180 [Phlh-17:split-Caspase + coel:GFP] IV; vtIs1 [dat-1p::GFP + rol-6(su1006)] V*
ASJ1470	*kcc-3(ok228) II; vtIs1[dat-1p::GFP + rol-6(su1006)] V*
ASJ1509	*kgb-1 (km21) IV; vtIs1 [dat-1p::GFP + rol-6(su1006)] V*
ASJ1506	*vtIs1 [dat-1p::GFP + rol-6(su1006)] V; mek-1(ks54) sek-1(qd127) X*
ASJ484	*otIs181[dat-1::mCherry + ttx-3::mCherry] III; smIs34[ced-1p::ced-1::GFP + rol-6(su1006)]*
ASJ574	*unc-13(e51) I; vtIs1 V*
ASJ1078	*unc-31(e928) IV; vtIs1 V*
ASJ1496	*dnaEx666[Pdpy-7:MEGF10:SL2:mKate2]; ced-1(e1754) I; vtIs1 V*
ASJ1501	*dnaEx670[Pmyo-3:MEGF10:SL2:mKate2 + coel:RFP]; ced-1(e1754) I; vtIs1 V*

Plasmids

The human MEGF10 cDNA was ordered from SinoBiological (HG16064-UT). To generate the body wall muscle MEGF10 rescue construct, MEGF10 was PCR amplified and cloned into ASJ356 (P_{myo-3}:CED-1A:SL2:mKate2) using *AscI*/*NheI* restriction sites to generate ASJ600/655 (P_{myo-3}:hMEGF10:SL2:mKate2); ASJ600 was injected into *vtIs1;ced-1(e1754)* worms at 20ng/µL with 20ng/µL of $P_{unc-122}$:RFP as a co-injection marker.

To generate the epithelial MEGF10 rescue construct, P_{dpy-7} was restriction digested from ASJ157 (P_{dpy-7}:CED-1A:SL2:mKate2) using *SphI/NotI* restriction sites and cloned into ASJ600 to generate ASJ601/602 (P_{dpy-7}:hMEGF10:SL2:mKate2); ASJ601 was injected into *vtIs1;ced-1(e1754)* worms at 20ng/µL.

6-hydroxydopamine treatment

Treatment with 6-hydroxydopamine was done as previously described with modifications (Nass et al., 2002; Offenburger et al., 2018a). 10 gravid adult worms were picked off a mixed population 6cm plate and placed into a well of a 96-well plate containing 70µL of M9 buffer. Worms were left shaking overnight (~18-24 hours) at 500 RPM on a plate shaker. This would allow any eggs that were laid by the gravid adult animals to hatch and arrest at the L1 stage. The next morning, 30µL of the hatched worms were added to a separate 96-well plate with 10µL of 200mM L-ascorbic acid (Sigma CAS #50-81-7) and then 10µL of a 5x 6-OHDA stock (Sigma CAS #28094-15-7) was added to a final volume of 50 µL (or L-Ascorbic acid alone as control). The plate was shaken on a horizontal shaker for 1hr at 500 RPM, after which 150µL of M9 was added to each well to oxidize the 6-OHDA and stop the reaction. Worms were then transferred

using a glass pipette to an OP50 seeded plate and left uncovered for 5-10 minutes in a fume hood to dry. At this point, adults or eggs that were accidentally transferred are picked off to ensure only L1-arrested animals remain. Plates were then covered and incubated at 20ºC. 6-OHDA treatments in L3 animals were done as previously described in Chapter 2.

In all paradigms, I exposed staged animals to a given concentration of 6-OHDA for 1 hour and examined CEP neurons via fluorescent reporters for changes in morphology as a basis for degeneration. CEP neurons were then scored for clearance 24 hours, 48 hours, and 72 hours after 50mM 6-OHDA treatment. CEP neurons were visualized using the *vtIs1* or *otIs181* transgenes expressing GFP or mCherry under the *dat-1* promoter, respectively, as noted (Bertrand and Hobert, 2009; Nass et al., 2002). CEP neurons were scored for intact and visible cell bodies. CEP neurons were scored as (1) non-rounded if the cell body was visible and maintained its gross shape, (2) rounded if the cell body was visible but looked rounded or spherical, or (3) missing if there was no cell body visible or detectable fluorescent signal. Percent of CEP neurons visible were calculated against total number of CEP neurons expected (4 per animal).

Microscopy

Worms were immobilized on 2% agar pads using 1% tetramisole hydrochloride (Sigma CAS #16595-80-5) dissolved in M9 buffer. Images were acquired on a Deltavision Elite RoHS wide-field deconvolution system with Ultimate Focus (GE), a PlanApo 60×/1.42 NA or OLY 100×/1.40 NA oil-immersion objective and a DV Elite CMOS Camera. Images were processed using ImageJ, FIJI.

Fluorescence Intensity Quantification

Images for fluorescence intensity measurements were taken on the same day using random sampling at 32% T with an exposure time of 0.001172 seconds. Raw images were deconvolved and then sum Z-projected before taking fluorescence measurements. We used ImageJ FIJI for all fluorescence measurements. For the *Pdat*-1:GFP experiments, an ROI was drawn around a CEPD soma, and two smaller ROIs were carefully drawn in the area between the pharyngeal bulbs to take 2 background measurements. The Integrated Density was measured for each ROI. The corrected total cell fluorescence (CTCF) for each animal was calculated by subtracting the background integrated density from the integrated density of the tissue-specific ROI for each cell.

Statistical Analysis

All statistical analysis was performed using GraphPad Prism 11. To evaluate changes in CEP neurodegeneration, a Fisher's Exact Test was used. To compare changes in fluorescence intensities, the non-parametric Mann-Whitney test was used.

Chapter 4

DISCUSSION

This thesis has focused on understanding the role of glia, muscle, and epithelial cells in the degeneration and clearance of dopaminergic neurons in *C. elegans* Parkinson's disease models. In Chapter 1, I reviewed previous literature to provide context on our current knowledge on how phagocytosis mechanisms and non-neural tissues impact PD degeneration. In Chapter 2, I discuss a submitted manuscript that details how epithelial and muscle cells engulf degenerating dopaminergic CEP neurons via the engulfment receptor CED-1 and how the CEPsh glial cells are neurotoxic to CEP neurons. Finally, in chapter 3 I describe experiments that examine the neuroprotective or degenerative roles of candidate genes in 6-OHDA degeneration of CEP neurons.

In this Chapter, I expand on these findings and contextualize them with the current knowledge in the field. I further discuss pressing questions, future experimental directions, and the implications of these findings in the broader scientific world. Some segments of this discussion are published in Rojas et al (JCB, in review, 2025) and merged with additional points.

Epithelia and muscle impact PD neurodegeneration

While PD has broad CNS and PNS involvement, and PD genes can be broadly expressed, roles of non-neuronal cells remain underexplored in PD. My work reveals epithelia and muscle as phagocytes for degenerating CEP neurons. While their roles as phagocytes is not yet implicated in PD, both cell types can act as phagocytes in other contexts: both epithelia and muscle engulf axon debris post-injury and developmentally apoptotic cells in *C. elegans* (Chiu et

al., 2018; Hsieh et al., 2012; Nichols et al., 2016; Reddien and Horvitz, 2004); *Drosophila* muscle engulf presynaptic debris at the NMJ (Fuentes-Medel et al., 2009); and zebrafish skin Langerhans cells engulf axon debris (Peterman et al., 2023). Thus, a role for epithelial and muscle cells as phagocytes appears to be conserved across species. In PD, skin epithelial α-synuclein levels are used as diagnostic biomarkers, and clinical and animal model studies show skeletal muscle atrophy and increased intramuscular α-synuclein (Gibbons et al., 2024; Yang et al., 2023). How either cell type accumulates α-synuclein or how this impacts PD progression in humans awaits inquiry. It would be interesting to explore how α-synuclein expression in *C. elegans* epithelia and muscle affect their ability to phagocytose. Several studies indicate that α-synuclein oligomers can inhibit microglial phagocytosis (Joers et al., 2017; Tremblay et al., 2019). In addition, astrocyte uptake of α-synuclein can lead to lysosome dysfunction, suggesting that engulfing α-synuclein may disrupt phagolysosome functioning (Tremblay et al., 2019). Whether these disruptions in phagocytic activity are detrimental to dopamine neurons remains unclear.

CED-1/MEGF10 regulates neurodegeneration and corpse clearance in PD models

CED-1 orthologs Draper and MEGF10 engulf Aβ in Alzheimer's models in flies and in cell culture and they regulate glial pruning in development (Chung et al., 2013; Hong et al., 2016; Ray et al., 2017; Singh et al., 2010). However, phagocytic receptors that clear degenerating dopamine neurons in Parkinson's disease had not been identified (Tremblay et al., 2019). My work reveals the conserved CED-1/MEGF10/Draper as the phagocytic receptor in both 6-OHDA and α-synuclein *C. elegans* models of PD. Loss of *ced-1* blocks dopamine neurodegeneration after neurotoxic insult and protects some dopamine-driven animal behaviors.

Our results also indicate that CED-1 driven phagocytosis may exacerbate neuron death by "assisted" suicide or phagoptosis. Previous studies have proposed phagoptosis as a mechanism for dopaminergic death in PD, but such a mechanism has not yet been reported for PD to our knowledge (Brown and Neher, 2014). However, my work is reminiscent of developmental apoptosis in *C. elegans* where engulfment similarly aids cell death (Hoeppner et al., 2001; Johnsen and Horvitz, 2016; Reddien et al., 2001).

How CED-1 drives cell death of engulfed neurons remains unclear. Previous work has shown that during development, CED-1 can drive an unequal segregation of apoptotic potential in dividing cells such that the cell destined to die has increased CED-3 expression (Chakraborty et al., 2015). Thus, CED-1 recruitment to dying CEP neurons may increase CED-3 expression. However, given that CED-3 mutations do not affect CEP degeneration after 6-OHDA exposure, this is not likely (Nass et al., 2002). Another possibility is that CED-1 recruitment drives necrotic or autophagic cell death mechanisms in CEP neurons. My work found that loss of ANOH-1/TMEM16F partially protected CEP neurons from degeneration suggesting a necrotic-like mechanism that mediates PS exposure. In combination with previous work showing that loss of CED-3 and CED-4 have no effect on CEP degeneration after 6-OHDA exposure, my work suggests that CEP neurons degenerate in a necrotic-like fashion (Nass et al., 2002). Interestingly, a missense mutation with enhanced TMEM16F scramblase function was identified in an Ashkenazi Jewish PD population, and TMEM16F lesions in cell culture exhibit reduced PS and α-synuclein spread (Cohen-Adiv et al., 2024). Thus, a potential model could be that ANOH-1-dependent PS exposure recruits CED-1 to trigger engulfment, thereby driving spread of α-synuclein into the phagocytic cell. In addition to necrotic death, it is possible that autophagic cell

death mechanisms are also at play since previous work showed that inhibiting autophagy in CEP neurons protected them against 6-OHDA (Donato et al., 2025).

CED-1 has also been shown to regulate innate immune signaling pathways. *ced-1* loss can both protect animals against pathogenic bacteria via PMK-1/MPK-1 signaling or enhance infection by downregulating the unfolded protein response (Haskins et al., 2008; Wan et al., 2021). PMK-1 signaling has been shown to regulate protective responses to oxidative stress (Andrusiak and Jin, 2016). In addition, CED-1 mediated clearance of axonal debris by muscle cells required the JNK signaling molecules *mlk-1* and *mek-1* (Chiu et al., 2018). Previous work showed no effect of *pmk-1* or *kgb-1* mutations on ADE and CEP degeneration after 6-OHDA exposure; however, in that study they scored ADE and CEP together rather than looking at effects on CEP or ADE cells alone (Offenburger et al., 2018a). My preliminary work suggests that KGB-1 drives CEP degeneration while SEK-1 protects CEP neurons. SEK-1 is known to act upstream of PMK-1 to regulate oxidative stress responses (Andrusiak and Jin, 2016). Thus, loss of CED-1 may protect CEP neurons by upregulating anti-oxidative stress genes such as PMK-1, SEK-1, or SKN-1.

In addition, my finding that over-expressing CED-1 in epithelia but not muscle exacerbates CEPD and CEPV degeneration implies a non-cell autonomous mode of signaling. Given that epithelia cells could only engulf CEPV neurons, it is surprising that CED-1 overexpression in epithelia also drives degeneration in CEPD neurons. Given these, I hypothesize a two-step mechanism of action: CED-1 is first recruited to dying CEP neurons by rate-limiting PS. This recruitment signals back to degenerating CEP neurons to regulate autophagic or necrotic signaling to aid in the killing of the neuron. Subsequent downstream signaling through CED-1 aids both the clearance of CEP corpses via engulfment and the

facilitation of neuron-death through SEK-1/PMK-1/SKN-1 MAPK signaling in the epithelia. In the future, I can test these ideas by looking at double mutants of *ced-1* with *pmk-1*, *sek-1*, and *skn-1*. I hypothesize that these double mutants would have persisting cell corpses but would have levels of degeneration similar to or higher than WT animals. In the future it would be interesting to examine whether activation of MAPK signaling is used to protect or to promote the degeneration of neurons in the context of PD and whether this is conserved throughout animals.

Whether MEGF10 activation in astrocytes mediates immune signaling or MAPK signaling is unknown. In mammalian systems, astrocytes communicate extensively with microglia to modulate the release of cytokines and neuromodulators (Tremblay et al., 2019). Microglial phagocytosis also appears to require p38 MAPK signaling (Tanaka et al., 2009). Thus, one possibility is that astrocytes use MEGF10 to survey for neuronal stress or damage and this in turn causes increased microglial activation and phagocytosis. Indeed, in *Drosophila,* axonal injury induces glial activation through Draper and subsequently JNK signaling to mediate axon debris engulfment and Draper upregulation (Lu et al., 2017). My preliminary findings on *kgb-1* and *mek-1;sek-1* show that JNK signaling may be dispensable for corpse engulfment but is necessary for mediating protective or toxic responses. However, I find that *ced-1* expression levels do not change in response to 6-OHDA toxicity.

My work also suggests that CED-1 clustering and not CED-1 expression levels mediates CEP degeneration and clearance. How is CED-1 recruited to degenerating CEP neurons? Recent studies have shown that CED-7 and CED-6 work redundantly to correctly localize CED-1 to the plasma membrane (Harders et al., 2024). In addition, CED-1 clustering around apoptotic corpses is regulated by CED-7 as *ced-7* mutants are unable to cluster CED-1 around apoptotic corpses (Zhou et al., 2001). Interestingly, the intracellular domain of CED-1 is not necessary for its

clustering, whereas loss of its extracellular domain results in diffuse CED-1 expression and no clustering around cell corpses (Zhou et al., 2001). Altogether, I believe that the interactions between the extracellular domain of CED-1 with PS mediates the clustering around degenerating CEP neurons. To test this idea, I could perform cell rescue experiments with a truncated form of CED-1 which lacks its intracellular or extracellular domains and examine its clustering around degenerating CEP neurons. I suspect that only CED-1 missing its extracellular domain will be unable to cluster around CEP neurons. These experiments will also help to determine whether the intracellular domain of CED-1, which is known to be necessary for the engulfment of cell corpses, is also necessary for the engulfment and degeneration of CEP neurons. Interestingly, the CED-1 orthologs, MEGF10 and MEGF11, are known to act as adhesion molecules (Suzuki and Nakayama, 2007). CED-1 is also posited to have adhesion-like properties that help severed axons regenerate (Chiu et al., 2018). Thus, I hypothesize that PS-CED-1 interactions help stabilize CED-1 at the plasma membrane through its adhesive properties. CED-1 then initiates a signaling cascade through CED-6 and CED-7 to both recruit more CED-1 and promote engulfment. In future studies, it will be interesting to examine whether loss of CED-6 or CED-7 prevents the clustering of CED-1 in the context of CEP degeneration.

How MEGF10 clusters to engulf neurons is unknown. Studies in Draper found that, in contrast to CED-1, the intracellular region was necessary for clustering around PS (Williamson and Vale, 2018). Both MEGF10 and Draper share similar intracellular protein domains such as an ITAM domain that is absent in CED-1 (Vargas-Franco et al., 2022). Thus, MEGF10 may require intracellular signaling and phosphorylation to mediate its clustering. In future studies, it would be interesting to perform site-direction mutagenesis in MEGF10 models to understand how its intracellular and extracellular domains mediate its clustering.

In addition to being expressed in astrocytes, MEGF10 is also expressed in muscle satellite cells (Holterman et al., 2007). In muscle satellite cells, MEGF10 is important for myogenesis and muscle cell regeneration possibly through Notch signaling (Holterman et al., 2007; Li et al., 2021; Richardson et al., 2025; Saha et al., 2017). In fact, biallelic mutations in MEGF10 cause the severe myopathy EMARDD (early myopathy, areflexia, respiratory distress and dysphagia) in humans (Croci et al., 2022). The physiological roles of MEGF10 and how mutations in it can cause EMARDD are currently being studied. Recent work has shown that MEGF10 is also expressed in perisynaptic Schwann cells and is highly localized to neuromuscular junctions (NMJs)(Juros et al., 2024). Loss of MEGF10 in mice caused perisynaptic Schwann cell migration into the synaptic cleft of the NMJ which is known to cause instability of the junction (Juros et al., 2024). In light of my findings, whether these Schwann cells use MEGF10 to engulf or promote the degeneration of motor neurons or muscle cells at NMJs would be an interesting follow-up study. In fact, sarcopenia, or the progressive decline of muscle mass and function, is common in patients with PD (Gui et al., 2025). Whether this sarcopenia is due to disruptions in MEGF10 functioning at NMJs or in perisynaptic Schwann cells would be interesting to study.

Glial control of activity and degeneration of dopamine neurons

We found that *C. elegans* astrocyte-like CEPsh glia actively react to CEP neuron stress post 6-OHDA insult. They also regulate dopamine levels, primarily via the rate-limiting enzyme *cat-2*/tyrosine hydroxylase, which impairs dopamine-related behavior when CEPsh glia are ablated but protects CEP neurons against neurotoxic and genetic insult. Thus, in addition to validating a neuroprotective role for CAT-2/TH, we find that glia are neurotoxic to dopamine

neurons. Together, this provides mechanistic insight into how astrocyte-like glia respond to neurotoxic insults. In humans, L-DOPA supplementation is the "gold standard" treatment for Parkinson's disease. However, the role of L-DOPA or CAT-2/TH in mediating protection or degeneration of dopamine neurons remains contentious (Lipski et al., 2011). Here we show a potential neuroprotective effect of L-DOPA synthesis for both toxin- and α-synuclein-induced degeneration by upregulating *cat-2*/TH suggesting a shared underlying mechanism of protection.

Whether the protection seen in α-synuclein overexpression is also due to *cat-2* is an important follow-up experiment for future studies. How CEPsh glial cells regulate the expression of *cat-2* in dopamine neurons remains unknown. One possibility is that loss of CEPsh glia disrupts synaptic connectivity between CEP neurons and other neurons in the nerve ring. Changes in synaptic connectivity could then lead to compensatory changes in dopamine synthesis gene expression. To test this idea, future studies could visualize CEP synapses in WT and CEPsh ablated animals using a known pre-synaptic marker such as CLA-1. Another possibility could be that the inability for CEP neurons to properly embed their cilia into the cuticle in CEPsh ablated animals could disrupt dopamine signaling. A recent study demonstrated that the ciliary protein BBS-1 regulates dopamine signaling through DAT-1 expression regulation (Refai et al., 2024). One way to test this idea would be to measure *cat-2* expression levels in whole animal *dyf-11* cilia mutants and in CEP-targeted knockdown of *dyf-11.*

We were surprised to find GFP aggregations in CEPsh glia following 6-OHDA treatment. To my knowledge, CEPsh glia do not express DAT-1 or CAT-1 transporters, so it is unlikely that 6-OHDA has entered the CEPsh glia in that manner. Thus, how CEPsh glia are sensing the degeneration from CEP neurons is unclear. Interestingly, CEPsh glia also express CED-1 (Purice et al., 2023). One tantalizing possibility is that CEPsh glia use CED-1 to monitor for exposed PS

as a sign of neuronal stress. To test this idea, I could examine GFP aggregation in CEPsh glia in *ced-1* mutants following 6-OHDA exposure. In this case, I would expect to see no increase in GFP aggregation.

In my thesis work, I also found that loss of the glutamate transporters GLT-1 and GLT-3 result in increased degeneration of CEP neurons possibly through increased glutamate signaling onto CEP neurons. Previous work has shown that increased glutamate signaling can induce degeneration of CEP neurons (Gibson et al., 2018). In addition, dysregulation of glutamate synthesis is thought to be a potential driver of dopaminergic degeneration in PD (Iovino et al., 2020). My thesis work supports this idea of glutamate excitotoxicity. However, in contrast to other studies, I did not see a decrease in glutamate transporter expression following 6-OHDA treatment (Pajarillo et al., 2019). One possible explanation is that I only examined their expression 24h after 6-OHDA treatment. It would be interesting to see if there are changes in gene expression at later time points. However, if our results hold true, it implies that glutamate antagonists could be a potential therapeutic avenue for slowing down the degeneration of dopamine neurons in the substantia nigra in PD. Indeed, one clinical study showed that use of a weak NMDA receptor antagonist improved the survival of patients with PD (Uitti et al., 1996). However, global blockade of glutamate signaling can lead to adverse side-effects (Zhang et al., 2019b). Thus, in future studies, it would be interesting to evaluate the protective effects of glutamate antagonists that target other glutamate receptors that may be specific to those expressed in the substantia nigra.

Limitations

Using *C. elegans* to study dopamine degeneration in PD presents a few limitations. First, *C. elegans* do not natively express α-synuclein. In addition, it remains unclear if the neurodegenerative effects of α-synuclein in *C. elegans* are mechanistically similar to the neurodegenerative effects in humans or other model systems. Second, my studies focused primarily on the larval stages of *C. elegans.* However, PD is a disease that is associated with aging. Thus, by looking at larval stages, we do not consider the effect of aging on dopamine degeneration. It would be interesting to investigate whether older animals are susceptible to 6-OHDA and if the phagocytic capabilities of the epithelia or muscle are impacted in older animals. Finally, while *C. elegans* dopamine neurons regulate locomotion behaviors similar to dopamine neurons in humans, we are unable to study how loss of these neurons may impact non-motor behaviors such as anxiety and depression. Thus, studies of PD in *C. elegans* may be limited to understanding just the cellular and molecular effects on dopamine neurons and its surrounding tissues.

While my studies demonstrated a role for epithelia and muscle in engulfing CEP neurons, we cannot rule out the involvement of other cell types such as the pharynx or nearby neurons in engulfing the degenerating CEP neurons. Indeed, previous work has shown that neurons also express MEGF10, and I show that PDE neurons also express CED-1 (Fujita et al., 2017). In addition, there is CED-1 expression in several tissues surrounding the CEP neurons that may be neuronal (Zhou et al., 2001). However, whether these neurons are using these receptors to engulf other cells remains unclear.

Finally, I show that CED-1 overexpression in epithelia but not muscle can promote CEP degeneration to levels higher than wildtype. However, these overexpression lines are in the form

of extrachromosomal arrays meaning that the level of expression per animal and per cell type can vary. Thus, one possibility is that the amount of CED-1 expressed in the muscle was not high enough to drive degeneration but was sufficient to promote engulfment. To test this idea, I could inject a higher concentration of CED-1 under the *myo-3* muscle promoter. Likewise, I could reduce the expression of CED-1 in epithelia as a corollary experiment.

Conclusions

In conclusion, my dissertation work makes the following contributions to the field:

1) the identification of CED-1 as the engulfment receptor that mediates clearance of degenerating dopamine neurons in two PD models in *C. elegans*
2) the identification of epithelial and muscle cells as the phagocytes that use CED-1 to engulf the degenerating CEP neuron somas
3) CEPsh glia are neurotoxic by regulating *cat-2*/TH levels in dopamine neurons
4) CEPsh glia regulate *cat-1*/VMAT2 expression in CEP neurons
5) CED-1 clustering around exposed phosphatidylserine in CEP neurons drives neuron degeneration and clearance
6) CED-1 promotes the degeneration of CEP neurons

I believe my thesis work was fruitful and helped identify a phagocytic receptor that is used to engulf degenerating dopamine neurons in two Parkinson's disease models. In addition, I provide evidence for the role of non-neuronal cells in the pathogenesis of Parkinson's disease neurodegeneration. My work then suggests that Parkinson's disease may be a dysfunction in cells of multiple organ systems rather than a dysfunction of just neurons in the brain. Thus, I believe

that understanding how PD affects muscle and epithelial tissues in other tissues of the body will be essential for developing new therapeutics and interventions. Just as the careful observations of past scientists and medical practitioners helped us to gain insight into Parkinson's disease and glial functioning today, I hope my work will provide an opportunity for novel insights into Parkinson's disease and the role of glia in neurodegenerative disorders.

REFERENCES

The following are the references for Chapters 1, 3, and 4.

Abbott, N.J., 2002. Astrocyte–endothelial interactions and blood–brain barrier permeability. J. Anat. 200, 629–638. https://doi.org/10.1046/j.1469-7580.2002.00064.x

Abdo, H., Calvo-Enrique, L., Lopez, J.M., Song, J., Zhang, M.-D., Usoskin, D., El Manira, A., Adameyko, I., Hjerling-Leffler, J., Ernfors, P., 2019. Specialized cutaneous Schwann cells initiate pain sensation. Science 365, 695–699. https://doi.org/10.1126/science.aax6452

Alberts, B., Johnson, A., Lewis, J., Raff, M., Roberts, K., Walter, P., 2002. Sensory Epithelia, in: Molecular Biology of the Cell. 4th Edition. Garland Science.

Allen, N.J., Eroglu, C., 2017. Cell Biology of Astrocyte-Synapse Interactions. Neuron 96, 697–708. https://doi.org/10.1016/j.neuron.2017.09.056

Alvarez-Suarez, P., Gawor, M., Prószyński, T.J., 2020. Perisynaptic schwann cells - The multitasking cells at the developing neuromuscular junctions. Semin. Cell Dev. Biol., Differentiation of skeletal muscles 104, 31–38. https://doi.org/10.1016/j.semcdb.2020.02.011

Andrusiak, M.G., Jin, Y., 2016. Context Specificity of Stress-activated Mitogen-activated Protein (MAP) Kinase Signaling: The Story as Told by *Caenorhabditis elegans**. J. Biol. Chem. 291, 7796–7804. https://doi.org/10.1074/jbc.R115.711101

Barcia, C., Ros, C.M., Ros-Bernal, F., Gómez, A., Annese, V., Carrillo-de Sauvage, M.A., Yuste, J.E., Campuzano, C.M., de Pablos, V., Fernández-Villalba, E., Herrero, M.T., 2013. Persistent phagocytic characteristics of microglia in the substantia nigra of long-term Parkinsonian macaques. J. Neuroimmunol. 261, 60–66. https://doi.org/10.1016/j.jneuroim.2013.05.001

Barcomb, K., Ford, C.P., 2023. Alterations in neurotransmitter co-release in Parkinson's disease. Exp. Neurol. 370, 114562. https://doi.org/10.1016/j.expneurol.2023.114562

Beccano-Kelly, D.A., Kuhlmann, N., Tatarnikov, I., Volta, M., Munsie, L.N., Chou, P., Cao, L.-P., Han, H., Tapia, L., Farrer, M.J., Milnerwood, A.J., 2014. Synaptic function is modulated by LRRK2 and glutamate release is increased in cortical neurons of G2019S LRRK2 knock-in mice. Front. Cell. Neurosci. 8. https://doi.org/10.3389/fncel.2014.00301

Bertrand, V., Hobert, O., 2009. Linking Asymmetric Cell Division to the Terminal Differentiation Program of Postmitotic Neurons in *C. elegans*. Dev. Cell 16, 563–575. https://doi.org/10.1016/j.devcel.2009.02.011

Bigdai, E.V., Samoilov, V.O., 2022. Role of Neurotransmitters in the Functioning of Olfactory Sensory Neurons. J. Evol. Biochem. Physiol. 58, 865–874. https://doi.org/10.1134/S0022093022030206

Bisht, K., Okojie, K.A., Sharma, K., Lentferink, D.H., Sun, Y.-Y., Chen, H.-R., Uweru, J.O., Amancherla, S., Calcuttawala, Z., Campos-Salazar, A.B., Corliss, B., Jabbour, L., Benderoth, J., Friestad, B., Mills, W.A., Isakson, B.E., Tremblay, M.-È., Kuan, C.-Y., Eyo, U.B., 2021. Capillary-associated microglia regulate vascular structure and function through PANX1-P2RY12 coupling in mice. Nat. Commun. 12, 5289. https://doi.org/10.1038/s41467-021-25590-8

Bitanihirwe, B.K.Y., Lizano, P., Woo, T.-U.W., 2022. Deconstructing the functional neuroanatomy of the choroid plexus: an ontogenetic perspective for studying neurodevelopmental and neuropsychiatric disorders. Mol. Psychiatry 27, 3573–3582. https://doi.org/10.1038/s41380-022-01623-6

Blum, D., Torch, S., Lambeng, N., Nissou, M.-F., Benabid, A.-L., Sadoul, R., Verna, J.-M., 2001. Molecular pathways involved in the neurotoxicity of 6-OHDA, dopamine and MPTP: contribution to the apoptotic theory in Parkinson's disease. Prog. Neurobiol. 65, 135–172. https://doi.org/10.1016/S0301-0082(01)00003-X

Bodea, L.-G., Wang, Y., Linnartz-Gerlach, B., Kopatz, J., Sinkkonen, L., Musgrove, R., Kaoma, T., Muller, A., Vallar, L., Monte, D.A.D., Balling, R., Neumann, H., 2014. Neurodegeneration by Activation of the Microglial Complement–Phagosome Pathway. J. Neurosci. 34, 8546–8556. https://doi.org/10.1523/JNEUROSCI.5002-13.2014

Braak, H., Del Tredici, K., Rüb, U., de Vos, R.A.I., Jansen Steur, E.N.H., Braak, E., 2003. Staging of brain pathology related to sporadic Parkinson's disease. Neurobiol. Aging 24, 197–211. https://doi.org/10.1016/s0197-4580(02)00065-9

Brenner, S., 1974. The Genetics of CAENORHABDITIS ELEGANS. Genetics 77, 71–94.

Brown, G.C., Neher, J.J., 2014. Microglial phagocytosis of live neurons. Nat. Rev. Neurosci. 15, 209–216. https://doi.org/10.1038/nrn3710

Cabello, J., Neukomm, L.J., Günesdogan, U., Burkart, K., Charette, S.J., Lochnit, G., Hengartner, M.O., Schnabel, R., 2010. The Wnt pathway controls cell death engulfment, spindle orientation, and migration through CED-10/Rac. PLoS Biol. 8, e1000297. https://doi.org/10.1371/journal.pbio.1000297

Cabello, J., Sämann, J., Gómez-Orte, E., Erazo, T., Coppa, A., Pujol, A., Büssing, I., Schulze, B., Lizcano, J.M., Ferrer, I., Baumeister, R., Dalfo, E., 2014. PDR-1/hParkin negatively regulates the phagocytosis of apoptotic cell corpses in Caenorhabditis elegans. Cell Death Dis. 5, e1120. https://doi.org/10.1038/cddis.2014.57

Calabresi, P., Mechelli, A., Natale, G., Volpicelli-Daley, L., Di Lazzaro, G., Ghiglieri, V., 2023. Alpha-synuclein in Parkinson's disease and other synucleinopathies: from overt neurodegeneration back to early synaptic dysfunction. Cell Death Dis. 14, 176. https://doi.org/10.1038/s41419-023-05672-9

Cao, S., Gelwix, C.C., Caldwell, K.A., Caldwell, G.A., 2005. Torsin-Mediated Protection from Cellular Stress in the Dopaminergic Neurons of Caenorhabditis elegans. J. Neurosci. 25, 3801–3812. https://doi.org/10.1523/JNEUROSCI.5157-04.2005

Chakraborty, S., Lambie, E.J., Bindu, S., Mikeladze-Dvali, T., Conradt, B., 2015. Engulfment pathways promote programmed cell death by enhancing the unequal segregation of apoptotic potential. Nat. Commun. 6, 10126. https://doi.org/10.1038/ncomms10126

Chalazonitis, A., Rao, M., Sulzer, D., 2022. Similarities and differences between nigral and enteric dopaminergic neurons unravel distinctive involvement in Parkinson's disease. Npj Park. Dis. 8, 1–16. https://doi.org/10.1038/s41531-022-00308-9

Chang, K.-H., Chen, C.-M., 2020. The Role of Oxidative Stress in Parkinson's Disease. Antioxidants 9, 597. https://doi.org/10.3390/antiox9070597

Chase, D.L., Pepper, J.S., Koelle, M.R., 2004. Mechanism of extrasynaptic dopamine signaling in Caenorhabditis elegans. Nat. Neurosci. 7, 1096–1103. https://doi.org/10.1038/nn1316

Chelur, D.S., Chalfie, M., 2007. Targeted cell killing by reconstituted caspases. Proc. Natl. Acad. Sci. U. S. A. 104, 2283–2288. https://doi.org/10.1073/pnas.0610877104

Chen, Y.-Z., Klöditz, K., Lee, E.-S., Nguyen, D.P., Yuan, Q., Johnson, J., Lee-yow, Y., Hall, A., Mitani, S., Xia, N.-S., Fadeel, B., Xue, D., 2019. Structure and function analysis of the C. elegans aminophospholipid translocase TAT-1. J. Cell Sci. 132, jcs227660. https://doi.org/10.1242/jcs.227660

Chisholm, A.D., Horvitz, H.R., 1995. Patterning of the Caenorhabditis elegans head region by the Pax-6 family member vab-3. Nature 377, 52–55. https://doi.org/10.1038/377052a0

Chiu, H., Zou, Y., Suzuki, N., Hsieh, Y.-W., Chuang, C.-F., Wu, Y.-C., Chang, C., 2018. Engulfing cells promote neuronal regeneration and remove neuronal debris through distinct biochemical functions of CED-1. Nat. Commun. 9, 4842. https://doi.org/10.1038/s41467-018-07291-x

Chung, W.-S., Baldwin, K.T., Allen, N.J., 2024. Astrocyte Regulation of Synapse Formation, Maturation, and Elimination. Cold Spring Harb. Perspect. Biol. 16, a041352. https://doi.org/10.1101/cshperspect.a041352

Chung, W.-S., Clarke, L.E., Wang, G.X., Stafford, B.K., Sher, A., Chakraborty, C., Joung, J., Foo, L.C., Thompson, A., Chen, C., Smith, S.J., Barres, B.A., 2013. Astrocytes mediate synapse elimination through MEGF10 and MERTK pathways. Nature 504, 394–400. https://doi.org/10.1038/nature12776

Clairembault, T., Leclair-Visonneau, L., Coron, E., Bourreille, A., Le Dily, S., Vavasseur, F., Heymann, M.-F., Neunlist, M., Derkinderen, P., 2015. Structural alterations of the intestinal

epithelial barrier in Parkinson's disease. Acta Neuropathol. Commun. 3, 12. https://doi.org/10.1186/s40478-015-0196-0

Clark, A.S., Huayta, J., Morton, K.S., Meyer, J.N., San-Miguel, A., 2024. Morphological hallmarks of dopaminergic neurodegeneration are associated with altered neuron function in Caenorhabditis elegans. Neurotoxicology 100, 100–106. https://doi.org/10.1016/j.neuro.2023.12.005

Clark, S.G., Shurland, D.-L., Meyerowitz, E.M., Bargmann, C.I., van der Bliek, A.M., 1997. A dynamin GTPase mutation causes a rapid and reversible temperature-inducible locomotion defect in C. elegans. Proc. Natl. Acad. Sci. U. S. A. 94, 10438–10443. https://doi.org/10.1073/pnas.94.19.10438

Cohen-Adiv, S., Amer-Sarsour, F., Berdichevsky, Y., Boxer, E., Goldstein, O., Gana-Weisz, M., Tripathi, U., Rike, W.A., Prag, G., Gurevich, T., Giladi, N., Stern, S., Orr-Urtreger, A., Friedmann-Morvinski, D., Ashkenazi, A., 2024. TMEM16F regulates pathologic α-synuclein secretion and spread in cellular and mouse models of Parkinson's disease. Aging Cell e14387. https://doi.org/10.1111/acel.14387

Conradt, B., Wu, Y.-C., Xue, D., 2016. Programmed Cell Death During Caenorhabditis elegans Development. Genetics 203, 1533–1562. https://doi.org/10.1534/genetics.115.186247

Cook, S.J., Jarrell, T.A., Brittin, C.A., Wang, Y., Bloniarz, A.E., Yakovlev, M.A., Nguyen, K.C.Q., Tang, L.T.-H., Bayer, E.A., Duerr, J.S., Bülow, H.E., Hobert, O., Hall, D.H., Emmons, S.W., 2019. Whole-animal connectomes of both Caenorhabditis elegans sexes. Nature 571, 63–71. https://doi.org/10.1038/s41586-019-1352-7

Cooper, J.F., Spielbauer, K.K., Senchuk, M.M., Nadarajan, S., Colaiácovo, M.P., Van Raamsdonk, J.M., 2018. α-synuclein expression from a single copy transgene increases sensitivity to stress and accelerates neuronal loss in genetic models of Parkinson's disease. Exp. Neurol. 310, 58–69. https://doi.org/10.1016/j.expneurol.2018.09.001

Coutinho-Budd, J., Freeman, M.R., Ackerman, S., 2024. Glial Regulation of Circuit Wiring, Firing, and Expiring in the Drosophila Central Nervous System. Cold Spring Harb. Perspect. Biol. 16, a041347. https://doi.org/10.1101/cshperspect.a041347

Croci, C., Traverso, M., Baratto, S., Iacomino, M., Pedemonte, M., Caroli, F., Scala, M., Bruno, C., Fiorillo, C., 2022. Congenital myopathy associated with a novel mutation in MEGF10 gene, myofibrillar alteration and progressive course. Acta Myol. 41, 111–116. https://doi.org/10.36185/2532-1900-076

Damier, P., Hirsch, E.C., Agid, Y., Graybiel, A.M., 1999. The substantia nigra of the human brain. II. Patterns of loss of dopamine-containing neurons in Parkinson's disease. Brain J. Neurol. 122 (Pt 8), 1437–1448. https://doi.org/10.1093/brain/122.8.1437

Damisah, E.C., Hill, R.A., Rai, A., Chen, F., Rothlin, C.V., Ghosh, S., Grutzendler, J., 2020. Astrocytes and microglia play orchestrated roles and respect phagocytic territories during neuronal corpse removal in vivo. Sci. Adv. 6, eaba3239. https://doi.org/10.1126/sciadv.aba3239

Danese, A., Leo, S., Rimessi, A., Wieckowski, M.R., Fiorica, F., Giorgi, C., Pinton, P., 2021. Cell death as a result of calcium signaling modulation: A cancer-centric prospective. Biochim. Biophys. Acta BBA - Mol. Cell Res. 1868, 119061. https://doi.org/10.1016/j.bbamcr.2021.119061

Darland-Ransom, M., Wang, X., Sun, C.-L., Mapes, J., Gengyo-Ando, K., Mitani, S., Xue, D., 2008. Role of C. elegans TAT-1 protein in maintaining plasma membrane phosphatidylserine asymmetry. Science 320, 528–531. https://doi.org/10.1126/science.1155847

Day, J.O., Mullin, S., 2021. The Genetics of Parkinson's Disease and Implications for Clinical Practice. Genes 12, 1006. https://doi.org/10.3390/genes12071006

de Ceglia, R., Ledonne, A., Litvin, D.G., Lind, B.L., Carriero, G., Latagliata, E.C., Bindocci, E., Di Castro, M.A., Savtchouk, I., Vitali, I., Ranjak, A., Congiu, M., Canonica, T., Wisden, W., Harris, K., Mameli, M., Mercuri, N., Telley, L., Volterra, A., 2023. Specialized astrocytes mediate glutamatergic gliotransmission in the CNS. Nature 622, 120–129. https://doi.org/10.1038/s41586-023-06502-w

Delenclos, M., Burgess, J.D., Lamprokostopoulou, A., Outeiro, T.F., Vekrellis, K., McLean, P.J., 2019. Cellular models of alpha-synuclein toxicity and aggregation. J. Neurochem. 150, 566–576. https://doi.org/10.1111/jnc.14806

Depboylu, C., Stricker, S., Ghobril, J.-P., Oertel, W.H., Priller, J., Höglinger, G.U., 2012. Brain-resident microglia predominate over infiltrating myeloid cells in activation, phagocytosis and interaction with T-lymphocytes in the MPTP mouse model of Parkinson disease. Exp. Neurol. 238, 183–191. https://doi.org/10.1016/j.expneurol.2012.08.020

Derk, J., Jones, H.E., Como, C., Pawlikowski, B., Siegenthaler, J.A., 2021. Living on the Edge of the CNS: Meninges Cell Diversity in Health and Disease. Front. Cell. Neurosci. 15. https://doi.org/10.3389/fncel.2021.703944

Derkinderen, P., 2017. LRRK2 Expression in the Enteric Nervous System: ENSuring Its Significance. Dig. Dis. Sci. 62, 826–827. https://doi.org/10.1007/s10620-017-4500-7

Dias, V., Junn, E., Mouradian, M.M., 2013. The Role of Oxidative Stress in Parkinson's Disease. J. Park. Dis. 3, 461. https://doi.org/10.3233/JPD-130230

Dickson, D.W., Braak, H., Duda, J.E., Duyckaerts, C., Gasser, T., Halliday, G.M., Hardy, J., Leverenz, J.B., Del Tredici, K., Wszolek, Z.K., Litvan, I., 2009. Neuropathological assessment of Parkinson's disease: refining the diagnostic criteria. Lancet Neurol. 8, 1150–1157. https://doi.org/10.1016/S1474-4422(09)70238-8

Ding, X.-B., Wang, X.-X., Xia, D.-H., Liu, H., Tian, H.-Y., Fu, Y., Chen, Y.-K., Qin, C., Wang, J.-Q., Xiang, Z., Zhang, Z.-X., Cao, Q.-C., Wang, W., Li, J.-Y., Wu, E., Tang, B.-S., Ma, M.-M., Teng, J.-F., Wang, X.-J., 2021. Impaired meningeal lymphatic drainage in patients with idiopathic Parkinson's disease. Nat. Med. 27, 411–418. https://doi.org/10.1038/s41591-020-01198-1

Doherty, J., Sheehan, A.E., Bradshaw, R., Fox, A.N., Lu, T.-Y., Freeman, M.R., 2014. PI3K Signaling and Stat92E Converge to Modulate Glial Responsiveness to Axonal Injury. PLOS Biol. 12, e1001985. https://doi.org/10.1371/journal.pbio.1001985

Donato, A., Ritchie, F.K., Lu, L., Wadia, M., Martinez-Marmol, R., Kaulich, E., Sankorrakul, K., Lu, H., Coakley, S., Coulson, E.J., Hilliard, M.A., 2025. OSP-1 protects neurons from autophagic cell death induced by acute oxidative stress. Nat. Commun. 16, 300. https://doi.org/10.1038/s41467-024-55105-0

Dorsey, E.R., Sherer, T., Okun, M.S., Bloem, B.R., 2018. The Emerging Evidence of the Parkinson Pandemic. J. Park. Dis. 8, S3–S8. https://doi.org/10.3233/JPD-181474

Dowling, L.R., Strazzari, M.R., Keely, S., Kaiko, G.E., 2022. Enteric nervous system and intestinal epithelial regulation of the gut-brain axis. J. Allergy Clin. Immunol. 150, 513–522. https://doi.org/10.1016/j.jaci.2022.07.015

Ellis, R.E., Jacobson, D.M., Horvitz, H.R., 1991. Genes required for the engulfment of cell corpses during programmed cell death in Caenorhabditis elegans. Genetics 129, 79–94. https://doi.org/10.1093/genetics/129.1.79

Fan, X., Agid, Y., 2018. At the Origin of the History of Glia. Neuroscience 385, 255–271. https://doi.org/10.1016/j.neuroscience.2018.05.050

Fearnley, J.M., Lees, A.J., 1991. Ageing and Parkinson's disease: substantia nigra regional selectivity. Brain J. Neurol. 114 (Pt 5), 2283–2301. https://doi.org/10.1093/brain/114.5.2283

Feinberg, E.H., Vanhoven, M.K., Bendesky, A., Wang, G., Fetter, R.D., Shen, K., Bargmann, C.I., 2008. GFP Reconstitution Across Synaptic Partners (GRASP) defines cell contacts and synapses in living nervous systems. Neuron 57, 353–363. https://doi.org/10.1016/j.neuron.2007.11.030

Fourgeaud, L., Través, P.G., Tufail, Y., Leal-Bailey, H., Lew, E.D., Burrola, P.G., Callaway, P., Zagórska, A., Rothlin, C.V., Nimmerjahn, A., Lemke, G., 2016. TAM receptors regulate multiple features of microglial physiology. Nature 532, 240–244. https://doi.org/10.1038/nature17630

Fuentes-Medel, Y., Logan, M.A., Ashley, J., Ataman, B., Budnik, V., Freeman, M.R., 2009. Glia and Muscle Sculpt Neuromuscular Arbors by Engulfing Destabilized Synaptic Boutons and Shed Presynaptic Debris. PLoS Biol. 7, e1000184. https://doi.org/10.1371/journal.pbio.1000184

Fujita, Y., Maeda, T., Kamaishi, K., Saito, R., Chiba, K., Shen, X., Zou, K., Komano, H., 2017. Expression of MEGF10 in cholinergic and glutamatergic neurons. Neurosci. Lett. 653, 25–30. https://doi.org/10.1016/j.neulet.2017.05.029

Fullard, M.E., Morley, J.F., Duda, J.E., 2017. Olfactory Dysfunction as an Early Biomarker in Parkinson's Disease. Neurosci. Bull. 33, 515–525. https://doi.org/10.1007/s12264-017-0170-x

Furuta, Y., Pena-Ramos, O., Li, Z., Chiao, L., Zhou, Z., 2021. Calcium ions trigger the exposure of phosphatidylserine on the surface of necrotic cells. PLoS Genet. 17, e1009066. https://doi.org/10.1371/journal.pgen.1009066

Gaeta, A.L., Caldwell, K.A., Caldwell, G.A., 2019a. Found in Translation: The Utility of C. elegans Alpha-Synuclein Models of Parkinson's Disease. Brain Sci. 9, 73. https://doi.org/10.3390/brainsci9040073

Gaeta, A.L., Caldwell, K.A., Caldwell, G.A., 2019b. Found in Translation: The Utility of C. elegans Alpha-Synuclein Models of Parkinson's Disease. Brain Sci. 9, 73. https://doi.org/10.3390/brainsci9040073

Gcwensa, N.Z., Russell, D.L., Cowell, R.M., Volpicelli-Daley, L.A., 2021. Molecular Mechanisms Underlying Synaptic and Axon Degeneration in Parkinson's Disease. Front. Cell. Neurosci. 15. https://doi.org/10.3389/fncel.2021.626128

Ghose, P., Wehman, A.M., 2021. The developmental and physiological roles of phagocytosis in *Caenorhabditis elegans*, in: Jarriault, S., Podbilewicz, B. (Eds.), Current Topics in Developmental Biology, Nematode Models of Development and Disease. Academic Press, pp. 409–432. https://doi.org/10.1016/bs.ctdb.2020.09.001

Gibbons, C.H., Levine, T., Adler, C., Bellaire, B., Wang, N., Stohl, J., Agarwal, P., Aldridge, G.M., Barboi, A., Evidente, V.G.H., Galasko, D., Geschwind, M.D., Gonzalez-Duarte, A., Gil, R., Gudesblatt, M., Isaacson, S.H., Kaufmann, H., Khemani, P., Kumar, R., Lamotte, G., Liu, A.J., McFarland, N.R., Miglis, M., Reynolds, A., Sahagian, G.A., Saint-Hillaire, M.-H., Schwartzbard, J.B., Singer, W., Soileau, M.J., Vernino, S., Yerstein, O., Freeman, R., 2024. Skin Biopsy Detection of Phosphorylated α-Synuclein in Patients With Synucleinopathies. JAMA 331, 1298–1306. https://doi.org/10.1001/jama.2024.0792

Gibson, C.L., Balbona, J.T., Niedzwiecki, A., Rodriguez, P., Nguyen, K.C.Q., Hall, D.H., Blakely, R.D., 2018. Glial loss of the metallo β-lactamase domain containing protein, SWIP-10, induces age- and glutamate-signaling dependent, dopamine neuron degeneration. PLoS Genet. 14, e1007269. https://doi.org/10.1371/journal.pgen.1007269

Gilleard, J.S., Barry, J.D., Johnstone, I.L., 1997. cis Regulatory Requirements for Hypodermal Cell-Specific Expression of the Caenorhabditis elegans Cuticle Collagen Gene dpy-7. Mol. Cell. Biol. 17, 2301–2311. https://doi.org/10.1128/MCB.17.4.2301

Gómez-Benito, M., Granado, N., García-Sanz, P., Michel, A., Dumoulin, M., Moratalla, R., 2020a. Modeling Parkinson's Disease With the Alpha-Synuclein Protein. Front. Pharmacol. 11, 356. https://doi.org/10.3389/fphar.2020.00356

Gómez-Benito, M., Granado, N., García-Sanz, P., Michel, A., Dumoulin, M., Moratalla, R., 2020b. Modeling Parkinson's Disease With the Alpha-Synuclein Protein. Front. Pharmacol. 11, 356. https://doi.org/10.3389/fphar.2020.00356

Goudeau, J., Sharp, C.S., Paw, J., Savy, L., Leonetti, M.D., York, A.G., Updike, D.L., Kenyon, C., Ingaramo, M., 2021. Split-wrmScarlet and split-sfGFP: tools for faster, easier fluorescent labeling of endogenous proteins in Caenorhabditis elegans. Genetics 217, iyab014. https://doi.org/10.1093/genetics/iyab014

Gröger, A., Kolb, R., Schäfer, R., Klose, U., 2014. Dopamine Reduction in the Substantia Nigra of Parkinson's Disease Patients Confirmed by In Vivo Magnetic Resonance Spectroscopic Imaging. PLOS ONE 9, e84081. https://doi.org/10.1371/journal.pone.0084081

Gui, M., Lv, L., Hu, S., Qin, L., Wang, C., 2025. Sarcopenia in Parkinson's disease: from pathogenesis to interventions. Metabolism 169, 156272. https://doi.org/10.1016/j.metabol.2025.156272

Gulbransen, B.D., Sharkey, K.A., 2012. Novel functional roles for enteric glia in the gastrointestinal tract. Nat. Rev. Gastroenterol. Hepatol. 9, 625–632. https://doi.org/10.1038/nrgastro.2012.138

Haddad, D., Nakamura, K., 2015. Understanding the susceptibility of dopamine neurons to mitochondrial stressors in Parkinson's disease. FEBS Lett. 589, 3702–3713. https://doi.org/10.1016/j.febslet.2015.10.021

Hamon, Y., Trompier, D., Ma, Z., Venegas, V., Pophillat, M., Mignotte, V., Zhou, Z., Chimini, G., 2006. Cooperation between Engulfment Receptors: The Case of ABCA1 and MEGF10. PLoS ONE 1, e120. https://doi.org/10.1371/journal.pone.0000120

Hardaway, J.A., Sturgeon, S.M., Snarrenberg, C.L., Li, Z., Xu, X.Z.S., Bermingham, D.P., Odiase, P., Spencer, W.C., Miller, D.M., Carvelli, L., Hardie, S.L., Blakely, R.D., 2015. Glial Expression of the Caenorhabditis elegans Gene swip-10 Supports Glutamate Dependent Control of Extrasynaptic Dopamine Signaling. J. Neurosci. 35, 9409–9423. https://doi.org/10.1523/JNEUROSCI.0800-15.2015

Harders, R.H., Morthorst, T.H., Landgrebe, L.E., Lande, A.D., Fuglsang, M.S., Mortensen, S.B., Feteira-Montero, V., Jensen, H.H., Wesseltoft, J.B., Olsen, A., 2024. CED-6/GULP and components of the clathrin-mediated endocytosis machinery act redundantly to correctly display CED-1 on the cell membrane in Caenorhabditis elegans. G3 GenesGenomesGenetics 14, jkae088. https://doi.org/10.1093/g3journal/jkae088

Haskins, K.A., Russell, J.F., Gaddis, N., Dressman, H.K., Aballay, A., 2008. Unfolded Protein Response Genes Regulated by CED-1 are Required for Caenorhabditis elegans Innate Immunity. Dev. Cell 15, 87–97. https://doi.org/10.1016/j.devcel.2008.05.006

Hengartner, M.O., Robert Horvitz, H., 1994. Programmed cell death in *Caenorhabditis elegans*. Curr. Opin. Genet. Dev. 4, 581–586. https://doi.org/10.1016/0959-437X(94)90076-F

Hernandez-Baltazar, D., Zavala-Flores, L.M., Villanueva-Olivo, A., 2017. The 6-hydroxydopamine model and parkinsonian pathophysiology: Novel findings in an older model. Neurol. Barc. Spain 32, 533–539. https://doi.org/10.1016/j.nrl.2015.06.011

Hoeppner, D.J., Hengartner, M.O., Schnabel, R., 2001. Engulfment genes cooperate with ced-3 to promote cell death in Caenorhabditis elegans. Nature 412, 202–206. https://doi.org/10.1038/35084103

Holterman, C.E., Le Grand, F., Kuang, S., Seale, P., Rudnicki, M.A., 2007. Megf10 regulates the progression of the satellite cell myogenic program. J. Cell Biol. 179, 911–922. https://doi.org/10.1083/jcb.200709083

Hong, S., Beja-Glasser, V.F., Nfonoyim, B.M., Frouin, A., Li, S., Ramakrishnan, S., Merry, K.M., Shi, Q., Rosenthal, A., Barres, B.A., Lemere, C.A., Selkoe, D.J., Stevens, B., 2016. Complement and microglia mediate early synapse loss in Alzheimer mouse models. Science 352, 712–716. https://doi.org/10.1126/science.aad8373

Hsieh, H.-H., Hsu, T.-Y., Jiang, H.-S., Wu, Y.-C., 2012. Integrin α PAT-2/CDC-42 signaling is required for muscle-mediated clearance of apoptotic cells in Caenorhabditis elegans. PLoS Genet. 8, e1002663. https://doi.org/10.1371/journal.pgen.1002663

Hsu, T.-Y., Wu, Y.-C., 2010. Engulfment of apoptotic cells in C. elegans is mediated by integrin alpha/SRC signaling. Curr. Biol. CB 20, 477–486. https://doi.org/10.1016/j.cub.2010.01.062

Iovino, L., Tremblay, M.E., Civiero, L., 2020a. Glutamate-induced excitotoxicity in Parkinson's disease: The role of glial cells. J. Pharmacol. Sci. 144, 151–164. https://doi.org/10.1016/j.jphs.2020.07.011

Iovino, L., Tremblay, M.E., Civiero, L., 2020b. Glutamate-induced excitotoxicity in Parkinson's disease: The role of glial cells. J. Pharmacol. Sci. 144, 151–164. https://doi.org/10.1016/j.jphs.2020.07.011

Iram, T., Ramirez-Ortiz, Z., Byrne, M.H., Coleman, U.A., Kingery, N.D., Means, T.K., Frenkel, D., El Khoury, J., 2016. Megf10 Is a Receptor for C1Q That Mediates Clearance of Apoptotic Cells by Astrocytes. J. Neurosci. 36, 5185–5192. https://doi.org/10.1523/JNEUROSCI.3850-15.2016

Jiang, Y., Horner, V., Liu, J., 2005. The HMX homeodomain protein MLS-2 regulates cleavage orientation, cell proliferation and cell fate specification in the C. eleganspostembryonic mesoderm. Development 132, 4119–4130. https://doi.org/10.1242/dev.01967

Joers, V., Tansey, M.G., Mulas, G., Carta, A.R., 2017. Microglial phenotypes in Parkinson's disease and animal models of the disease. Prog. Neurobiol., Multiple Mechanisms of Neurodegeneration and Progression 155, 57–75. https://doi.org/10.1016/j.pneurobio.2016.04.006

Johnsen, H.L., Horvitz, H.R., 2016. Both the apoptotic suicide pathway and phagocytosis are required for a programmed cell death in Caenorhabditis elegans. BMC Biol. 14, 39. https://doi.org/10.1186/s12915-016-0262-5

Juros, D., Avila, M.F., Hastings, R.L., Pendragon, A., Wilson, L., Kay, J., Valdez, G., 2024. Cellular and molecular alterations to muscles and neuromuscular synapses in a mouse model of MEGF10-related myopathy. Skelet. Muscle 14, 10. https://doi.org/10.1186/s13395-024-00342-6

Jyothi, H.J., Vidyadhara, D.J., Mahadevan, A., Philip, M., Parmar, S.K., Manohari, S.G., Shankar, S.K., Raju, T.R., Alladi, P.A., 2015. Aging causes morphological alterations in astrocytes and microglia in human substantia nigra pars compacta. Neurobiol. Aging 36, 3321–3333. https://doi.org/10.1016/j.neurobiolaging.2015.08.024

Kam, T.-I., Park, H., Chou, S.-C., Van Vranken, J.G., Mittenbühler, M.J., Kim, H., A, M., Choi, Y.R., Biswas, D., Wang, J., Shin, Y., Loder, A., Karuppagounder, S.S., Wrann, C.D., Dawson, V.L., Spiegelman, B.M., Dawson, T.M., 2022. Amelioration of pathologic α-synuclein-induced Parkinson's disease by irisin. Proc. Natl. Acad. Sci. 119, e2204835119. https://doi.org/10.1073/pnas.2204835119

Katz, M., Corson, F., Iwanir, S., Biron, D., Shaham, S., 2018. Glia Modulate a Neuronal Circuit for Locomotion Suppression during Sleep in C. elegans. Cell Rep. 22, 2575–2583. https://doi.org/10.1016/j.celrep.2018.02.036

Katz, M., Corson, F., Keil, W., Singhal, A., Bae, A., Lu, Y., Liang, Y., Shaham, S., 2019. Glutamate spillover in C. elegans triggers repetitive behavior through presynaptic activation of MGL-2/mGluR5. Nat. Commun. 10, 1882. https://doi.org/10.1038/s41467-019-09581-4

Khakh, B.S., Sofroniew, M.V., 2015. Diversity of astrocyte functions and phenotypes in neural circuits. Nat. Neurosci. 18, 942–952. https://doi.org/10.1038/nn.4043

Kordower, J.H., Olanow, C.W., Dodiya, H.B., Chu, Y., Beach, T.G., Adler, C.H., Halliday, G.M., Bartus, R.T., 2013. Disease duration and the integrity of the nigrostriatal system in Parkinson's disease. Brain 136, 2419–2431. https://doi.org/10.1093/brain/awt192

Kouli, A., Torsney, K.M., Kuan, W.-L., 2018. Parkinson's Disease: Etiology, Neuropathology, and Pathogenesis, in: Stoker, T.B., Greenland, J.C. (Eds.), Parkinson's Disease: Pathogenesis and Clinical Aspects. Codon Publications, Brisbane (AU).

Kozlowski, C., Hadyniak, S.E., Kay, J.N., 2024. Retinal neurons establish mosaic patterning by excluding homotypic somata from their dendritic territories. Cell Rep. 43, 114615. https://doi.org/10.1016/j.celrep.2024.114615

Langen, U.H., Ayloo, S., Gu, C., 2019. Development and Cell Biology of the Blood-Brain Barrier. Annu. Rev. Cell Dev. Biol. 35, 591–613. https://doi.org/10.1146/annurev-cellbio-100617-062608

Lashuel, H.A., Overk, C.R., Oueslati, A., Masliah, E., 2013. The many faces of α-synuclein: from structure and toxicity to therapeutic target. Nat. Rev. Neurosci. 14, 38–48. https://doi.org/10.1038/nrn3406

Lee, K.H., Cha, M., Lee, B.H., 2021. Crosstalk between Neuron and Glial Cells in Oxidative Injury and Neuroprotection. Int. J. Mol. Sci. 22, 13315. https://doi.org/10.3390/ijms222413315

Li, C., Vargas-Franco, D., Saha, M., Davis, R.M., Manko, K.A., Draper, I., Pacak, C.A., Kang, P.B., 2021. Megf10 deficiency impairs skeletal muscle stem cell migration and muscle regeneration. FEBS Open Bio 11, 114–123. https://doi.org/10.1002/2211-5463.13031

Li, S., Le, W., 2017. Milestones of Parkinson's Disease Research: 200 Years of History and Beyond. Neurosci. Bull. 33, 598–602. https://doi.org/10.1007/s12264-017-0178-2

Li, Z., Venegas, V., Nagaoka, Y., Morino, E., Raghavan, P., Audhya, A., Nakanishi, Y., Zhou, Z., 2015. Necrotic Cells Actively Attract Phagocytes through the Collaborative Action of Two Distinct PS-Exposure Mechanisms. PLoS Genet. 11, e1005285. https://doi.org/10.1371/journal.pgen.1005285

Lipski, J., Nistico, R., Berretta, N., Guatteo, E., Bernardi, G., Mercuri, N.B., 2011. l-DOPA: A scapegoat for accelerated neurodegeneration in Parkinson's disease? Prog. Neurobiol. 94, 389–407. https://doi.org/10.1016/j.pneurobio.2011.06.005

Liu, K.E., Raymond, M.H., Ravichandran, K.S., Kucenas, S., 2022. Clearing Your Mind: Mechanisms of Debris Clearance After Cell Death During Neural Development. Annu. Rev. Neurosci. 45, 177–198. https://doi.org/10.1146/annurev-neuro-110920-022431

Lu, N., Yu, X., He, X., Zhou, Z., 2009. Detecting Apoptotic Cells and Monitoring Their Clearance in the Nematode Caenorhabditis elegans. Methods Mol. Biol. Clifton NJ 559, 357–370. https://doi.org/10.1007/978-1-60327-017-5_25

Lu, T.-Y., MacDonald, J.M., Neukomm, L.J., Sheehan, A.E., Bradshaw, R., Logan, M.A., Freeman, M.R., 2017. Axon degeneration induces glial responses through Draper-TRAF4-JNK signalling. Nat. Commun. 8, 14355. https://doi.org/10.1038/ncomms14355

MacDonald, J.M., Beach, M.G., Porpiglia, E., Sheehan, A.E., Watts, R.J., Freeman, M.R., 2006. The Drosophila cell corpse engulfment receptor Draper mediates glial clearance of severed axons. Neuron 50, 869–881. https://doi.org/10.1016/j.neuron.2006.04.028

Mapes, J., Chen, Y.-Z., Kim, A., Mitani, S., Kang, B.-H., Xue, D., 2012. CED-1, CED-7, and TTR-52 Regulate Surface Phosphatidylserine Expression on Apoptotic and Phagocytic Cells. Curr. Biol. 22, 1267–1275. https://doi.org/10.1016/j.cub.2012.05.052

Marrocco, E., Indrieri, A., Esposito, F., Tarallo, V., Carboncino, A., Alvino, F.G., De Falco, S., Franco, B., De Risi, M., De Leonibus, E., 2020. α-synuclein overexpression in the retina leads to vision impairment and degeneration of dopaminergic amacrine cells. Sci. Rep. 10, 9619. https://doi.org/10.1038/s41598-020-66497-6

Martin, C.G., Bent, J.S., Hill, T., Topalidou, I., Singhvi, A., 2024. Epithelial UNC-23 limits mechanical stress to maintain glia-neuron architecture in C. elegans. Dev. Cell 59, 1668-1688.e7. https://doi.org/10.1016/j.devcel.2024.04.005

Martin-Lopez, E., Vidyadhara, D.J., Liberia, T., Meller, S.J., Harmon, L.E., Hsu, R.M., Spence, N., Brennan, B., Han, K., Yücel, B., Chandra, S.S., Greer, C.A., 2023. α-Synuclein Pathology and Reduced Neurogenesis in the Olfactory System Affect Olfaction in a Mouse Model of Parkinson's Disease. J. Neurosci. Off. J. Soc. Neurosci. 43, 1051–1071. https://doi.org/10.1523/JNEUROSCI.1526-22.2022

Masoudi, N., Ibanez-Cruceyra, P., Offenburger, S.-L., Holmes, A., Gartner, A., 2014a. Tetraspanin (TSP-17) Protects Dopaminergic Neurons against 6-OHDA-Induced Neurodegeneration in C. elegans. PLOS Genet. 10, e1004767. https://doi.org/10.1371/journal.pgen.1004767

Masoudi, N., Ibanez-Cruceyra, P., Offenburger, S.-L., Holmes, A., Gartner, A., 2014b. Tetraspanin (TSP-17) protects dopaminergic neurons against 6-OHDA-induced neurodegeneration in C. elegans. PLoS Genet. 10, e1004767. https://doi.org/10.1371/journal.pgen.1004767

McCarroll, S.A., Li, H., Bargmann, C.I., 2005. Identification of Transcriptional Regulatory Elements in Chemosensory Receptor Genes by Probabilistic Segmentation. Curr. Biol. 15, 347–352. https://doi.org/10.1016/j.cub.2005.02.023

McDonald, P.W., Hardie, S.L., Jessen, T.N., Carvelli, L., Matthies, D.S., Blakely, R.D., 2007. Vigorous motor activity in Caenorhabditis elegans requires efficient clearance of dopamine mediated by synaptic localization of the dopamine transporter DAT-1. J. Neurosci. Off. J. Soc. Neurosci. 27, 14216–14227. https://doi.org/10.1523/JNEUROSCI.2992-07.2007

Mello, C.C., Kramer, J.M., Stinchcomb, D., Ambros, V., 1991. Efficient gene transfer in C.elegans: extrachromosomal maintenance and integration of transforming sequences. EMBO J. 10, 3959–3970. https://doi.org/10.1002/j.1460-2075.1991.tb04966.x

Miyabayashi, T., Palfreyman, M.T., Sluder, A.E., Slack, F., Sengupta, P., 1999. Expression and Function of Members of a Divergent Nuclear Receptor Family in *Caenorhabditis elegans*. Dev. Biol. 215, 314–331. https://doi.org/10.1006/dbio.1999.9470

Montanari, M., Imbriani, P., Bonsi, P., Martella, G., Peppe, A., 2023. Beyond the Microbiota: Understanding the Role of the Enteric Nervous System in Parkinson's Disease from Mice to Human. Biomedicines 11, 1560. https://doi.org/10.3390/biomedicines11061560

Morales, I., Sanchez, A., Rodriguez-Sabate, C., Rodriguez, M., 2017. Striatal astrocytes engulf dopaminergic debris in Parkinson's disease: A study in an animal model. PloS One 12, e0185989. https://doi.org/10.1371/journal.pone.0185989

Moskal, N., Visanji, N.P., Gorbenko, O., Narasimhan, V., Tyrrell, H., Nash, J., Lewis, P.N., McQuibban, G.A., 2023. An AI-guided screen identifies probucol as an enhancer of mitophagy through modulation of lipid droplets. PLoS Biol. 21, e3001977. https://doi.org/10.1371/journal.pbio.3001977

Murphy, K.T., Lynch, G.S., 2023. Impaired skeletal muscle health in Parkinsonian syndromes: clinical implications, mechanisms and potential treatments. J. Cachexia Sarcopenia Muscle 14, 1987–2002. https://doi.org/10.1002/jcsm.13312

Nagata, S., Suzuki, J., Segawa, K., Fujii, T., 2016. Exposure of phosphatidylserine on the cell surface. Cell Death Differ. 23, 952–961. https://doi.org/10.1038/cdd.2016.7

Nass, R., Blakely, R.D., 2003. The Caenorhabditis elegans Dopaminergic System: Opportunities for Insights into Dopamine Transport and Neurodegeneration. Annu. Rev. Pharmacol. Toxicol. 43, 521–544. https://doi.org/10.1146/annurev.pharmtox.43.100901.135934

Nass, R., Hall, D.H., Miller, D.M., Blakely, R.D., 2002a. Neurotoxin-induced degeneration of dopamine neurons in Caenorhabditis elegans. Proc. Natl. Acad. Sci. U. S. A. 99, 3264–3269. https://doi.org/10.1073/pnas.042497999

Nass, R., Hall, D.H., Miller, D.M., Blakely, R.D., 2002b. Neurotoxin-induced degeneration of dopamine neurons in Caenorhabditis elegans. Proc. Natl. Acad. Sci. 99, 3264–3269. https://doi.org/10.1073/pnas.042497999

Neumann, H., Kotter, M.R., Franklin, R.J.M., 2009. Debris clearance by microglia: an essential link between degeneration and regeneration. Brain J. Neurol. 132, 288–295. https://doi.org/10.1093/brain/awn109

Nichols, A.L.A., Meelkop, E., Linton, C., Giordano-Santini, R., Sullivan, R.K., Donato, A., Nolan, C., Hall, D.H., Xue, D., Neumann, B., Hilliard, M.A., 2016. The Apoptotic Engulfment Machinery Regulates Axonal Degeneration in C. elegans Neurons. Cell Rep. 14, 1673–1683. https://doi.org/10.1016/j.celrep.2016.01.050

Niemann, N., Billnitzer, A., Jankovic, J., 2021. Parkinson's disease and skin. Parkinsonism Relat. Disord. 82, 61–76. https://doi.org/10.1016/j.parkreldis.2020.11.017

Nikoletopoulou, V., Tavernarakis, N., 2014. Necrotic Cell Death in *Caenorhabditis elegans*, in: Ashkenazi, A., Wells, J.A., Yuan, J. (Eds.), Methods in Enzymology, Regulated Cell Death Part B. Academic Press, pp. 127–155. https://doi.org/10.1016/B978-0-12-801430-1.00006-8

Offenburger, S.-L., Ho, X.Y., Tachie-Menson, T., Coakley, S., Hilliard, M.A., Gartner, A., 2018a. 6-OHDA-induced dopaminergic neurodegeneration in Caenorhabditis elegans is promoted by the engulfment pathway and inhibited by the transthyretin-related protein TTR-33. PLOS Genet. 14, e1007125. https://doi.org/10.1371/journal.pgen.1007125

Offenburger, S.-L., Ho, X.Y., Tachie-Menson, T., Coakley, S., Hilliard, M.A., Gartner, A., 2018b. 6-OHDA-induced dopaminergic neurodegeneration in Caenorhabditis elegans is promoted by the engulfment pathway and inhibited by the transthyretin-related protein TTR-33. PLoS Genet. 14. https://doi.org/10.1371/journal.pgen.1007125

Offenburger, S.-L., Jongsma, E., Gartner, A., 2018c. Mutations in Caenorhabditis elegans neuroligin-like glit-1, the apoptosis pathway and the calcium chaperone crt-1 increase dopaminergic neurodegeneration after 6-OHDA treatment. PLoS Genet. 14, e1007106. https://doi.org/10.1371/journal.pgen.1007106

Offenburger, S.-L., Jongsma, E., Gartner, A., 2018d. Mutations in Caenorhabditis elegans neuroligin-like glit-1, the apoptosis pathway and the calcium chaperone crt-1 increase dopaminergic neurodegeneration after 6-OHDA treatment. PLoS Genet. 14. https://doi.org/10.1371/journal.pgen.1007106

O'Gorman Tuura, R.L., Baumann, C.R., Baumann-Vogel, H., 2018. Beyond Dopamine: GABA, Glutamate, and the Axial Symptoms of Parkinson Disease. Front. Neurol. 9. https://doi.org/10.3389/fneur.2018.00806

Pajarillo, E., Rizor, A., Lee, J., Aschner, M., Lee, E., 2019. The role of astrocytic glutamate transporters GLT-1 and GLAST in neurological disorders: Potential targets for neurotherapeutics. Neuropharmacology 161, 107559. https://doi.org/10.1016/j.neuropharm.2019.03.002

Parfejevs, V., Debbache, J., Shakhova, O., Schaefer, S.M., Glausch, M., Wegner, M., Suter, U., Riekstina, U., Werner, S., Sommer, L., 2018. Injury-activated glial cells promote wound healing of the adult skin in mice. Nat. Commun. 9, 236. https://doi.org/10.1038/s41467-017-01488-2

Parkinson, J., 2002. An Essay on the Shaking Palsy. J. Neuropsychiatry Clin. Neurosci. 14, 223–236. https://doi.org/10.1176/jnp.14.2.223

Pérez-Acuña, D., Rhee, K.H., Shin, S.J., Ahn, J., Lee, J.-Y., Lee, S.-J., 2023. Retina-to-brain spreading of α-synuclein after intravitreal injection of preformed fibrils. Acta Neuropathol. Commun. 11, 83. https://doi.org/10.1186/s40478-023-01575-0

Peterman, E., Quitevis, E.J.A., Black, E.C., Horton, E.C., Aelmore, R.L., White, E., Sagasti, A., Rasmussen, J.P., 2023. Zebrafish cutaneous injury models reveal that Langerhans cells engulf

axonal debris in adult epidermis. Dis. Model. Mech. 16, dmm049911. https://doi.org/10.1242/dmm.049911

Petratou, D., Fragkiadaki, P., Lionaki, E., Tavernarakis, N., 2024. Assessing locomotory rate in response to food for the identification of neuronal and muscular defects in C. elegans. STAR Protoc. 5, 102801. https://doi.org/10.1016/j.xpro.2023.102801

Pierce, M.L., Weston, M.D., Fritzsch, B., Gabel, H.W., Ruvkun, G., Soukup, G.A., 2008. MicroRNA-183 family conservation and ciliated neurosensory organ expression. Evol. Dev. 10, 106–113. https://doi.org/10.1111/j.1525-142X.2007.00217.x

Poewe, W., Seppi, K., Tanner, C.M., Halliday, G.M., Brundin, P., Volkmann, J., Schrag, A.-E., Lang, A.E., 2017. Parkinson disease. Nat. Rev. Dis. Primer 3, 1–21. https://doi.org/10.1038/nrdp.2017.13

Purice, M.D., Quitevis, E.J.A., Manning, R.S., Severs, L.J., Tran, N.-T., Sorrentino, V., Setty, M., Singhvi, A., 2023. Molecular heterogeneity of C. elegans glia across sexes. BioRxiv Prepr. Serv. Biol. 2023.03.21.533668. https://doi.org/10.1101/2023.03.21.533668

Purice, M.D., Ray, A., Münzel, E.J., Pope, B.J., Park, D.J., Speese, S.D., Logan, M.A., 2017. A novel Drosophila injury model reveals severed axons are cleared through a Draper/MMP-1 signaling cascade. eLife 6, e23611. https://doi.org/10.7554/eLife.23611

Purice, M.D., Severs, L.J., Singhvi, A., 2024. Glia in Invertebrate Models: Insights from Caenorhabditis elegans, in: Blanco-Suarez, E., Farhy-Tselnicker, I. (Eds.), Astrocyte-Neuron Interactions in Health and Disease. Springer Nature Switzerland, Cham, pp. 19–49. https://doi.org/10.1007/978-3-031-64839-7_2

Raiders, S., Black, E.C., Bae, A., MacFarlane, S., Klein, M., Shaham, S., Singhvi, A., 2021a. Glia actively sculpt sensory neurons by controlled phagocytosis to tune animal behavior. eLife 10, e63532. https://doi.org/10.7554/eLife.63532

Raiders, S., Han, T., Scott-Hewitt, N., Kucenas, S., Lew, D., Logan, M.A., Singhvi, A., 2021b. Engulfed by Glia: Glial Pruning in Development, Function, and Injury across Species. J. Neurosci. 41, 823. https://doi.org/10.1523/JNEUROSCI.1660-20.2020

Rapti, G., Li, C., Shan, A., Lu, Y., Shaham, S., 2017. Glia initiate brain assembly through non-canonical Chimaerin/Furin axon guidance in C. elegans. Nat. Neurosci. 20, 1350. https://doi.org/10.1038/nn.4630

Raudino, F., 2012. The Parkinson disease before James Parkinson. Neurol. Sci. 33, 945–948. https://doi.org/10.1007/s10072-011-0816-9

Ray, A., Speese, S.D., Logan, M.A., 2017. Glial Draper Rescues Aβ Toxicity in a Drosophila Model of Alzheimer's Disease. J. Neurosci. Off. J. Soc. Neurosci. 37, 11881–11893. https://doi.org/10.1523/JNEUROSCI.0862-17.2017

Ray, S., Gurung, P., Manning, R.S., Kravchuk, A.A., Singhvi, A., 2024. Neuron cilia restrain glial KCC-3 to a microdomain to regulate multisensory processing. Cell Rep. 43, 113844. https://doi.org/10.1016/j.celrep.2024.113844

Reddien, P.W., Cameron, S., Horvitz, H.R., 2001. Phagocytosis promotes programmed cell death in C. elegans. Nature 412, 198–202. https://doi.org/10.1038/35084096

Reddien, P.W., Horvitz, H.R., 2004a. The engulfment process of programmed cell death in caenorhabditis elegans. Annu. Rev. Cell Dev. Biol. 20, 193–221. https://doi.org/10.1146/annurev.cellbio.20.022003.114619

Reddien, P.W., Horvitz, H.R., 2004b. The engulfment process of programmed cell death in caenorhabditis elegans. Annu. Rev. Cell Dev. Biol. 20, 193–221. https://doi.org/10.1146/annurev.cellbio.20.022003.114619

Reemst, K., Noctor, S.C., Lucassen, P.J., Hol, E.M., 2016. The Indispensable Roles of Microglia and Astrocytes during Brain Development. Front. Hum. Neurosci. 10, 566. https://doi.org/10.3389/fnhum.2016.00566

Refai, O., Rodriguez, P., Gichi, Z., Blakely, R.D., 2024. Forward genetic screen of the C. elegans million mutation library reveals essential, cell-autonomous contributions of BBSome proteins to dopamine signaling. J. Neurochem. 168, 2073–2091. https://doi.org/10.1111/jnc.16188

Richardson, L., Hughes, R., Johnson, C.A., Egginton, S., Peckham, M., 2025. The role of MEGF10 in myoblast fusion and hypertrophic response to overload of skeletal muscle. J. Muscle Res. Cell Motil. 1–18. https://doi.org/10.1007/s10974-024-09686-4

Roux, A.E., Langhans, K., Huynh, W., Kenyon, C., 2016. Reversible Age-Related Phenotypes Induced during Larval Quiescence in C. elegans. Cell Metab. 23, 1113–1126. https://doi.org/10.1016/j.cmet.2016.05.024

Rueda-Carrasco, J., Sokolova, D., Lee, S., Childs, T., Jurčáková, N., Crowley, G., De Schepper, S., Ge, J.Z., Lachica, J.I., Toomey, C.E., Freeman, O.J., Hardy, J., Barnes, S.J., Lashley, T., Stevens, B., Chang, S., Hong, S., 2023. Microglia-synapse engulfment via PtdSer-TREM2 ameliorates neuronal hyperactivity in Alzheimer's disease models. EMBO J. 42, e113246. https://doi.org/10.15252/embj.2022113246

Rui, Q., Ni, H., Li, D., Gao, R., Chen, G., 2018. The Role of LRRK2 in Neurodegeneration of Parkinson Disease. Curr. Neuropharmacol. 16, 1348–1357. https://doi.org/10.2174/1570159X16666180222165418

Saha, M., Mitsuhashi, S., Jones, M.D., Manko, K., Reddy, H.M., Bruels, C.C., Cho, K.-A., Pacak, C.A., Draper, I., Kang, P.B., 2017. Consequences of MEGF10 deficiency on myoblast function and Notch1 interactions. Hum. Mol. Genet. 26, 2984–3000. https://doi.org/10.1093/hmg/ddx189

Sawin, E.R., Ranganathan, R., Horvitz, H.R., 2000. C. elegans locomotory rate is modulated by the environment through a dopaminergic pathway and by experience through a serotonergic pathway. Neuron 26, 619–631. https://doi.org/10.1016/s0896-6273(00)81199-x

Schober, A., 2004a. Classic toxin-induced animal models of Parkinson's disease: 6-OHDA and MPTP. Cell Tissue Res. 318, 215–224. https://doi.org/10.1007/s00441-004-0938-y

Schober, A., 2004b. Classic toxin-induced animal models of Parkinson's disease: 6-OHDA and MPTP. Cell Tissue Res. 318, 215–224. https://doi.org/10.1007/s00441-004-0938-y

Shehadeh, J., Double, K.L., Murphy, K.E., Bobrovskaya, L., Reyes, S., Dunkley, P.R., Halliday, G.M., Dickson, P.W., 2019. Expression of tyrosine hydroxylase isoforms and phosphorylation at serine 40 in the human nigrostriatal system in Parkinson's disease. Neurobiol. Dis. 130, 104524. https://doi.org/10.1016/j.nbd.2019.104524

Singh, T.D., Park, S.-Y., Bae, J., Yun, Y., Bae, Y.-C., Park, R.-W., Kim, I.-S., 2010. MEGF10 functions as a receptor for the uptake of amyloid-β. FEBS Lett. 584, 3936–3942. https://doi.org/10.1016/j.febslet.2010.08.050

Singhvi, A., Liu, B., Friedman, C.J., Fong, J., Lu, Y., Huang, X.-Y., Shaham, S., 2016. A Glial K/Cl Transporter Controls Neuronal Receptive Ending Shape by Chloride Inhibition of an rGC. Cell 165, 936–948. https://doi.org/10.1016/j.cell.2016.03.026

Singhvi, A., Shaham, S., Rapti, G., 2024. Glia Development and Function in the Nematode Caenorhabditis elegans. Cold Spring Harb. Perspect. Biol. a041346. https://doi.org/10.1101/cshperspect.a041346

Stiernagle, T., 2006. Maintenance of C. elegans, in: WormBook: The Online Review of C. Elegans Biology [Internet]. WormBook.

Sulston, J., Dew, M., Brenner, S., 1975. Dopaminergic neurons in the nematode Caenorhabditis elegans. J. Comp. Neurol. 163, 215–226. https://doi.org/10.1002/cne.901630207

Sulston, J.E., Schierenberg, E., White, J.G., Thomson, J.N., 1983. The embryonic cell lineage of the nematode Caenorhabditis elegans. Dev. Biol. 100, 64–119. https://doi.org/10.1016/0012-1606(83)90201-4

Suzuki, E., Nakayama, M., 2007. The mammalian Ced-1 ortholog MEGF10/KIAA1780 displays a novel adhesion pattern. Exp. Cell Res. 313, 2451–2464. https://doi.org/10.1016/j.yexcr.2007.03.041

Tabrez, S., Jabir, N.R., Shakil, S., Greig, N.H., Alam, Q., Abuzenadah, A.M., Damanhouri, G.A., Kamal, M.A., 2012. A Synopsis on the Role of Tyrosine Hydroxylase in Parkinson's Disease. CNS Neurol. Disord. Drug Targets 11, 395–409. https://doi.org/10.2174/187152712800792785

Tambasco, N., Romoli, M., Calabresi, P., 2018. Levodopa in Parkinson's Disease: Current Status and Future Developments. Curr. Neuropharmacol. 16, 1239–1252. https://doi.org/10.2174/1570159X15666170510143821

Tamo, W., Imaizumi, T., Tanji, K., Yoshida, H., Mori, F., Yoshimoto, M., Takahashi, H., Fukuda, I., Wakabayashi, K., Satoh, K., 2002. Expression of α-synuclein, the precursor of non-amyloid β component of Alzheimer's disease amyloid, in human cerebral blood vessels. Neurosci. Lett. 326, 5–8. https://doi.org/10.1016/S0304-3940(02)00297-5

Tamo, W., Imaizumi, T., Tanji, K., Yoshida, H., Takanashi, S., Wakabayashi, K., Takahashi, R., Hattori, N., Satoh, K., 2007. Parkin is expressed in vascular endothelial cells. Neurosci. Lett. 419, 199–201. https://doi.org/10.1016/j.neulet.2007.04.023

Tanaka, T., Ueno, M., Yamashita, T., 2009. Engulfment of Axon Debris by Microglia Requires p38 MAPK Activity*. J. Biol. Chem. 284, 21626–21636. https://doi.org/10.1074/jbc.M109.005603

Tremblay, M.-E., Cookson, M.R., Civiero, L., 2019a. Glial phagocytic clearance in Parkinson's disease. Mol. Neurodegener. 14, 16. https://doi.org/10.1186/s13024-019-0314-8

Tremblay, M.-E., Cookson, M.R., Civiero, L., 2019b. Glial phagocytic clearance in Parkinson's disease. Mol. Neurodegener. 14, 16. https://doi.org/10.1186/s13024-019-0314-8

Uitti, R.J., Rajput, A.H., Ahlskog, J.E., Offord, K.P., Schroeder, D.R., Ho, M.M., Prasad, M., Rajput, A., Basran, P., 1996. Amantadine treatment is an independent predictor of improved survival in Parkinson's disease. Neurology 46, 1551–1556. https://doi.org/10.1212/wnl.46.6.1551

Vargas-Franco, D., Kalra, R., Draper, I., Pacak, C.A., Asakura, A., Kang, P.B., 2022. The Notch signaling pathway in skeletal muscle health and disease. Muscle Nerve 66, 530–544. https://doi.org/10.1002/mus.27684

Veys, L., Vandenabeele, M., Ortuño-Lizarán, I., Baekelandt, V., Cuenca, N., Moons, L., De Groef, L., 2019. Retinal α-synuclein deposits in Parkinson's disease patients and animal models. Acta Neuropathol. (Berl.) 137, 379–395. https://doi.org/10.1007/s00401-018-01956-z

Vijayaraghavan, T., Dhananjay, S., Ho, X.Y., Giordano-Santini, R., Hilliard, M., Neumann, B., 2023. The dynamin GTPase mediates regenerative axonal fusion in Caenorhabditis elegans by regulating fusogen levels. PNAS Nexus 2, pgad114. https://doi.org/10.1093/pnasnexus/pgad114

Vilalta, A., Brown, G.C., 2018. Neurophagy, the phagocytosis of live neurons and synapses by glia, contributes to brain development and disease. FEBS J. 285, 3566–3575. https://doi.org/10.1111/febs.14323

Villalba, R.M., Smith, Y., 2018. Loss and remodeling of striatal dendritic spines in Parkinson's disease: from homeostasis to maladaptive plasticity? J. Neural Transm. Vienna Austria 1996 125, 431–447. https://doi.org/10.1007/s00702-017-1735-6

Vozdek, R., Pramstaller, P.P., Hicks, A.A., 2022a. Functional Screening of Parkinson's Disease Susceptibility Genes to Identify Novel Modulators of α-Synuclein Neurotoxicity in Caenorhabditis elegans. Front. Aging Neurosci. 14, 806000. https://doi.org/10.3389/fnagi.2022.806000

Vozdek, R., Pramstaller, P.P., Hicks, A.A., 2022b. Functional Screening of Parkinson's Disease Susceptibility Genes to Identify Novel Modulators of α-Synuclein Neurotoxicity in Caenorhabditis elegans. Front. Aging Neurosci. 14, 806000. https://doi.org/10.3389/fnagi.2022.806000

Wadsworth, W.G., Bhatt, H., Hedgecock, E.M., 1996. Neuroglia and pioneer neurons express UNC-6 to provide global and local netrin cues for guiding migrations in C. elegans. Neuron 16, 35–46. https://doi.org/10.1016/s0896-6273(00)80021-5

Walsh, K.T., Zemper, A.E., 2019. The Enteric Nervous System for Epithelial Researchers: Basic Anatomy, Techniques, and Interactions With the Epithelium. Cell. Mol. Gastroenterol. Hepatol. 8, 369–378. https://doi.org/10.1016/j.jcmgh.2019.05.003

Wan, J., Yuan, L., Jing, H., Zheng, Q., Xiao, H., 2021. Defective apoptotic cell clearance activates innate immune response to protect Caenorhabditis elegans against pathogenic bacteria. Virulence 12, 75–83. https://doi.org/10.1080/21505594.2020.1857982

Wang, J., Wang, F., Mai, D., Qu, S., 2020. Molecular Mechanisms of Glutamate Toxicity in Parkinson's Disease. Front. Neurosci. 14. https://doi.org/10.3389/fnins.2020.585584

Wang, X., Li, W., Zhao, D., Liu, B., Shi, Y., Chen, B., Yang, H., Guo, P., Geng, X., Shang, Z., Peden, E., Kage-Nakadai, E., Mitani, S., Xue, D., 2010. C. elegans transthyretin-like protein TTR-52 mediates recognition of apoptotic cells by the CED-1 phagocyte receptor. Nat. Cell Biol. 12, 655–664. https://doi.org/10.1038/ncb2068

Wang, X., Wu, Y.-C., Fadok, V.A., Lee, M.-C., Gengyo-Ando, K., Cheng, L.-C., Ledwich, D., Hsu, P.-K., Chen, J.-Y., Chou, B.-K., Henson, P., Mitani, S., Xue, D., 2003. Cell corpse engulfment mediated by C. elegans phosphatidylserine receptor through CED-5 and CED-12. Science 302, 1563–1566. https://doi.org/10.1126/science.1087641

Wang, X., Yang, C., 2016. Programmed cell death and clearance of cell corpses in Caenorhabditis elegans. Cell. Mol. Life Sci. 73, 2221–2236. https://doi.org/10.1007/s00018-016-2196-z

Weingarten, C.P., Sundman, M.H., Hickey, P., Chen, N., 2015. Neuroimaging of Parkinson's disease: Expanding views. Neurosci. Biobehav. Rev. 59, 16–52. https://doi.org/10.1016/j.neubiorev.2015.09.007

White, J.G., Southgate, E., Thomson, J.N., Brenner, S., 1986. The structure of the nervous system of the nematode Caenorhabditis elegans. Philos. Trans. R. Soc. Lond. B. Biol. Sci. 314, 1–340. https://doi.org/10.1098/rstb.1986.0056

Williamson, A.P., Vale, R.D., 2018. Spatial control of Draper receptor signaling initiates apoptotic cell engulfment. J. Cell Biol. 217, 3977–3992. https://doi.org/10.1083/jcb.201711175

Wu, Y., O'Toole, E.T., Girard, M., Ritter, B., Messa, M., Liu, X., McPherson, P.S., Ferguson, S.M., De Camilli, P., 2014. A dynamin 1-, dynamin 3- and clathrin-independent pathway of synaptic vesicle recycling mediated by bulk endocytosis. eLife 3, e01621. https://doi.org/10.7554/eLife.01621

Xiong, Y., Dawson, T.M., Dawson, V.L., 2017. Models of LRRK2-Associated Parkinson's Disease. Adv. Neurobiol. 14, 163–191. https://doi.org/10.1007/978-3-319-49969-7_9

Yamada, K., Hirotsu, T., Matsuki, M., Butcher, R.A., Tomioka, M., Ishihara, T., Clardy, J., Kunitomo, H., Iino, Y., 2010. Olfactory plasticity is regulated by pheromonal signaling in Caenorhabditis elegans. Science 329, 1647–1650. https://doi.org/10.1126/science.1192020

Yang, H., Chen, Y.-Z., Zhang, Y., Wang, X., Zhao, X., Godfroy, J.I., Liang, Q., Zhang, M., Zhang, T., Yuan, Q., Ann Royal, M., Driscoll, M., Xia, N.-S., Yin, H., Xue, D., 2015. A lysine-rich motif in the phosphatidylserine receptor PSR-1 mediates recognition and removal of apoptotic cells. Nat. Commun. 6, 5717. https://doi.org/10.1038/ncomms6717

Yang, Q., Wang, Y., Zhao, C., Pang, S., Lu, J., Chan, P., 2023. α-Synuclein aggregation causes muscle atrophy through neuromuscular junction degeneration. J. Cachexia Sarcopenia Muscle 14, 226–242. https://doi.org/10.1002/jcsm.13123

Yang, S., Zhou, J., Li, D., 2021. Functions and Diseases of the Retinal Pigment Epithelium. Front. Pharmacol. 12, 727870. https://doi.org/10.3389/fphar.2021.727870

Yarychkivska, O., Sharmin, R., Elkhalil, A., Ghose, P., 2024. Apoptosis and beyond: A new era for programmed cell death in *Caenorhabditis elegans*. Semin. Cell Dev. Biol., C. elegans as a model for health and disease 154, 14–22. https://doi.org/10.1016/j.semcdb.2023.02.003

Yoshimura, S., Murray, J.I., Lu, Y., Waterston, R.H., Shaham, S., 2008. mls-2 and vab-3 Control glia development, hlh-17/Olig expression and glia-dependent neurite extension in C. elegans. Dev. Camb. Engl. 135, 2263–2275. https://doi.org/10.1242/dev.019547

Yu, X., Ji, C., Shao, A., 2020. Neurovascular Unit Dysfunction and Neurodegenerative Disorders. Front. Neurosci. 14. https://doi.org/10.3389/fnins.2020.00334

Yu, X., Odera, S., Chuang, C.-H., Lu, N., Zhou, Z., 2006. *C. elegans* Dynamin Mediates the Signaling of Phagocytic Receptor CED-1 for the Engulfment and Degradation of Apoptotic Cells. Dev. Cell 10, 743–757. https://doi.org/10.1016/j.devcel.2006.04.007

Yuan, L., Li, P., Jing, H., Zheng, Q., Xiao, H., 2022. trim-21 promotes proteasomal degradation of CED-1 for apoptotic cell clearance in C. elegans. eLife 11, e76436. https://doi.org/10.7554/eLife.76436

Zhang, X., Zhang, R., Nisa Awan, M.U., Bai, J., 2022. The Mechanism and Function of Glia in Parkinson's Disease. Front. Cell. Neurosci. 16, 903469. https://doi.org/10.3389/fncel.2022.903469

Zhang, Y., Meng, X., Jiao, Z., Liu, Y., Zhang, X., Qu, S., 2020. Generation of a Novel Mouse Model of Parkinson's Disease via Targeted Knockdown of Glutamate Transporter GLT-1 in the Substantia Nigra. ACS Chem. Neurosci. 11, 406–417. https://doi.org/10.1021/acschemneuro.9b00609

Zhang, Y., Wang, H., Kage-Nakadai, E., Mitani, S., Wang, X., 2012. C. elegans secreted lipid-binding protein NRF-5 mediates PS appearance on phagocytes for cell corpse engulfment. Curr. Biol. CB 22, 1276–1284. https://doi.org/10.1016/j.cub.2012.06.004

Zhang, Zhu, Zhang, S., Fu, P., Zhang, Zhang, Lin, K., Ko, J.K.-S., Yung, K.K.-L., 2019a. Roles of Glutamate Receptors in Parkinson's Disease. Int. J. Mol. Sci. 20, 4391. https://doi.org/10.3390/ijms20184391

Zhang, Zhu, Zhang, S., Fu, P., Zhang, Zhang, Lin, K., Ko, J.K.-S., Yung, K.K.-L., 2019b. Roles of Glutamate Receptors in Parkinson's Disease. Int. J. Mol. Sci. 20, 4391. https://doi.org/10.3390/ijms20184391

Zhao, C., Wang, C., Zhang, H., Yan, W., 2023. A mini-review of the role of vesicular glutamate transporters in Parkinson's disease. Front. Mol. Neurosci. 16, 1118078. https://doi.org/10.3389/fnmol.2023.1118078

Zhivotovsky, B., Orrenius, S., 2011. Calcium and cell death mechanisms: a perspective from the cell death community. Cell Calcium 50, 211–221. https://doi.org/10.1016/j.ceca.2011.03.003

Zhou, Z., Hartwieg, E., Horvitz, H.R., 2001. CED-1 is a transmembrane receptor that mediates cell corpse engulfment in C. elegans. Cell 104, 43–56. https://doi.org/10.1016/s0092-8674(01)00190-8

Zhou, Z.D., Yi, L.X., Wang, D.Q., Lim, T.M., Tan, E.K., 2023. Role of dopamine in the pathophysiology of Parkinson's disease. Transl. Neurodegener. 12, 44. https://doi.org/10.1186/s40035-023-00378-6

Zou, W., Lu, Q., Zhao, D., Li, W., Mapes, J., Xie, Y., Wang, X., 2009. Caenorhabditis elegans Myotubularin MTM-1 Negatively Regulates the Engulfment of Apoptotic Cells. PLOS Genet. 5, e1000679. https://doi.org/10.1371/journal.pgen.1000679

Zou, W., Pu, T., Feng, W., Lu, M., Zheng, Y., Du, R., Xiao, M., Hu, G., 2019. Blocking meningeal lymphatic drainage aggravates Parkinson's disease-like pathology in mice overexpressing mutated α-synuclein. Transl. Neurodegener. 8, 7. https://doi.org/10.1186/s40035-019-0147-y

Zuchero, J.B., Barres, B.A., 2015. Glia in mammalian development and disease. Dev. Camb. Engl. 142, 3805. https://doi.org/10.1242/dev.129304